Nina Zupančič

ŠTUDIJSKO GRADIVO ZA VAJE IZ GEOKEMIJE

Ljubljana, februar 2004

Kollinson H., 1993, using

The major elements (Chapter 3) are the elements which predominate in any rock analysis. They are Si, Ti, Al, Fe, Mn, Mg, Ca, Na, K and P, and their concentrations are expressed as a weight per cent (wt %) of the oxide (Table 1.1). Major element determinations are usually made only for cations and it is assumed that they are accompanied by an appropriate amount of oxygen. Thus the sum of the major element oxides will total to about 100 % and the analysis total may be used as a rough guide to its reliability. Iron may be determined as FeO and Fe_2O_3, but is sometimes expressed as 'total Fe' and given as either $FeO_{(tot)}$ or $Fe_2O_{3(tot)}$.

Trace elements (Chapter 4) are defined as those elements which are present at less than the 0.1 % level and their concentrations are expressed in parts per million (ppm) or more rarely in parts per billion (ppb; 1 billion = 10^9) of the element (Table 1.1). Convention is not always followed however, and trace element concentrations exceeding the 0.1 % (1000 ppm) level are sometimes cited. The trace elements of importance in geochemistry are identified in Table 1.5 and shown in Figure 4.1.

Some elements behave as a major element in one group of rocks and as a trace element in another group of rocks. An example is the element K, which is a major constituent of rhyolites, making up more than 4 wt % of the rock and forming an essential structural part of minerals such as orthoclase and biotite. In some basalts, however, K concentrations are very low and there are no K-bearing phases. In this case K behaves as a trace element.

Volatiles such as H_2O, CO_2 and S are normally included in the major element analysis (Table 1.1). Water combined within the lattice of silicate minerals and released above 110 °C is described as H_2O+. Water present simply as dampness in the rock powder and driven off by heating below 110 °C is quoted as H_2O- and is not an important constituent of the rock. Sometimes the total volatile content of the rock is determined by ignition at 1000 °C and is expressed as 'loss on ignition' (Lechler and Desilets, 1987).

Isotopes are subdivided into radiogenic and stable isotopes. **Radiogenic isotopes** (Chapter 6) include those isotopes which decay spontaneously due to their natural radioactivity and those which are the final daughter products of such a decay scheme. They include the parent–daughter element pairs Rb–Sr, Sm–Nd, U–Pb, Th–Pb and K–Ar. They are expressed as ratios either in absolute terms $^{87}Sr/^{86}Sr$ (e.g.) or relative to a standard (the ε-notation) (Table 1.1).

Stable isotope studies in geology (Chapter 7) concentrate on the naturally occurring isotopes of light elements such as H, O, C and S which may be fractionated on the basis of mass differences between the isotopes of the element. For example, the isotope ^{18}O is 12.5 % heavier than the isotope ^{16}O and the two are fractionated during the evaporation of water. Stable isotopes contribute significantly to an understanding of fluid and volatile species in geology. They are expressed as ratios relative to a standard using the δ-notation (Table 1.1)

The major part of this book discusses the four main types of geochemical data outlined above and shows how they can be used to identify geochemical processes. In addition, Chapter 5 has been included to show the way in which trace and major element chemistry is used to determine the tectonic setting of some igneous and sedimentary rocks. Chapter 2 discusses some of the particular statistical problems which arise when analysing geochemical data-sets, and some recommendations are made about permissible and impermissible methods of data presentation.

In this introductory chapter we consider three topics: (1) the geochemical processes which are likely to be encountered in nature and their geochemical signatures; (2) the interaction between geological fieldwork and the interpretation of geochemical data; and (3) the different analytical methods currently in use in modern geochemistry.

1.2 Geological processes and their geochemical signatures

A major purpose of this text is to show how geochemical data can be used to identify geological processes. In this section the main geochemical signatures of igneous, sedimentary and metamorphic processes are briefly summarized and presented in graphical (Figures 1.1 to 1.3) and in tabular form (Tables 1.2 to 1.4). This brief survey is augmented by fuller discussions elsewhere in the text. Each of the Tables 1.2 to 1.4 lists the geological processes which may have a geochemical signature and identifies the sections in the book where the particular process is described and characterized using major or trace elements, and radiogenic or stable isotopes.

1.2.1 Processes which control the chemical composition of igneous rocks

The chemical composition and mineralogy of the source region exerts a fundamental control over the chemistry of magmatic rocks. The major and trace element composition of a melt is determined by the type of melting process and the degree of partial melting, although the composition of the melt can be substantially modified *en route* to the surface (Figure 1.1). The source region is best characterized by its radiogenic isotope composition because isotope ratios are not modified during partial melting and magma chamber processes. The composition of the source itself is a function of mixing processes in the source region. This is particularly pertinent to studies of the mantle, and in the last decade important advances have been made in understanding mantle dynamics through the isotopic study of mantle-derived oceanic basalts (see Section 6.3.6).

Most magmatic rocks are filtered through a magma chamber prior to their emplacement at or near the surface. Magma chamber processes frequently modify the chemical composition of the primary magma, produced by partial melting of the source, through fractional crystallization, magma mixing, contamination or a dynamic mixture of several of these processes. Resolving the chemical effects of these different processes requires the full range of geochemical tools — major and trace element studies coupled with the measurement of both radiogenic and stable isotope compositions. Excellent and detailed discussions of magma chamber processes are given by Hall (1987 — Chapter 7) and Wilson (1989 — Chapter 4).

Following emplacement or eruption, igneous rocks may be chemically modified, either by outgassing or by interaction with a fluid. The outgassing of igneous rocks chiefly affects the stable isotope chemistry whereas interaction with a fluid may affect all aspects of the rock chemistry. Ideally, igneous rocks selected for chemical analysis are completely fresh, but sometimes this cannot be achieved. For example, samples from the seafloor have most probably been subjected to weathering or even hydrothermal alteration by seawater. Many igneous plutonic bodies initiate, on emplacement, hydrothermal groundwater circulation in the surrounding country rocks, thus leading to the chemical alteration of the igneous pluton itself. Metamorphosed igneous rocks are also likely to be chemically modified by the interaction with a fluid phase, as is discussed below.

1.2.2 Processes which control the chemical composition of sedimentary rocks

The chemical composition of the provenance is probably the major control on the chemistry of sedimentary rocks although this can be greatly modified by subsequent processes (Figure 1.2). The composition of the provenance is a function of tectonic setting. Weathering conditions may leave their signature in the resultant sediment and major element studies of sedimentary rocks indicate that sometimes the former weathering conditions can be recognized from the chemistry of the sediments (Section 3.3.1). Significant chemical changes may also take place during transport: some trace elements become concentrated in the clay component and in the heavy mineral fraction whilst others are diluted in a quartz-rich coarse fraction. These processes are to a large extent also dependent upon the length of time spent between erosion and deposition.

Chemical changes during deposition will depend upon the depositional environment, which is chiefly controlled by subsidence rate. Chemical and biochemical processes controlling element solubilities in seawater, submarine weathering and redox conditions are also important for particular types of sediment. Post-depositional processes are best investigated using stable isotopes. The stable isotopes of oxygen and hydrogen are important tracers for different types of water, vital in the study of diagenetic fluids. Carbon and oxygen isotopes are used in the study of limestone diagenesis. The temperature-dependent fractionation of oxygen isotopes can be used to calculate the geothermal gradient during diagenesis and allows some control on the burial history of the rock.

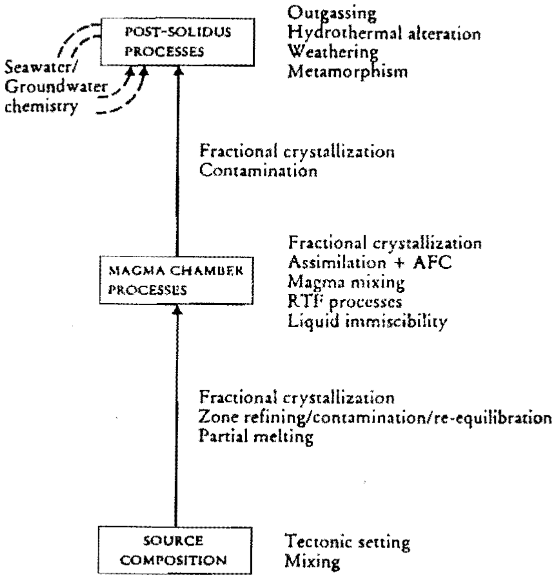

Figure 1.1 Flow diagram showing the principal processes which control the chemical composition of igneous rocks.

1.2.3 Processes which control the chemical composition of metamorphic rocks

The principal control on the chemical composition of a metamorphic rock is the composition of the pre-metamorphic protolith. Sometimes metamorphic recrystallization may be isochemical but most commonly there is a change in chemical composition (Figure 1.3). This is principally controlled by the movement of fluids and the thermal conditions during metamorphism. Metamorphism is frequently accompanied by deformation; particularly at high metamorphic grades, there may be tectonic interleaving of different protolith compositions which gives rise to a metamorphic rock of mixed parentage.

The ingress and expulsion of water during metamorphism, chiefly as a consequence of hydration and dehydration reactions, may give rise to changes in the chemical composition of the parent rock as a consequence of particular elements becoming mobile in the fluid. These processes are controlled by the composition of the fluid phase, its temperature and the ratio of metamorphic fluid to the host rock.

At high metamorphic grades and frequently in the presence of a hydrous fluid, melting may take place. The segregation and removal of this melt will clearly differentiate the parental rock into two compositionally distinct components — restite and melt. In this case, the precise nature of the chemical change is governed by the degree of melting and the melting process.

Chemical change in metamorphic rocks in the absence of a fluid phase is

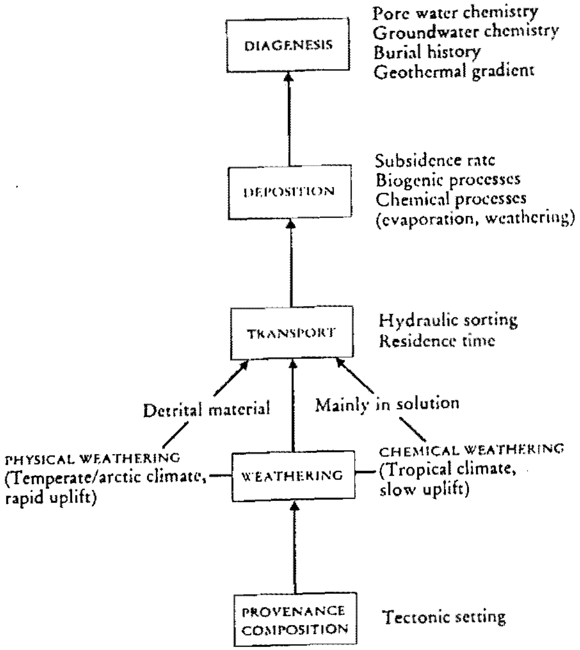

Figure 1.2 Flow diagram showing the principal processes which control the chemical composition of sedimentary rocks.

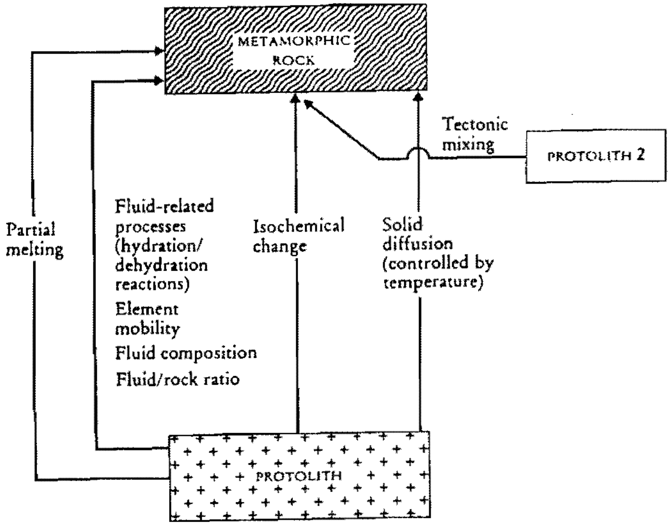

Figure 1.3 Flow diagram showing the principal processes which control the chemical composition of metamorphic rocks.

governed by diffusion of ions in the solid state. This is in response to changing mineral stabilities and metamorphic reactions — a function of the P–T conditions of metamorphism.

1.3 Geological controls on geochemical data

Geochemical investigations are most fruitful when a particular model or hypothesis is being tested. This ultimately hinges upon a clear understanding of the geological relationships. Thus, any successful geochemical investigation must be based upon a proper understanding of the geology of the area. It is not sufficient to carry out a 'smash and grab raid', returning to the laboratory with large numbers of samples, if the relationship between the samples is unknown and their relationship to the regional geology is unclear. It is normal to use the geology to interpret the geochemistry. Rarely is the converse true, for at best the results are ambiguous.

As an example, consider a migmatitic terrain in which there are several generations of melt produced from a number of possible sources. A regional study in which samples are collected on a grid pattern may have a statistically accurate feel and yet will provide limited information on the origin of the migmatite complex. What is required in such a study is the mapping of the age relationships between the units present, at the appropriate scale, followed by the careful sampling of each unit. This then allows chemical variations within the units to be investigated and models tested for the relationships between units. A fundamental thesis of this book is therefore that geochemical investigations must always be carried out in the light of a clear understanding of the geological relationships.

This approach leads naturally to the way in which geochemical data are presented. In the main this presentation is as bivariate (and trivariate) plots in which the variables are the geochemical data; a discussion of these plots forms the major part of this book. However, if the geology is also considered, then the additional variables of time and space may be plotted as well. Clearly, it can be informative on some occasions to examine chemical variations with time in a sedimentary pile. Furthermore, it is often valuable to examine the spatial distribution of geochemical data. This can vary over the entire range of geological investigations from the micro- to the global scale. Compare for example the 'map' of lead-isotopic analyses in a single galena grain (Shimizu and Hart, 1982) with the projection of isotopic anomalies in the Earth's mantle onto a world map, described by Hart (1984). Both are instructive.

Where has all the old crust gone?

Richard W. Carlson

Geophysicists have come to believe that the Earth was covered with a thick crust more than four billion years ago. New measurements challenge that theory, indicating the importance of crustal destruction in Earth's early history.

V 10 - 15 [illegible]
[illegible] [illegible]
[illegible] !

VIEWED as a huge chemical factory, the Earth has been trying for 4.5 billion years to separate its chemical constituents into stable, density-stratified layers. Dense iron–nickel alloys, which do not dissolve in the silicate mantle, fell to form the core; volatile compounds were distilled from the interior to make the atmosphere and oceans; and melts of the mantle rose to the surface to form the crust. Most of the core formation and a large fraction of the volatile degassing from the mantle were completed in the first billion years of Earth's history. Evidence for similarly efficient crust formation on the early Earth has been suggested by recent studies of preserved rocks 3.5 to 3.9 billion years old[1,2]. However, data reported by Vervoort *et al.*[3] on page 624 of this issue contradict that evidence, and raise the questions: why did the Earth not form an extensive early crust or, if it did, where has all this old crust gone?

Current ideas of planet formation suggest a very energetic early Earth. Large planetesimals (rock and ice bodies that condensed in the early Solar System) collided violently with the Earth during the latter stages of formation, and transformed their kinetic energy into heat within the growing planet. The sinking of iron alloys to form the core released gravitational potential energy as additional heat. Radioactive elements, perhaps including those that have long-since decayed away, such as aluminium-26 and iron-60 which have half-lives of about a million years, contributed further to heating the early Earth's interior.

Models developed as a result of our visits to the Moon suggest that this energetic formation resulted in planetary interiors that were either largely or totally molten. Upon cooling and crystallization, these 'magma oceans' would have transferred dense material to the core and buoyant crystallizing minerals, such as plagioclase, to the surface. The Moon illustrates this effect clearly in its thick, plagioclase-rich crust; in a mantle showing the complementary chemical signature of plagioclase removal; and in the fact that radiometric dating shows this chemical separation of crust from mantle on the Moon to have been nearly complete 4.35 to 4.4 billion years ago.

Exploration for ancient terrestrial crust has been intense, but so far the oldest rocks found on the Earth are only 3.96 billion years old[4], although a few sub-millimetre-sized grains of the particularly sturdy mineral zircon have been found in western Australia that have ages (measured by radiometric dating) approaching 4.2 billion years[5]. On the Earth, the lack of preserved ancient crust does not necessarily mean that such crust never existed, because the plate tectonic cycle provides a clear method of crustal destruction through subduction into the deep mantle at convergent plate boundaries, and replacement by new crust produced along ocean ridges.

The 3.54-billion-year-old Ngwane gneiss of Swaziland, southern Africa. This gneiss is composed of feldspar-rich (light coloured bands) and amphibole-rich (dark) material intermixed by metamorphism. The 'stirring' is shown clearly by the feldspar-rich layer folded into an 's' shape on the right-hand side of the photograph. Metamorphism is probably also responsible for altering neodymium isotope ratios to indicate falsely a thick crust on the early Earth.

In seeking information on Earth's first crust, one can remove the effects of more than 3 billion years of plate tectonics by looking at the ratios of different radiogenic isotopes in the oldest preserved crustal rocks at the time of their formation. The chemical changes associated with crust formation result in abundance ratios of parent to daughter elements that differ between the crust, its complementary melt-depleted mantle and mantle unaffected by melt removal. Over time, these distinct parent/daughter ratios produce different daughter-element isotopic compositions. This is demonstrated well in the volcanic rocks erupted today along the Earth's ocean ridges, which show very clearly that the mantle providing these magmas is a complementary residue to the continental crust.

Three of the radioactive decay systems that have been used for this purpose are rubidium–strontium, samarium–neodymium and lutetium–hafnium. Neodymium data taken in the early 1980s (ref. 6) from crustal rocks 2.7 to 3.8 billion years old showed clearly that, 3.8 billion years ago, the mantle had already been depleted by extraction of crust. The deviation of these data from those expected for an undepleted mantle was not large, however, and failed to provide evidence for the existence of large volumes of crust produced by magma ocean crystallization. More recent data, particularly for the oldest preserved crustal rocks[1,2], show much wider initial neodymium isotope variation, implying the existence of large volumes of crust in the Hadean era (the geological period between Earth's formation and creation of the oldest preserved crust).

Calculating initial isotopic compositions of old rocks, however, relies on the unverifiable assumption that the parent/daughter ratio of the sample has remained constant since rock formation. In general, the assumption is a good one, but crust that has floated around Earth's surface for billions of years has had many opportunities for collisions with other crustal blocks, which can lead to metamorphism of the constituent rocks (see figure). If that changes the parent/daughter ratio of a sample of old crust long after rock formation, the initial isotopic composition will be obscured. Because of the ease with which the rubidium/strontium ratio of a rock can be changed by metamorphism, attempts to study crustal development by examination of that radiometric system have all but been abandoned. Samarium and neodymium, being neighbouring lanthanide elements and insoluble in most metamorphic fluids, are more immune than rubidium to migration during metamorphism, but the question that must be faced is, are they absolutely immobile?

To avoid this problem, Vervoort *et al.* examined the lutetium–hafnium radiometric system in the mineral zircon. Zircon is well known to geochronologists because it incorporates high quantities of uranium but almost no lead during its formation, and so is extremely useful for precise uranium–lead geochronology. Furthermore, it is a very stable mineral during metamorphic processes. For lutetium–hafnium studies, zircon offers the additional advantage that hafnium is an abundant element whereas its parent lutetium is present only in trace amounts. Consequently, the lutetium/hafnium ratio of zircon is near zero, necessitating only minor corrections to measured hafnium isotopic compositions.

Vervoort and colleagues show that the initial hafnium isotope compositions of zircons from Greenland rocks 3.6 to 3.8 billion years old indicate a mantle source that was mildly depleted by melt removal in the Hadean era. However, the range of initial neodymium isotope composition of the same rocks is much larger than is compatible with the observed variation in hafnium, implying that the more extreme values of neodymium composition observed in ancient continental rocks are the result of metamorphic perturbations, and not an indication of large amounts of ancient crust.

We are faced with a troubling lack of evidence for large volumes of Hadean crust on Earth. Perhaps we are looking for the wrong type of crust? The lunar example of a plagioclase-rich flotation crust is probably not appropriate for the Earth, where much greater interior pressures promote crystallization of the dense mineral garnet, which would consume the aluminium necessary for plagioclase formation. Another explanation, but by no means the only one, is that vigorous convection in the early mantle was particularly good at mixing away evidence of earlier crust–mantle differentiation. If this is the case, the Earth's surface in the Hadean may have been covered with a thin and transient basaltic crust, much like the current situation in the ocean basins where new crust formed along ocean ridges survives at the surface for, at most, a couple of hundred million years before it plunges back into the mantle in a subduction zone. The continent–ocean distinction, unique to the Earth among the terrestrial planets, may not be a primary feature of Earth, but rather one reflecting the losing battle of plate tectonics to stir back the 'slag'-separating from the mantle 'foundry'. ☐

1. Gibbsova prosta energija formacije FeO pri standardnih pogojih je -251.1 kJ. Ali je značaj Al, Ba, Ca, Cd, Cu, Mg, Ni, Pb, Si, Sn in W pri the pogojih litofilen ali siderofilen?
2. Ali sta pri 827°C Zn in Sn siderofilna ali litofilna?
3. Kakšna je povezava med Goldschmidtovo razdelitvijo prvin in periodnim sistemom?
4. Kaj pomeni trditev, da je Cu bolj halkofilen kot Zr ali Pt?
5. Katero glavno prvino ali prvine lahko nadomešča Ba^{2+}, Cr^{3+} in Y^{3+}?
6. Zakaj so plagioklazi, ki se izločijo bolj zgodaj v kristalizacijskem zaporedju bogatejši s Ca, tisti ki se izločijo kasneje pa z Na?
7. Katere prvine označujemo z LILE, HFSE in REE?
8. Kaj pomeni, da je neka prvina inkompatibilna?
9. Na diagramih prikaži trend spreminjanja vsebnosti K, Ca, Ba, Mg in Cr z naraščajočo diferenciacijo ter razloži diagrame. Podatki so v priloženi tabeli.
10. Vanadij je obilnejši kot bor, vendar pa tako v magmatskih kot v sedimentnih kamninah pogosteje zasledimo borove minerale kot vanadijeve. Razloži zakaj.
11. Za vsako od razmerij ugotovi ali bo običajno višje v mafičnih ali felsičnih magmatskih kamninah ter navedi zakaj: Sr/Ba, B/Mn, Li/Mg, Pb/Rb in Cr/Al.
12. Katera razmerja med prvinami bodo višja v evaporitih, katera v glinavcih? Zakaj? Sr/Na, K/Rb, Mg/Mn
13. Li in Cs se koncentrirata v pozno nastalih sljudah v pegmatitih, čeprav sta njuna ionska radija zelo različna. Navedi zakaj.
14. Zakaj se našteti pari prvin običajno ne zamenjujejo izomorfno: Li - Na, Fe - Li, Mg - Nb, Mn - Pt, Ca - Rb, Cu - Na, C - Si, Se - Li, Cd - Na in Cl - F.
15. Zakaj so Ga minerali izredno redki, minerali mnogo manj obilnih prvin kot so Sn, U in W pa dokaj običajni?
16. Zakaj so najobilnejše prvine v morski vodi Na, K, Mg, Ca, S in Cl?
17. Zakaj sta U in Th bolj obilna v granitih kot v ultramafičnih kamninah?
18. Večina REE je obilnejših v granitih kot v bazaltih. Zakaj je Eu izjema?
19. Kaj je to normalizacija REE?
20. Zakaj se pri interpretaciji uporabljajo normalizirani in ne normalni vzorci REE?

Krauskopf K. B. & Bird D. K., 1995 · Introduction to Geochemistry

CHAPTER
20

DISTRIBUTION OF THE ELEMENTS

The central problem of geochemistry was defined by the Norwegian geochemist V. M. Goldschmidt, early in the 20th century, to be "the determination of the distribution of the elements in materials of the Earth and the reasons for this distribution." In a sense we have been working with this problem from the start of Chapter 1, but our emphasis has been on the role of particular elements in geologic processes as seen from a chemical standpoint. Now we set out to address Goldschmidt's problem more directly.

Basic facts about element distribution are already familiar, just from ordinary experience and from discussions in preceding chapters. Igneous rocks have a characteristic group of elements (Chap. 17), sulfide ores another group (Chap. 19), carbonate sediments another group (Chap. 3), salt deposits still another (Chap. 14). To refine such generalizations, in particular to see how the rarer elements are distributed in various environments, we need a classification, a way of grouping the elements so that their properties may be related to geologic behavior. One such scheme is Mendeleev's periodic table, an overall grouping according to chemical properties that is familiar from elementary chemistry and that we introduced in a geological context back in Chapter 5 (Table 5-3). A few highlights of this table should be recalled.

Elements in each column of the table are closely related in their electronic structures and chemical properties. Resemblances are especially strong among the metallic elements in columns toward the left side of the table and among the nonmetallic elements on the right. On these left and right sides the properties of rare elements, both chemical and geological, can be predicted with considerable accuracy from properties of the better known elements in the same column. The transition elements in the middle of the table, mostly metals, are less regular in their relationships, and prediction of properties is less satisfactory. Two special groups of elements, the actinides and lanthanides, are singled out because they are so very similar among themselves in their properties and in the structures of their atoms. From these relations in Mendeleev's table many useful general statements about the distribution of the rarer elements in geologic materials are possible, but a more specific geochemical classification is also needed.

20-1 GOLDSCHMIDT'S GEOCHEMICAL CLASSIFICATION

One alternative classification was suggested by Goldschmidt in his early work on the rules of element distribution. This grouping of elements was an attempted answer to a hypothetical question: If the Earth at some time in the past was largely molten and if the molten material separated itself on cooling into a metal phase, a sulfide phase, and a silicate phase, how would the elements distribute themselves among these three materials? An answer can be sought from theoretical arguments and also from three kinds of observation: (1) the composition of meteorites, on the assumption that meteorites have an average composition similar to that of the primordial Earth and underwent a similar kind of differentiation; (2) analyses of metal, slag (silicate), and matte (sulfide) phases in metallurgical operations; and (3) the composition of silicate rocks, sulfide ores, and the rare occurrences of native iron found in the Earth's crust.

From a theoretical standpoint, consider first the expected distribution of elements between metallic iron and silicates, in a system with iron in excess. Metals more chemically active (in the sense of a higher free energy of oxidation) than iron would presumably combine with silica to form silicates, and the remaining silica would react so far as possible with iron. Metals less active than iron would have no chance to form silicates but would remain as free metals with the uncombined iron. In other words, the fate of any given metal should depend entirely on the free energy of formation of its silicate (Sec. 7-4). Data on formation energies of silicates are not complete, but to a good approximation we can substitute the free energies of oxides, since in the formation of a silicate the energy of the reaction (with Me standing for any metal)

$$\mathrm{Me} + 1/2\mathrm{O}_2 \rightleftharpoons \mathrm{MeO} \qquad (20\text{-}1)$$

is always much larger than the energy of the reaction

$$\mathrm{MeO} + \mathrm{SiO}_2 \rightleftharpoons \mathrm{MeSiO}_3. \qquad (20\text{-}2)$$

Free energies of formation of representative oxides are given in Table 20-1. From this list we could predict that the elements above iron would go preferentially into

TABLE 20.1
Free energies of formation of oxides per oxygen atom, kJ

	25°C	827°C
CaO	−604.0	−520.8
MgO	−569.4	−481.6
Al_2O_3	−527.4	−442.7
UO_2	−515.9	−447.2
TiO_2	−444.7	−371.9
SiO_2	−428.3	−356.8
MnO	−362.9	−304.3
K_2O	−322.1	−203.2
ZnO	−320.4	−237.9
WO_2	−266.9	−195.0
SnO_2	−259.9	−176.5
FeO	−251.1	−199.7
MoO_3	−222.7	−156.7
CoO	−214.2	−154.9
NiO	−211.7	−140.7
PbO	−188.9	−109.2
Cu_2O	−146.0	−86.9

The numbers are free energies of formation per oxygen atom, in kilojoules. The oxides are arranged in order of decreasing free energy at 25°C. *Source:* Robie et al. (1979).

the oxide (or silicate) phase, and those below iron into the metallic phase. The grouping is not entirely unambiguous, in that two elements (W and Sn) appear to stand above iron at low temperatures and below iron at high temperatures. Similar lists could be drawn up showing the expected distribution of metals between a metal phase and a sulfide phase with iron in excess, and between a sulfide phase and a silicate phase with silica in excess. So many additional assumptions are required, however, that the numerical values are not very helpful.

On the observational side, the compositions of the three phases (metal, sulfide, silicate) in meteorites and in smelter products are well-known. Analyses show that, with a few exceptions, elements above iron in Table 20-1 have higher concentrations in the silicate phases than the metal phases of both materials, and that most of the elements below iron are strongly concentrated in the sulfide phases. Occurrences of elements in silicate rocks, sulfide ores, and native iron agree fairly well with the distributions shown by the meteorite and smelter analyses. The lack of complete agreement is not surprising, as Goldschmidt pointed out, since the conditions of formation of sulfide ore deposits in nature are quite different from the conditions under which sulfides would separate from an artificial melt.

On the basis of such evidence, Goldschmidt suggested that the elements could be usefully grouped into those that preferentially occur with native iron and probably are concentrated in the Earth's iron core (*siderophile elements*); those concentrated in sulfides and therefore characteristic of sulfide ore deposits (*chalcophile elements*); and those that generally occur in or with silicates (*lithophile elements*). For completeness, elements that are prominent in air and other natural gases can be put in a fourth group, the *atmophile elements*. This classification, shown in Table 20-2, is clearly consistent with the data of Table 20-1.

As might be expected, Goldschmidt's classification is closely related to the periodic law. Comparison of Tables 20-2 and 5-3 shows that in general siderophile elements are concentrated in the center of the periodic table, lithophile elements to the left of center, chalcophile elements to the right, and atmophile elements on the extreme right. The classification can also be correlated with electrode potentials: siderophile elements are dominantly noble metals with low electrode potentials, lithophile elements are those with high potentials, and chalcophile elements have an intermediate position.

The grouping of elements shown in Table 20-2 can at best express only tendencies, not quantitative relationships. The different groups overlap, as is shown by the occurrence of many elements in more than one category. Iron, for example, is not only the principal element of the Earth's core but is also common in sulfide deposits and in igneous rocks. Such overlaps are inevitable in a classification that is based partly on distributions in very high-temperature processes and partly on distributions under ordinary surface conditions. Various refinements have been suggested, but there seems little point in trying to make the classification more quantitative or more detailed. It is useful simply as a rough qualitative expression of the geologic behavior of the elements.

TABLE 20-2
Goldschmidt's geochemical classification of the elements

Siderophile	Chalcophile	Lithophile	Atmophile
Fe Co Ni	Cu Ag (Au)[1]	Li Na K Rb Cs	H N (C) (O)
Ru Rh Pd	Zn Cd Hg	Be Mg Ca Sr Ba (Pb)	(F) (Cl) (Br) (I)
Re Os Ir Pt Au	Ga In Tl	B Al Sc Y REE[2]	He Ne Ar Kr Xe
Mo Ge Sn C P	(Ge) (Sn) Pb	(C) Si Ti Zr Hf Th	
(Pb) (As) (W)	As Sb Bi	(P) V Nb Ta	
	S Se Te	O Cr W U	
	(Fe) (Mo) (Re)	(Fe) Mn	
		F Cl Br I	
		(H) (Tl) (Ga) (Ge)	
		(N)	

[1] Parentheses around a symbol indicate that the element belongs primarily in another group, but has some characteristics that relate it to this group. For example, gold is dominantly siderophile, but (Au) appears in the chalcophile group because gold is often found in sulfide veins.
[2] REE = rare-earth elements.

20-2 DISTRIBUTION OF ELEMENTS IN IGNEOUS ROCKS

Point of View

The origin of many igneous rocks, as noted in previous discussions, is a subject of lively debate. Fortunately the various hypotheses of origin lead in general to similar predictions about the distribution of trace elements. To unify the discussion—but not to argue for one hypothesis over another—we start with the "classical" viewpoint that most igneous rocks can be thought of as formed by differentiation of basaltic magma, mafic minerals settling out first to form ultramafic rocks and the remaining melt changing in composition through the series gabbro → diorite → granodiorite → granite → pegmatite. We can speak then of "early-formed minerals" of high melting point, such as olivine and calcic plagioclase, "late-formed minerals" like alkali feldspars and biotite, and "residual fluids" of pegmatitic composition. We can work out semiempirical rules of behavior for various elements during such a differentiation process and compare our predictions with analyses. When this procedure is adopted, it turns out that agreement between predictions and analyses is surprisingly good, and surprisingly uniform from one set of igneous rocks to another.

This agreement, however, is not evidence in favor of the assumed crystallization-differentiation process for the origin of igneous rocks. The same sequence of rock compositions could be formed equally well (but in reverse order) by progressive anatexis of a shale or graywacke, proceeding from the composition of alkali granite through granodiorite, tonalite, and gabbro as more and more mafic material is incorporated into the melt. The same distribution of elements would be expected at comparable stages in this series as in the sequence formed by crystallization differentiation, provided that the composition of the starting material was reasonably close to the crustal average and provided that equilibrium was maintained during the melting. If marked departures from equilibrium occur, during either the fractional crystallization of a mafic magma or the progressive melting of average silicate material, the distribution of minor elements might be considerably different in corresponding parts of the two series. But ordinarily a close enough approach to equilibrium can be assumed so that the rare elements would be expected to distribute themselves according to uniform rules.

Thus the point of view that most igneous rocks have formed by crystallization differentiation, a point of view that underlies much of the following argument, is presented not as a hypothesis to be proved but as a framework to unify the discussion. When we speak of "early-formed minerals," for example, we shall mean minerals that *would* form early during differentiation, but that might equally well form late during metamorphism and anatexis.

Rules of Distribution

The general sequence of minerals that separate during differentiation of a silicate melt at low pressures is already familiar (Chap. 17). Most commonly olivine and calcic plagioclase crystallize first; as the temperature falls, part or all of the olivine reacts with the melt to form pyroxene, which is followed by amphibole and then biotite; the composition of plagioclase meanwhile becomes increasingly sodic; near the end of the crystallization, quartz and potash feldspar appear along with sodic plagioclase. If oxygen fugacity is low this scheme is altered, in that abundant iron remains longer in the melt; this means that ferrous silicates continue to crystallize until a late stage and that the accumulation of silica in the residual fluid is less pronounced. Many other variations are possible: an abundance of water in the melt would emphasize formation of hydrous minerals, abundant chlorine or fluorine or boron would lead to unusual minerals containing these elements, and at higher pressures the dominant early-crystallizing minerals would be garnet and soda-rich pyroxene rather than olivine and plagioclase. But for present purposes we restrict the discussion to the more usual pattern of differentiation, in which major elements drop out in a fairly uniform sequence: most of the magnesium and calcium leave the melt in early stages, and the alkali metals later; iron may be largely concentrated in early minerals or may appear at all stages; aluminum drops out in feldspars all during the differentiation process, and also in micas toward the end. Our objective now is to see how the behavior of the less common elements is related to these changes.

For an element to crystallize in a mineral of its own—a mineral in which it is a major constituent—requires that the element be present in the melt in appreciable amounts. If only a few ions of the element are present, they can be taken up by the crystal structures of the major silicates, either as isomorphous replacements of an abundant element or as random inclusions in the holes of a crystal lattice. *How much* of a given element can be accommodated in the silicate structures depends on the characteristics of its ions. The rare alkali metal rubidium, for example, is so similar to potassium that several tenths of a percent can be accommodated as replacements of Rb^+ for K^+ in micas and feldspars, and no separate rubidium mineral can form. The rare metal zirconium, on the other hand, cannot fit easily into common silicate structures, and even very small amounts of it go into separate crystals of the accessory mineral zircon. Some elements, like beryllium, boron, copper, and uranium, are capable neither of forming their own high-temperature minerals nor of substituting appreciably for common ions in silicate structures, and so are concentrated in the residual solutions that give rise to pegmatites and quartz-sulfide veins. What specific characteristics of an element determine which way it will behave?

The question takes us back to the discussion of isomorphism in Sec. 5-8. On the basis of that earlier treatment, a few rules can be formulated that are generally followed in the isomorphous replacement of one ion by another:

1. A minor element may substitute extensively for a major element if the ionic radii do not differ by more than about 15%.
2. Ions whose charges differ by one unit may substitute for one another, provided their radii are similar and provided the charge difference can be compensated by another substitution. For example, in plagioclase feldspar Na^+ readily substitutes

for Ca^{2+}, and the charge difference is compensated by substitution of Si^{4+} for Al^{3+}.

3. Of two ions that can occupy the same position in a crystal structure, the one that forms the stronger bonds with its neighbors is the one with the smaller radius, higher charge, or both.
4. Substitution of one ion for another may be very limited, even when the size criterion is fulfilled, if the bonds formed differ markedly in covalent character.

Leaving aside the question of bond character for the moment, we find abundant illustrations of the first three rules. We could predict, according to rules 1 and 2 and the table of ionic radii in Appendix VI, that Ba^{2+} would commonly substitute for K^+, Cr^{3+} for Fe^{3+}, Y^{3+} for Ca^{2+}; and these predictions fully accord with analytical data. From the third rule we could generalize that, in an isomorphous pair of compounds, the one containing ions of smaller radius and higher charge would have the higher melting point (because of the stronger bonding) and therefore would appear earlier in a crystallization sequence. Hence a minor element like Li, which substitutes extensively for Mg because of the similarity in their ionic radii, should be concentrated in late-forming Mg minerals rather than early ones because its single charge forms weaker bonds than the double charge on Mg^{2+}; this is borne out by the near absence of Li in olivine and its common presence as a substitute for Mg in the micas of pegmatites. Similarly Rb, having an ion similar in charge to K^+ but somewhat larger, should be enriched in late K minerals rather than early ones, a prediction that agrees with the observed concentration of Rb in the feldspars and micas of pegmatites.

The same rules, it should be noted, are illustrated beautifully by some of the major elements. In the isomorphous series of the olivines, forsterite has a higher melting point than fayalite and is enriched in early crystals (Prob. 17-3), corresponding with the fact that Mg^{2+} is a smaller ion than Fe^{2+}. Early crystals of plagioclase are Ca-rich, late crystals Na-rich (Sec. 17-3), in accordance with the higher charge of the Ca^{2+} ion. The rules are also similar to generalizations we have formulated regarding ion-exchange processes (Sec. 6-3), as they should be, because in both cases we are dealing with the relative strengths of bonds formed between ions and crystal structures.

The rules of substitution according to ionic radius work well as long as we limit discussion to elements in the first three columns of the periodic table, but with the remaining elements agreement between prediction and observation is often much less satisfactory. The ion Cu^+, for example, is similar in size and charge to Na^+, but copper shows no enrichment in sodium minerals. The ion Hg^{2+} closely resembles Ca^{2+} in size and charge, but is not concentrated in calcium minerals. The difficulty goes back to rule 4, the difference in bond character (or polarization): the ions Cu^+ and Hg^{2+} form bonds of markedly less ionic character with the anions of a crystal structure than do Na^+ and Ca^{2+} (last column of Appendix VI). This failure of the rules of substitution is reminiscent of the failure of predictions from simple geometry to account for crystal structures when strongly covalent bonds are involved (Sec. 5-4).

9

Examples of Minor-Element Distribution

To get a feeling for the effectiveness of the distribution rules in predicting the behavior of minor elements in igneous processes, we look now at some analytical data for typical rock sequences.

Table 20-3 shows average concentrations of major and minor elements in four rock series. The first series consists of worldwide averages for the major igneous rock types, and the other three give analyses for rocks in specific localities. The world-wide averages, of course, do not represent a sequence necessarily related by a differentiation process, but they are pertinent because trace elements would distribute themselves in much the same manner whether rocks form by differentiation or by anatexis during metamorphism. For each of the other three series there is good geological and chemical evidence that the rocks are actually members of a differentiation sequence. The Irish lavas show a fairly typical trend from olivine basalt to rhyolite, with a marked increase in silica and alkali metals and a decrease in iron; the Skaergaard rocks show a notable increase in iron and fairly constant silica until the very end of the differentiation process; the Hawaiian lavas are rich in soda and potash and show only a modest increase in silica. Thus the four sets of analyses enable us to compare the distribution of trace elements in three different kinds of differentiation sequences with the average distribution for igneous rocks in general.

Cursory examination of the data shows that the distribution has a certain amount of regularity, but also much apparently random variation. As so often happens in geochemistry, the numbers seem to follow a vague general rule that is subject to many exceptions. A little reflection will show that this is what we might expect. We are dealing, of course, with a very complicated process. The distribution is affected not only by the various trends of differentiation, but also by details of the way the trace elements enter into individual minerals. Other variables than ionic radius can affect the extent of substitution of one element by another, for example pressure, temperature, and overall rock composition. Furthermore, the steps in differentiation do not necessarily correspond from one set of analyses to another, nor do the extremes necessarily represent equivalent stages in differentiation; we have, in fact, no good way of even defining what we mean by "equivalent stages of differentiation." Recognizing these reasons for lack of complete regularity in the data, we can nevertheless draw useful conclusions from the analyses about general patterns of trace-element behavior.

Trends shown in the table can be visualized with the diagrams in Fig. 20-1. Lines on the figure represent analyses for various elements in the four categories of the world averages: ultramafic rocks, mafic rocks, intermediate rocks, and felsic rocks. These four rock types are shown, from left to right, by four points on each line. The heavy lines represent major elements (K, Ca, Al, Fe, Mg), and the light lines in each column represent possibly related minor elements. Scales are not uniform, so that absolute values cannot be compared from diagram to diagram. The lines simply show trends, the relative increases or decreases of different elements in going from ultramafic to felsic rocks.

TABLE 20-3

Average content of major and minor elements in four rock series[1]

		World averages				Tertiary lavas of NE Ireland				Skaergaard intrusive rocks				Hawaiian lavas				
	Ionic radii (Å)	Ultramafic rocks	Mafic rocks	Intermediate rocks	Felsic rocks	Olivine basalt	Tholeite basalt	Quartz trachyte	Rhyolite	Gabbro-picrite	Hyp-olivine gabbro	Ferrogabbro	Granophyre	Picrite-basalt	Basalt	Andesine andesite	Oligoclase andesite	Trachyte
Si^{4+}	0.26	19.0	24.0	26.0	32.3	21.1	24.3	30.0	35.2	19.3	21.6	20.3	31.2	22.3	24.0	23.7	24.4	29.0
Al^{3+}	0.54	0.5	8.8	8.9	7.7	7.8	7.5	7.5	6.5	4.6	8.9	7.7	6.7	4.9	6.8	8.7	8.8	9.9
Fe^{3+}	0.64	9.9	8.6	5.9	2.7	1.9	1.8	3.2	0.6	1.9	1.1	2.3	2.6	1.0	1.2	4.1	2.2	3.0
Fe^{2+}	0.78					6.7	6.5	2.2	0.3	8.2	8.1	17.1	3.9	8.1	7.3	4.8	5.7	0.1
Mg^{2+}	0.72	25.9	4.5	2.2	0.6	6.8	3.5	0.5	0.1	16.3	5.8	1.5	0.3	11.4	4.6	2.6	1.9	0.2
Ca^{2+}	1.00	0.7	6.7	4.7	1.6	7.1	7.1	1.5	0.6	4.7	8.1	6.5	2.0	5.5	7.5	4.6	4.5	0.6
Na^{+}	1.02	0.6	1.9	3.0	2.8	1.5	1.9	3.1	2.0	0.5	1.8	2.1	3.0	1.2	1.5	3.5	4.1	5.1
K^{+}	1.38	0.03	0.8	2.3	3.3	0.2	0.9	3.5	3.8	0.1	0.2	0.3	2.6	0.3	0.3	1.8	1.8	4.1
P^{5+}	0.17	170	1,400	1,600	700	970	1,260	535	90	90	260	5,000	1,500	1,000	1,140	740	4,060	1,050
Ga^{3+}	0.62	2	18	20	20	33	35	40	43	8	19	20	33	18	23	20	23	25
Cr^{3+}	0.62	2,000	200	50	25	1,600	150	50	<1	1,500	230	<1	11	1,750	470	<1	<1	20
Li^{+}	0.76	<1	15	20	40	8	18	65	80	2	2	3	20	1	2	15	20	30
Ni^{2+}	0.69	2,000	160	55	8	900	50	65	13	1,000	120	<2	9	950	85	7	13	15
Co^{2+}	0.75	200	45	10	5	140	110	8	2	90	48	20	5	75	35	14	6	2
V^{3+}	0.64	40	200	100	40	630	750	55	2	120	220	4	9	250	280	70	19	<5
Ti^{3+} [2]	0.67	300	9,000	8,000	2,300	7,000	6,700	3,200	700	9,000	5,000	15,000	5,000	12,000	20,000	16,000	15,000	2,000
Zr^{4+}	0.72	30	100	260	180	180	700	3,000	2,000	30	33	20	1,200	75	100	350	1,250	1,500
Mn^{2+}	0.83	1,500	2,000	1,200	600	1,380	1,360	1,200	130	1,200	700	3,300	800	860	1,010	1,710	1,010	1,170
Sc^{3+}	0.75	5	24	3	3	19	25	25	<10	<10	20	10	<10	<10	10	<10	<10	<10
Cu^{+} [2]	0.77	20	100	35	20	400	180	50	66	100	67	400	200	150	170	<10	<10	<10
Sr^{2+}	1.18	10	440	800	300	680	1,250	650	170	100	600	400	450	300	800	2,500	3,500	100
Pb^{2+}	1.19	<1	8	15	20	<20	25	43	43		No data					No data		
Ba^{2+}	1.35	1	300	650	830	310	1,350	2,000	2,300	10	18	60	1,100	110	120	600	1,000	800
Rb^{+}	1.52	2	45	100	200	3	90	1,000	930	<20	<20	<20	110	<20	<20	35	55	300

[1] Major elements in weight percent (of the elements, not the oxides), minor elments in parts per million.

[2] The elements Ti and Cu may also be present in part as other ions, Ti^{4+} (radius 0.61 Å) and Cu^{2+} (radius 0.73 Å).

Sources:

Ionic radii, Appendix VI.
World averages, Vinogradov (1962).
Irish lavas, Patterson (1952).
Skaergaard rocks, Wager and Mitchell (1951).
Hawaiian lavas, Wager and Mitchell (1953).

10

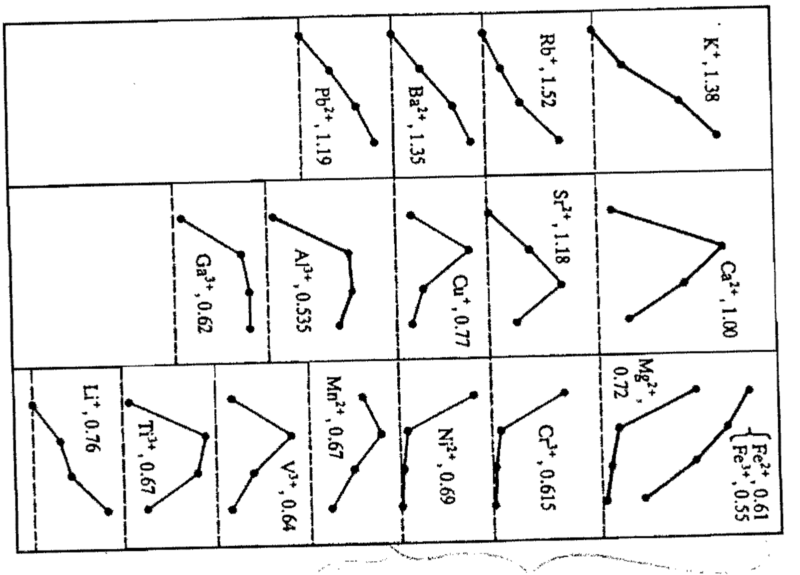

nadomeščajo Al

nadom. Fe

FIGURE 20-1
Trends of minor-element concentration in a differentiation sequence. Data from columns headed "world averages" in Table 20-3. The four points in each line represent concentrations in (from left to right) ultramafic rocks, mafic rocks, intermediate rocks, and felsic rocks. Scales are not uniform; lines show trends only. Heavy lines are trends for major elements, light lines for minor elements. Numbers beside symbols are ionic radii in angstroms.

The first column of Fig. 20-1 gives trends for three large cations that might be expected to substitute for K^{+} because of their size. The similarity in their lines is evident, suggesting that Rb^{+}, Ba^{2+}, and Pb^{2+} do indeed enter potassium minerals in small amounts and hence, like potassium, are concentrated in rocks formed late in the crystallization sequence. The similarity in trend is most marked for Rb^{+}; because of their double charge and smaller size, Ba^{2+} and Pb^{2+} tend to enter early potassium minerals, hence are not as strongly enriched at the felsic end of the series as is Rb^{+}. For these elements the rules of substitution work beautifully.

The second column shows the trend for calcium and the related minor element strontium. Here agreement with the rules is less clear. The ion Sr^{2+}, with a radius between those of Ca^{2+} and K^{+}, can substitute for both, so that its trend is a compromise between the trends for the two major elements. Except for its low abundance in ultramafic rocks, strontium remains fairly constant through the differentiation sequence, because calcium decreases as potassium increases. Copper, with an ionic radius close to that of calcium, has a somewhat similar trend line, but the similarity is probably fortuitous because a chalcophile element like copper forms dominantly covalent bonds with oxygen and cannot readily substitute for an element whose bonds are strongly ionic. Also in the second column are curves for aluminum and gallium, illustrating the great similarity of these two elements and the consequent extensive substitution of Ga^{3+} for Al^{3+} in aluminosilicate minerals.

In the third column of Fig. 20-1 are trend lines for several minor elements with ionic radii similar to those of iron and magnesium. The two major elements show a markedly decreasing abundance as differentiation proceeds, and most of the minor-element trend lines follow this pattern except that some have low concentrations at the ultramafic end of the series. Trends for Cr^{3+} and Ni^{2+} mimic that of Mg^{2+}, as would be expected from the extensive substitution of these metals in early formed Mg minerals (pyroxenes and olivines). Mn^{2+}, V^{3+}, and Ti^{3+} substitute more readily for Fe, and their trend lines are correspondingly similar except at the left-hand ends. Li^{+}, with its single positive charge, substitutes readily for Mg^{2+} only in the latest-formed magnesium minerals (especially micas), hence increases in abundance during the course of differentiation.

Analyses for the three differentiation series in Table 20-3 (northern Ireland, Skaergaard, and Hawaii) show trends similar to those for the world averages. There are a few conspicuous deviations, as might be expected because the rock series have different overall compositions and different degrees of differentiation, but nevertheless the trends displayed in Fig. 20-1 apparently represent a general pattern widely applicable to igneous rocks.

Regularities of Distribution in Igneous Rocks

Important features of this general pattern, as revealed by many analyses of rock series like those in Table 20-3, are the following:

1. Cations with large radii and low electric charges tend to substitute for potassium (radius of K^{+} = 1.38 Å), hence are concentrated in felsic rather than mafic rocks. These elements (Rb, Cs, Ba, Pb, Tl) are often called the *large-ion lithopile* group (LIL). Their abundance in a rock series is a good indication of the extent to which differentiation has sorted out constituents of the original igneous material. The rare-earth elements are often included here, although the substitution of their ions in late-forming minerals is mostly for Ca^{2+} rather than K^{+}.
2. Several cations with smaller radii and mostly with higher charges (U^{4+}, Th^{4+}, B^{3+}, Be^{2+}, Mo^{6+}, W^{6+}, Nb^{5+}, Ta^{5+}, Sn^{4+}, Zr^{4+}) also are concentrated at the felsic end of the series, not because of extensive substitution, but rather because their size and charge make their substitution for any major ions in common silicate minerals difficult. Differentiation segregates them into the late residual solutions, and if present in appreciable amounts they may form minerals of their own (uraninite, beryl, columbite, zircon, etc.). Because of the small size and high charge, the electric field associated with these ions is unusually strong, and they are often designated *high field-strength elements* (HFSE). Both LIL and HFSE elements, because their ions do not fit readily into the usual positions available in silicate structures, are described as *incompatible* elements.

3. Many elements whose ions have intermediate radii, especially metals of the transition groups, substitute readily for iron and magnesium, hence are abundant in the earlier members of the differentiation sequence. Some (Cr, Ni, Co) are strongly enriched with Mg in ultramafic rocks, others (Mn, V, Ti) have maximum abundance in gabbros and basalts.
4. Among the chalcophile elements, a few substitute to some extent for major cations in silicate structures (Pb^{2+} and Tl^{+} for K^{+}, Zn^{2+} for Fe^{2+} and Mg^{2+}, Bi^{3+} for Ca^{2+}), but for the most part these metals are left to accumulate in the residual solutions that may eventually form sulfide ores. In a magma containing abundant sulfur, part of the chalcophile elements may separate early in differentiation as an immiscible sulfide liquid. The traces of chalcophile metals commonly reported in ordinary igneous rocks may be present largely as tiny sulfide grains rather than as substitutes for major elements. This would explain, for example, the apparently erratic values for copper in the analyses of Table 20-3.
5. Some minor elements are so similar in size and chemical properties to major elements that normal differentiation cannot separate them effectively from their major relatives. Gallium is a good example: it is always present in aluminum minerals, and very seldom becomes sufficiently segregated to appear in a mineral of its own. Other closely related pairs are Rb and K, Hf and Zr, Cd and Zn. The rare members of these pairs are not particularly scarce metals, but they are little known because minerals in which they appear as major constituents are rare or nonexistent.

Thus the principal features of minor-element distribution in igneous rocks can be explained by the simple rules of substitution based on ionic charge and radius, supplemented by empirical statements about the behavior of elements whose bonds are largely covalent. The simple rules, however, have many exceptions, and details of the distribution would require more sophisticated analysis. We have spoken of the distribution, for example, as if it were influenced only by mineral structures in the crystallizing solids; a complete description would have to consider also structures in the silicate liquid with which the solids are in contact. Again, the transition elements show many apparent anomalies in the relative amounts that substitute for Mg^{2+} and the two ions of iron; the anomalies can be in large part clarified by considering effects on the strengths of directed bonds exerted by electric fields in different positions in crystal structures ("crystal-field effects"). Detailed study shows that relationships between major and minor elements in crystal structures are highly complex, so it seems remarkable that the simple rules work as well as they do.

One way to represent the distribution of minor elements is to set up a ratio of concentration in a mineral to concentration in the melt. This ratio, called the *partition coefficient*, is defined as

$$k_{\mathrm{Me}} = \frac{[\mathrm{Me}]_{\mathrm{mineral}}}{[\mathrm{Me}]_{\mathrm{melt}}}, \tag{20-3}$$

where the brackets are some measure of the concentration of a minor element represented by the symbol Me. As an example, elements that are largely incompatible with major elements of silicate minerals have values of k_{Me} much less than one. Analysis of measured concentrations of minor elements in minerals and matrix glasses of extrusive igneous rocks and from laboratory experiments shows that the partition coefficients for many minor elements are dependent on changes in temperature, pressure, and composition, as would be expected on thermodynamic grounds. In most cases these general trends can be predicted using the rules of distribution outlined above.

As an example of the temperature–pressure–composition relationships of partition coefficients, consider the partitioning of Ni between a melt and the mineral enstatite in the system NiO–MgO–SiO_2. At equilibrium we have

$$\underset{\mathrm{melt}}{\mathrm{Ni}^{2+}} + \underset{\mathrm{enstatite}}{\mathrm{MgSiO_3}} \rightleftharpoons \underset{\mathrm{melt}}{\mathrm{Mg}^{2+}} + \underset{\mathrm{Ni\text{-}enstatite}}{\mathrm{NiSiO_3}}, \tag{20-4}$$

and an equilibrium constant of

$$K = \frac{a_{\mathrm{Ni\text{-}enstatite}}\, a_{\mathrm{Mg\text{-}melt}}}{a_{\mathrm{Ni\text{-}melt}}\, a_{\mathrm{Mg\text{-}enstatite}}}. \tag{20-5}$$

If activities are expressed in terms of concentration (represented by brackets) and activity coefficients (λ),

$$K = \frac{[\mathrm{Ni}]_{\mathrm{enstatite}}}{[\mathrm{Ni}]_{\mathrm{melt}}} \frac{[\mathrm{Mg}]_{\mathrm{melt}}}{[\mathrm{Mg}]_{\mathrm{enstatite}}} \left(\frac{\lambda_{\mathrm{Ni\text{-}enstatite}} \lambda_{\mathrm{Mg\text{-}melt}}}{\lambda_{\mathrm{Ni\text{-}melt}} \lambda_{\mathrm{Mg\text{-}enstatite}}} \right). \tag{20-6}$$

The first ratio on the right-hand side is the partition coefficient for Ni [Eq. (20-3)]. Its temperature and pressure dependence will be determined, in part, by changes in the equilibrium constant which are governed by the enthalpy and volume of reaction (Sec. 8-5). How the partition coefficient will depend on composition is determined by the activity coefficients: for the melt, activity coefficients reflect melt structure and interaction among Ni and Mg with other melt components, and for enstatite, the coefficients are related to energetics of incorporating Ni and Mg into the mineral structure. All these properties, of course, are functions of temperature and pressure.

Rare-Earth Elements

The distribution of minor elements, as is evident from the simple rules of substitution, leads readily to speculation about the genesis and history of particular igneous rocks and rock associations. The rare-earth elements (REE, Table 5-3) provide a good example, and merit a brief digression.

Despite their name, the REE (Table 20-4) are not especially uncommon in Earth materials. The group as a whole makes up more than 200 ppm of average crust, and some of the individual elements are more abundant than such common metals as lead and copper. From the numbers in Appendix IV it is evident that all of this group, with the single exception of europium, are more concentrated in granite than in basalt, and that the differences are greater for the light elements (La–Sm) than for the heavier ones (Eu–Lu). These simple facts about abundances tell us that the REE are to some extent incompatible with the common ions of igneous magmas, the light ones (LREE) more incompatible than the heavy ones (HREE), and that Eu is something of a maverick.

TABLE 20-4
Rare-earth (lanthanide) elements

	Ions	Radii (Å) (6-coord)
Lanthanum	La^{3+}	1.03
Cerium	Ce^{3+}	1.01
Praseodymium	Pr^{3+}	0.99
Neodymium	Nd^{3+}	0.98
(Promethium)[1]	Pm^{3+}	0.97
Samarium	Sm^{3+}	0.96
Europium	Eu^{3+}	0.95
	Eu^{2+}	1.17
Gadolinium	Gd^{3+}	0.94
Terbium	Tb^{3+}	0.92
Dysprosium	Dy^{3+}	0.91
Holmium	Ho^{3+}	0.90
Erbium	Er^{3+}	0.89
Thulium	Tm^{3+}	0.88
Ytterbium	Yb^{3+}	0.87
Lutetium	Lu^{3+}	0.86

[1] Promethium does not occur in nature, but radioactive isotopes may be prepared artificially.
LREE: La–Sm HREE: Eu–Lu
Source: Shannon (1976).

Elements of this group are remarkable for the similarity in their chemical and physical properties, a similarity which means that they commonly occur together in natural environments and are difficult to separate in the laboratory. The whole assemblage occupies a single spot in Mendeleev's table (Table 5-3), in the third column and sixth period, from which we know immediately that these elements are active metals with a principal oxidation number of +3. The similar properties find a ready explanation in the electron structure of their atoms: all have three valence electrons, and each one differs from the preceding only in the addition of an electron in an f-orbital far down in the electron cloud. As might be expected, the increasing nuclear charge from one element to the next means a steadily decreasing ionic radius through the group (often called the "lanthanide contraction"). The slight decrease in size means slight differences in properties, which are reflected in differences in the distribution of these elements in geologic materials.

The high oxidation number and the large ionic radii (0.86–1.01 Å) mean that the entire group is incompatible in the common minerals of igneous rocks, as we have just guessed from the concentration differences between granite and basalt. The degree of incompatibility varies from mineral to mineral and from one element to another. Certainly the REE would not substitute readily for the smaller Fe^{2+} and Mg^{2+} ions (radii of 0.78 and 0.72 Å, respectively) in the early-crystallizing olivine and orthopyroxene of a mafic melt. Calcium ion is more similar in size (1.00 Å), and some rare-earth concentration is found in calcium materials, but the difference in oxidation number apparently keeps the substitution limited. So the REE by and large remain in the liquid during fractional crystallization, substituting to some extent for LIL elements in the later stages, and at the end may be concentrated enough to form their own minerals (for example, monazite, xenotime, allanite) in alkali granites and pegmatites.

Europium differs from its brethren in that it has an additional stable oxidation number of +2 (ionic radius 1.17 Å), and the relative amounts of Eu^{2+} and Eu^{3+} in a magma depend on its oxidation state. The divalent ion, as might be expected, substitutes readily for Ca^{2+} and even more readily for Sr^{2+} (1.18 Å), so that when plagioclase crystallizes from a mafic magma it often removes a good deal of europium from the liquid. (One other lanthanide, cerium, has an abnormal oxidation number, +4, when conditions are very oxidizing. This peculiarity has little importance in igneous processes, but explains much of cerium's behavior in surface waters and sediments.)

The slight differences in ionic size make the LREE somewhat more incompatible than the HREE, as we noted from abundance figures. Thus in the last residual fluid during crystallization of a magma, or in the earliest melt to form during anatexis, the LREE elements may be more concentrated than their heavier kin. This difference in properties makes analyses of the REE a useful tool in studies of the source and history of the magmas that formed various kinds of igneous rock.

To display analyses showing the distribution of REE in geologic materials, it is common to plot abundances against atomic number. Rather than simple concentrations, however, it is customary to plot ratios—ratios of the amount of each element in a given rock or mineral to the amount in material supposedly representing undifferentiated stuff from which the rock or mineral was derived. In igneous geochemistry the undifferentiated material is commonly taken to be an average of analyses of chondritic meteorites, on the plausible assumption that the Earth and meteorites were formed originally out of the same protoplanetary mixture. A sampling of such plots, showing lanthanide concentrations "normalized" to chondritic concentrations, is shown in Fig. 20-2. In effect, the lines on this figure record for different kinds of igneous rock the changes in REE distribution over the long times since their materials were part of the Earth's primeval substance.

Earth material not greatly differentiated from the original meteoritic composition should plot near the horizontal line representing the ratio "1" in Fig. 20-2. Such material might be a chunk of peridotite carried up from the mantle as a xenolith in a lava flow (line A). Basalt from the midocean ridges, representing material formed by partial melting of the upper mantle, would be expected to show increased concentrations of all the rare-earth elements, without much separation of LREE and HREE (line B). Further differentiation, leading to marked preferential increases of the light rare earths, is shown by lines C (rhyolite) and D (granite). Line D is noteworthy also because it shows a pronounced negative europium anomaly, presumably meaning that separation of Ca-rich plagioclase has played a role in its history. The frequent strong concentration of europium in plagioclase is strikingly shown by an analysis of anorthosite (line E), a rock consisting almost entirely of this mineral. And finally, line F shows an average analysis of the rare-earth content of North American shales, rocks that represent material formed by repeated differentiation by both igneous and sedimentary processes over long geologic times. It should be noted that Fig. 20-2 shows only a few selected analyses, and that actually curves for any of the various rock types show a great deal of variation. But the general trends of rare-earth behavior during igneous rock formation are well displayed.

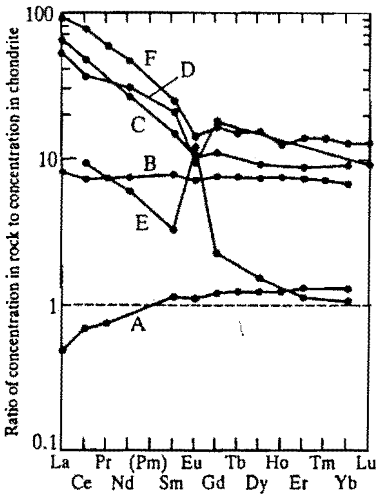

FIGURE 20-2
Chondrite-normalized rare-earth analyses for six rock samples. Each point is the ratio of the concentration of a rare-earth element to the concentration of the same element in an average chondrite meteorite. Rocks and sources: A: *Peridotite* xenolith from lava flow. Jagoutz, E.: *Proc. Lunar and Planetary Conference*, vol. 10, p. 2031, 1979. B: Mid-ocean ridge *basalt*. Langmuir, C. H., J. F. Bender, A. E. Bence, G. N. Hanson, and S. R. Taylor: *Earth and Planetary Science Letters*, vol. 36, p. 133, 1977. C: *Rhyolite*. Jahn, B. M., A. Y. Glikson, J. J. Peucat, and A. H. Hickman: *Geochim. et Cosmochim. Acta*, vol. 45, p. 1633, 1981. D: *Granite*. Shaw, S. E., and R. H. Flood: *Jour. Geophys. Research*, vol. 86, p. 10,530, 1981. E: *Anorthosite*. Simmons, E. C., and G. N. Hanson: *Contrib. Mineralogy and Petrology*, vol. 66, p. 119, 1978. F: North American *shales*. Haskin, L. A., M. A. Haskin, F. A. Frey, and T. R. Wildman, in Ahrens, L. A., ed.: *Origin and Distribution of the Elements*, Pergamon, Oxford, 1968, p. 899.

This sampling of conclusions that can be drawn from REE distributions is an illustration of the general rule that trace elements are often more sensitive indicators of an igneous rock's history than are its major elements. A rock with an unusual abundance of LIL elements (including LREE), for example, is almost surely the product of extreme differentiation—either the final residual liquid remaining after nearly complete crystallization of a magma, or the initial melt from heating a metamorphic rock, or perhaps the result of segregation of these elements in some previous episode of sedimentation or metamorphism. An igneous rock depleted in LIL elements presumably represents material left after the more easily melted fraction has been removed. Thus the concentrations of the rare-earth elements have proved particularly useful in working out details of igneous rock history.

21. Na diagramu Na_2O+K_2O/SiO_2 prikaži in razloži položaj naslednjih kamnin iz tabele 4-6: tholeiit, andezit, pantellerit, fonolit in nefelinit ter ga komentiraj.

22. Na AFM diagramu prikaži trenda razvoja tholeiitne in kalcijsko-alkalne magme (podatki v tabeli 4-6) ter ju razloži v skladu s slikami 8-9, 8-11 in 8-12.

23. Na diagramu (A/CNK)/SiO_2 prikaži položaj vzorca pohorskega granodiorita P104 (SiO_2 68%, Al_2O_3 16%, Fe_2O_3 3.25%, MgO 0.98%, CaO 3.3%, Na_2O 3.85%, K_2O 2.76%, TiO_2 0.28%). Ugotovi ali je a.) meta- ali peraluminijski in b.) ali pripada I ali S-tipu granita ter rezultat komentiraj.

24. Na trikotnem diagramu Ba-Rb-Sr prikaži položaj vzorca pohorskega granodiorita P101 (Ba 2375ppm, Rb 70ppm, Sr 900ppm) in komentiraj diferenciacijski trend.

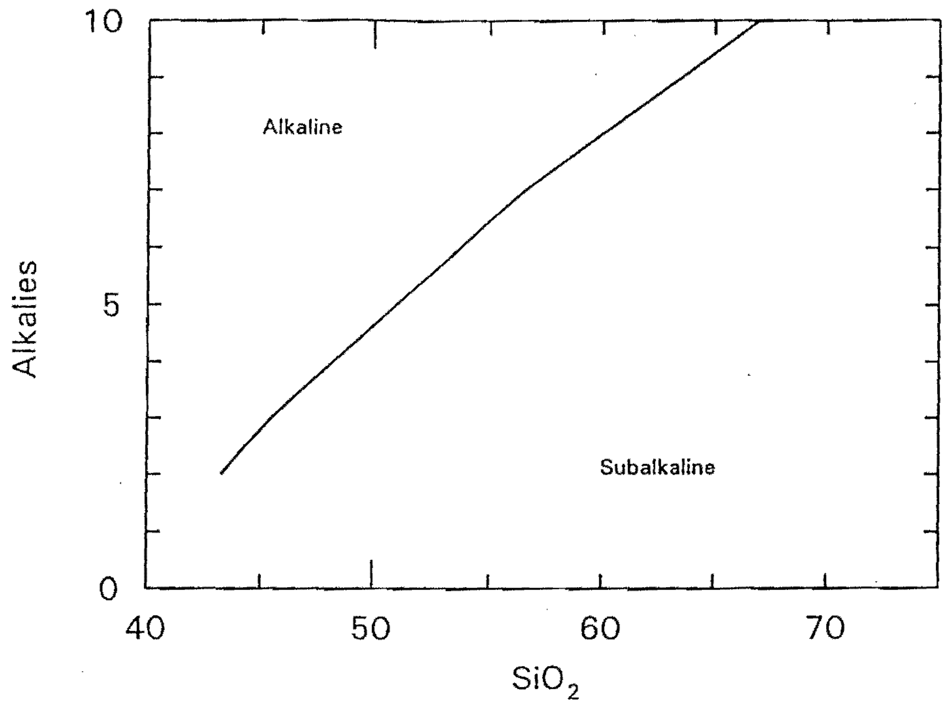
10
5
0
Alkalies
40
50
60
70
SiO$_2$
Alkaline
Subalkaline

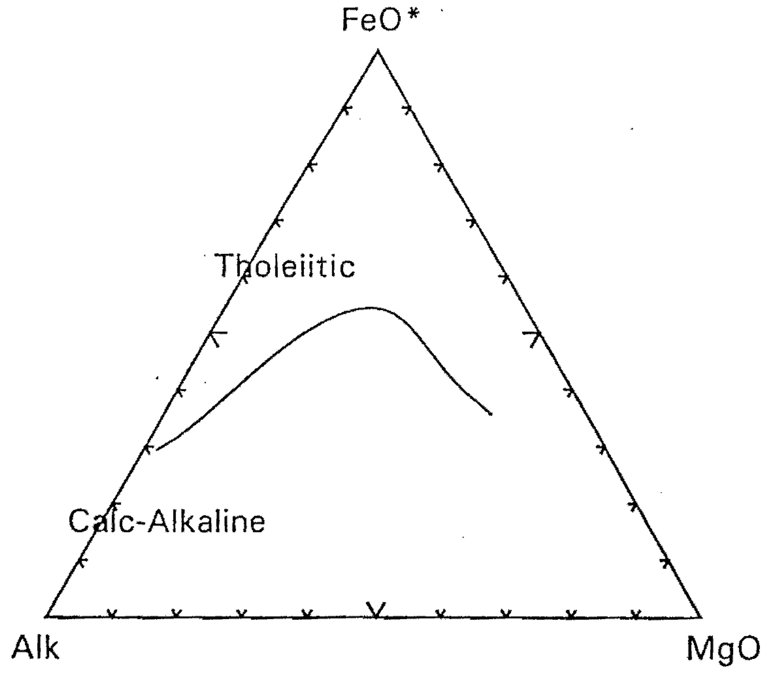
FeO*
Tholeiitic
Calc-Alkaline
Alk
MgO

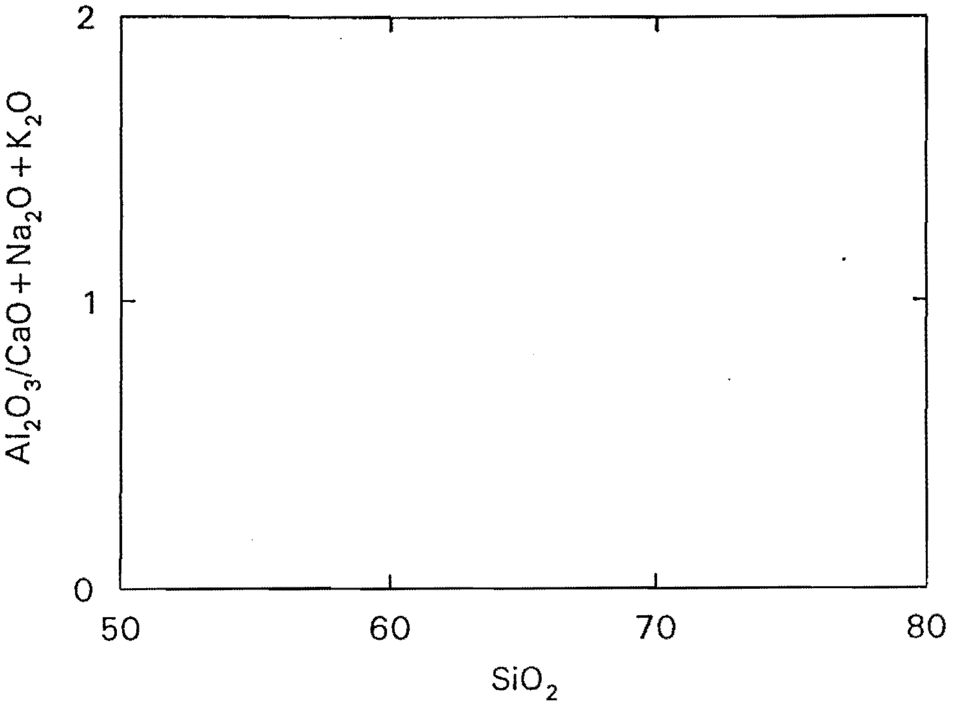
2
1
0
50
60
70
80
SiO$_2$
Al$_2$O$_3$/CaO+Na$_2$O+K$_2$O

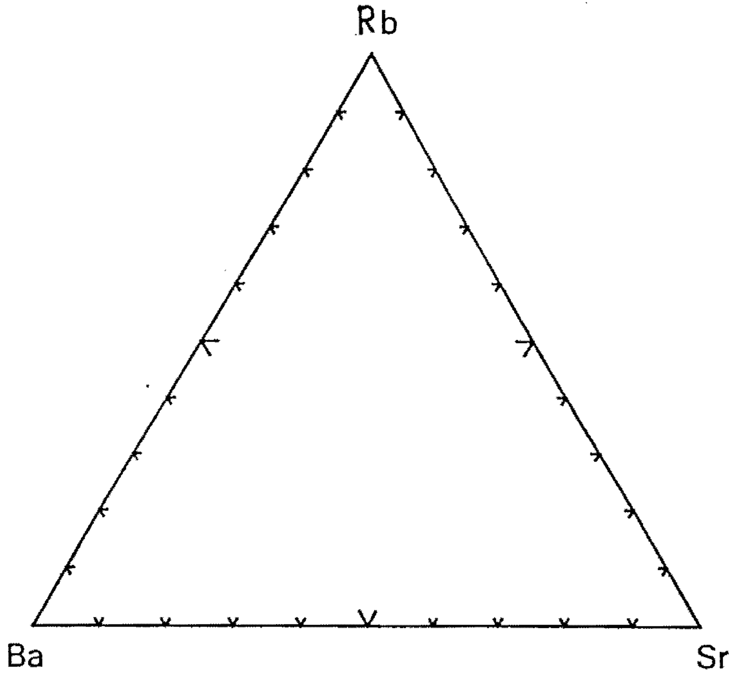
Rb
Ba
Sr

Philpotts, A. R., 1989: Petrography of Igneous and Metamorphic Rocks

17

The Irvine - Baragar Classification of Volcanic Rocks

In recent years the classification of volcanic rocks proposed by Irvine and Baragar (1971) has gained wide acceptance. It sets up divisions between different rock types based solely on common usage; that is, in practice most geologists associate a particular rock name with a certain compositional range. The scheme also incorporates the well-established fact that volcanic rocks fall into a number of distinct genetic series, which can be distinguished by simple chemical parameters. These series have the added significance that they can be correlated with distinct tectonic environments.

Volcanic rocks are classified by Irvine and Baragar into three main groups (Fig. 4-5), the *subalkaline*, the *alkaline*, and the *peralkaline* (alkali-rich). Most rocks belong to the first two groups, which are each subdivided into two subgroups. Assigning a rock to any one of these groups is based on simple chemical parameters or normative compositions. Before this is done, however, the chemical effects of alteration must be taken into account, if possible. Many volcanic rocks become oxidized, hydrated, or carbonated by hydrothermal activity during burial or during later metamorphism. These chemical changes can seriously affect the normative composition of a rock, which may, in turn, affect its classification. For example, conversion of ferrous iron to ferric during alteration results in smaller amounts of iron silicates being calculated in the norm; this then produces a norm that appears more saturated in silica than was the original rock. This type of alteration, however, can be corrected for, because in many unaltered volcanic rocks there is a strong positive correlation between the TiO_2 and Fe_2O_3 contents. The primary wt% Fe_2O_3 in many volcanic rocks is given approximately by (wt% TiO_2 + 1.5). H_2O and CO_2 are subtracted from the analysis and the total recalculated to 100%. Norm calculations are carried out according to the CIPW rules, but Irvine and Baragar chose to recalculate the normative minerals in terms of molecular rather than weight percentages. Thus, instead of multiplying the mole proportions by the weight factors given in Table 4-1, the mole proportions are simply recalculated to 100%. Finally, in expressing feldspar compositions, nepheline is recast as albite. Thus, the normative anorthite content is given by 100xAn/(An+Ab+5/3Ne). Analyses of typical samples of each of the main rock types in Irvine and Baragar's classification are given in Table 4-6.

Division into the three main groups is based on the alkali content of the rocks. Rocks in which the molecular amounts of (Na_2O + K_2O) > Al_2O_3 fall into the peralkaline group. These rocks typically contain aegerine or a sodic amphibole. The alkali content that separates the subalkaline from the alkaline groups varies with the silica content of the rock (Fig. 4-6). The equation for the boundary between these groups is given by

$$SiO_2 = -3.3539 \times 10^{-4} \times A^6 + 1.2030 \times 10^{-2} \times A^5 - 1.5188 \times 10^{-1} \times A^4 + 8.6096 \times 10^{-1} \times A^3 - 2.1111 \times A^2 + 3.9492 \times A + 39.0$$

where A = (Na_2O + K_2O). These two groups can also be distinguished in a plot of the normative contents of olivine - nepheline - quartz (Fig. 4-7). To plot a rock in this diagram the normative minerals are recast as follows: Ne' = Ne + 3/5 Ab, Q' = Q + 2/5 Ab + 1/4 Opx, Ol' = Ol + 3/4 Opx. The subalkaline rocks plot on the quartz side of the boundary line, whereas the alkaline ones plot on the nepheline side of it.

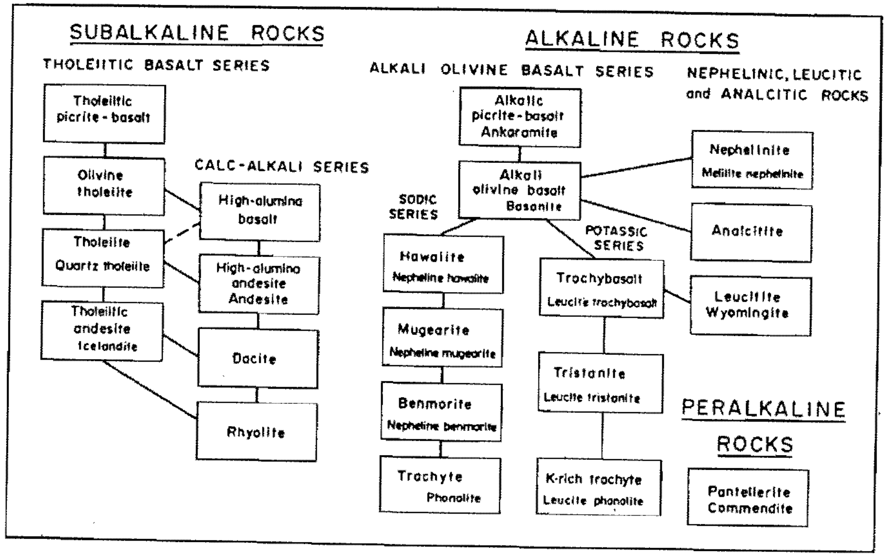

Figure 4-5 General classification scheme for the common volcanic rocks (after Irvine and Baragar, 1971). Lines joining boxes link commonly associated rocks. The small print within the boxes refers to variants of the main rock. (Published with permission of Canadian J. Earth Sci.)

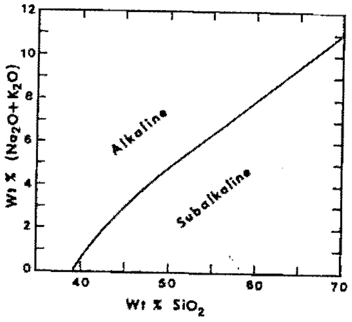

Figure 4-6 Alkalis-silica plot with line separating fields of alkaline and subalkaline rocks. (after Irvine and Baragar, 1971).

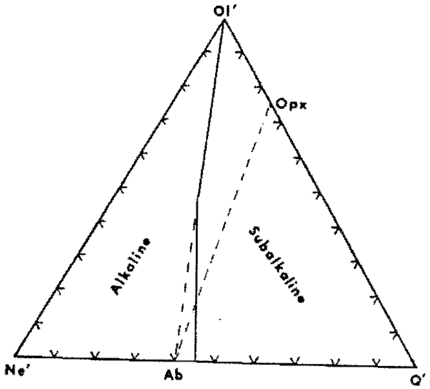

Figure 4-7 Ol'-Ne'-Q' projection with line separating fields of alkaline and subalkaline rocks. See text for explanation. Plot in % cation equivalents. (after Irvine and Baragar, 1971)

TABLE 4-6 Typical Analyses of the Rocks Listed in Fig. 4-5 (from Irvine and Baragar, 1971).

	SUBALKALINE ROCKS										PERALKALINE ROCKS	
	Tholeiitic basalt series					Calc-alkali series						
	Tholeiitic Picrite	Ol Tholeiite	Tholeiite	Tholeiitic Andesite	Icelandite	High Al Basalt	High Al Andesite	Andesite	Dacite	Rhyolite	Pantellerite	Commendite
SiO_2	46.4	49.2	53.8	58.3	61.8	49.1	58.6	60.0	69.7	73.2	69.8	75.2
TiO_2	2.0	2.3	2.0	1.7	1.3	1.5	0.8	1.0	0.4	0.1	0.4	0.1
Al_2O_3	8.5	13.3	13.9	13.8	15.4	17.7	17.4	16.0	15.2	14.0	7.4	12.0
Fe_2O_3	2.5	1.3	2.6	3.4	2.3	2.8	3.2	1.9	1.1	0.6	2.4	0.9
FeO	9.8	9.7	9.3	6.5	5.8	7.2	3.5	6.2	1.9	1.7	6.1	1.2
MnO	0.2	0.2	0.2	0.2	0.2	0.1	0.1	0.2	0.0	0.0	0.3	0.1
MgO	20.8	10.4	4.1	2.3	1.8	6.9	3.3	3.9	0.9	0.4	0.1	0.0
CaO	7.4	10.9	7.9	5.6	5.0	9.9	6.3	5.9	2.7	1.3	0.4	0.3
Na_2O	1.6	2.2	3.0	3.9	4.4	2.9	3.8	3.9	4.5	3.9	6.7	4.8
K_2O	0.3	0.5	1.5	1.9	1.6	0.7	2.0	0.9	3.0	4.1	4.3	4.7
P_2O_5	0.2	0.2	0.4	0.5	0.4	0.3	0.2	0.2	0.1	0.0	0.2	0.1

	ALKALINE ROCKS											ALKALINE ROCKS			
	Alkali olivine basalt series											Nephelinites etc.			
	Alkalic Picrite	Ankaramite	K-poor Alk basalt	K-rich Alk basalt	Trachybasalt	Hawaiite	Mugearite	Tristanite	Benmorite	Trachyte	Phonolite	Nephelinite	Analcitite	Leucitite	Wyomingite
SiO_2	46.6	44.1	45.4	42.4	46.5	47.9	49.7	55.8	55.6	60.7	60.6	39.7	49.0	46.2	54.1
TiO_2	1.8	2.7	3.0	4.1	3.1	3.4	2.1	1.8	0.9	0.5	0.0	2.8	0.7	1.2	2.3
Al_2O_3	8.2	12.1	14.7	14.1	16.7	15.9	17.0	19.0	16.4	20.5	18.3	11.4	13.0	14.4	9.9
Fe_2O_3	1.2	3.2	4.1	5.8	4.1	4.9	3.4	2.6	3.1	2.3	2.7	5.3	4.9	4.1	3.1
FeO	9.8	9.6	9.2	8.5	7.3	7.6	9.0	3.1	4.9	0.4	1.2	8.2	4.5	4.4	1.5
MnO	0.1	0.2	0.2	0.2	0.2	0.2	0.3	0.1	0.2	0.2	0.2	0.2	0.1	0.0	0.1
MgO	19.6	13.0	7.8	6.7	4.6	4.8	2.8	2.0	1.1	0.2	0.1	12.1	8.3	7.0	7.0
CaO	9.4	11.5	10.5	11.9	9.4	8.0	5.5	4.5	2.9	1.4	0.8	12.8	11.5	13.2	4.7
Na_2O	1.6	1.9	3.0	2.8	3.8	4.2	5.8	5.2	6.1	6.2	8.9	3.8	3.9	1.6	1.4
K_2O	1.2	0.7	1.0	2.0	3.1	1.5	1.9	4.1	3.5	6.7	5.1	1.2	3.0	6.4	11.4
P_2O_5	0.3	0.3	0.4	0.6	0.9	0.7	0.5	0.4	0.7	0.0	0.0	0.9	1.1	0.4	1.8

The subalkaline rocks are divided into the *calc-alkali* and *tholeiitic* series on the basis of their iron contents in the AFM plot (Fig. 4-8), where $A = Na_2O + K_2O$, $F = FeO + 0.8998xFe_2O_3$, and $M = MgO$ (all in wt%). This plot distinguishes intermediate members of these series very well, but at the mafic and felsic ends there is considerable overlap. Calc-alkali basalts and andesites, however, contain 16 to 20% Al_2O_3, which is considerably more than occurs in tholeiitic basalts and andesites which contain from 12 to 16%. At the extreme felsic end there is no satisfactory way of distinguishing calc-alkali and tholeiitic members; thus all granitic rocks are assigned to the calc-alkali series.

The alkaline rocks are divided into the *alkali olivine basalt* series and the *nephelinitic - leucitic - analcitic* series. Rocks of the latter series typically contain less than 45% SiO_2, have normative color indices greater than 50, and may contain normative leucite.

The naming of rocks within the various subgroups is based on normative plagioclase composition and on normative color index. In the various subalkaline series, the rocks range from *basalt* through *andesite* and *dacite* to *rhyolite* with decreasing normative anorthite content and decreasing normative color index (Fig. 4-9). Two series of rock names are used for the alkaline rocks, depending on whether they are sodic or potassic. This division is made on the basis of the normative feldspar composition (Fig. 4-10). With decreasing normative anorthite content, the sodic series passes from *alkali basalt* through *hawaiite*, *mugearite*, and *benmoreite* to *trachyte* (Fig. 4-11a), whereas the potassic series passes from *alkali basalt* through *trachybasalt* and *tristanite* to *trachyte* (Fig. 4-11b). At the mafic end of all of these series, basalts containing more than 25% normative olivine are named *picrites*; these rocks contain abundant phenocrystic olivine. *Ankaramites*, which belong to the alkaline group, contain abundant augite phenocrysts which cause the norm to have more than 20% clinopyroxene. Basalts containing more than 5% normative nepheline are named either *basanite* if they contain modal nepheline, or *basanitoid* if nepheline is not visible. Finally, nepheline-bearing trachyte is known as *phonolite*.

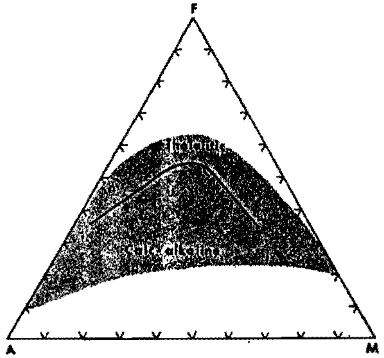

Figure 4-8 AFM plot showing line separating fields of tholeiitic and calc-alkaline rocks as proposed by Irvine and Baragar (1971).
$A = Na_2O+K_2O$; $F = FeO+0.8998Fe_2O_3$; $M = MgO$, all in weight percent.

Raymond, L.A., 1995: Petrology

Kuno (1959, 1966a, 1966b) recognized the importance of the relationship between Benioff-Wadati Zone and basalt chemistry. He related basalt chemistry to the *depth of generation* in the seismic zone (figure 7.17c). On the basis of major, trace, rare earth, and isotopic element data, plus phase equilibria, Brophy and Marsh (1986) and J. D. Myers (1988) supported Kuno's interpretation that high-alumina basalt liquids are primary magmas. In contrast, some theoretical, chemical, and experimental work on magma generation seems inconsistent with the depth-of-generation model (Gust and Perfit, 1987; Brophy, 1989b), making the model debatable.[89]

Models that attempt to account for major element and trace element differences within arc rocks and across volcanic arcs are generally complex (Ringwood, 1974; Kushiro, 1983; Myers, 1988). For example, Ringwood (1974), following Nicholls and Ringwood (1973), presented a model, here called the *pyrolite-pyroxenite model*, in which volcanism occurs in two phases (figure 7.17d). In this model, the physical-chemical history of the mantle rock, rather than simply the depth, controls rock chemistry. In the pyrolite-pyroxenite model, early, shallow, tholeiitic volcanism results from the following series of processes:

1. Dehydration of the subducting plate;
2. Partial melting of mantle pyrolite above the subduction zone;
3. Diapiric rise of pyrolite followed by separation and differentiation of tholeiitic magma in the upper mantle;
4. Eruption of tholeiites at the surface.

Later, deeper, calc-alkaline volcanism occurs after continued subduction converts oceanic crust to quartz eclogite, in the following sequence of events.

1. Dehydration of serpentine occurs in the subducting plate (to provide water).
2. Melting of quartz eclogite produces siliceous (e.g., rhyolitic) magmas.
3. Reaction of siliceous magmas with overlying mantle pyrolite produces garnet pyroxenite.
4. Diapiric rise of wet pyroxenite masses accompanies partial melting in the mantle to produce calc-alkaline magmas.
5. Eruption of calc-alkaline magmas occurs at the surface.

This complex model requires dehydration of the subducting slab and mixing of some subducted components (fluid and melt) with mantle rock that is later melted. The likelihood of dehydration is now widely accepted (Fyfe and McBirney, 1975; Delaney and Helgeson, 1978; Tatsumi, 1989),[90] and Pb and Be isotopes in arc rocks support the involvement of subducted materials in models of magma generation (J. D. Myers and Marsh, 1987; Morris and Tera, 1989). On the negative side, melting and assimilation experiments do not support the model (Stern and Wyllie, 1981; W. L. Huang and Wyllie, 1981; Sekine and Wyllie, 1983; Johnston and Wyllie, 1989). Still, the model is evolving. In an effort to explain the origin of source rocks for intraplate magmas, Ringwood (1982, 1985, 1990; Kesson and Ringwood, 1989) extended his model. The expanded version focuses on shearing at depths below 100 km along the subduction zone and hybridization of sheared, depleted mantle rocks by magmas derived from the subducting slab.

Clarke, D. B., 1992: Granitoid Rocks

to their conversation is, if anything, exceeded by their affection for the old. They are not about to drop granite. They say granodiorite when they are in church and granite the rest of the week.' In *this* book, the unmodified term 'granite' refers only to the QAP field in which plagioclase is 10–65% of total feldspar. 'Granitic' is an adjective meaning 'having the properties of a granite', but not necessarily referring only to granite *sensu stricto*. The term 'granitoid' will be used, as both an adjective and a noun, to refer generally to the whole family of granitic rocks from alkali feldspar granite to tonalite.

Although the classification system based on modal proportions of QAP is simple in theory, it is difficult in practice. Few alternatives to tedious slabbing, messy staining, and mindless point-counting exist. No wonder classifications based on chemical parameters developed.

1.2.2 Chemical classification (measured parameter)

We can make the transition from mineralogy to chemistry by using the mineralogical definitions above to set limits on the major element chemical compositions. Figure 1.3 translates the mineralogical limits of the granitoid family into chemical compositions, using a plagioclase composition of An_{50} and an alkali feldspar composition of $Kf_{90}Ab_{10}$. The derived upper and lower limits for SiO_2 are too high, partly because few granitoid rocks contain more than 45% quartz, and partly because relatively silica-poor ferromagnesian silicates are not included. With these provisos, the calculated compositions in Fig. 1.3 are approximately what we should expect for granitoid rocks. For comparison, Fig. 1.3 also shows the average composition of 363 North American granitoid rocks, and the estimated composition of the upper continental crust.

One simple way to avoid the slabbing, staining, and point-counting syndrome is to grind the rocks to powders and analyse them for their major elements. This chemical composition can then be reconstituted in terms of its mineralogy by calculating its mesonorm (Mielke and Winkler, 1979) or CIPW normative mineralogy. The amounts of normative quartz and feldspar can be plotted in QAP to determine the rock name. Streckeisen and Le Maitre (1979) and Debon and Le Fort (1982) have explored other relationships between the modal mineralogical and chemical systems of classification, but in igneous rocks it is rarely clear whether the mineralogy controls the chemistry of the rock, or whether the chemistry of the melt controls the mineralogy. (There is more about this philosophical problem in Chapter 4.)

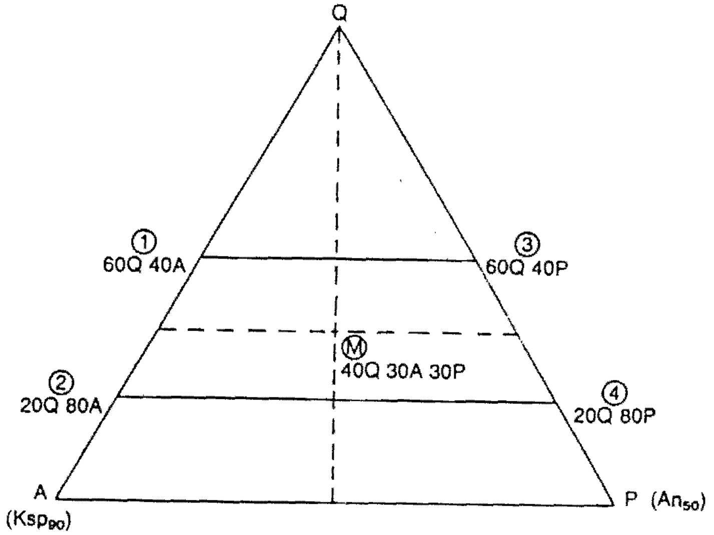

	1	2	3	4	M	MNAG*	U.CRUST**
SiO_2	72.1	86.0	83.9	67.9	77.4	69.7	66.0
TiO_2	–	–	–	–	–	0.4	0.5
Al_2O_3	14.7	7.4	10.2	20.3	13.2	14.7	15.2
FeO	–	–	–	–	–	3.2	4.5
MnO	–	–	–	–	–	0.1	0.1
MgO	–	–	–	–	–	1.2	2.2
CaO	–	–	2.8	5.6	2.1	2.7	4.2
Na_2O	1.00	0.5	3.1	6.2	2.7	3.7	3.9
K_2O	12.2	6.1	–	–	4.6	3.5	3.4
P_2O_5	–	–	–	–	–	0.2	0.1
Total	100.0	100.0	100.0	100.0	100.0	99.4	100.0
A/CNK***	1.00	1.00	1.00	1.00	1.00	1.02	0.86

* Mean of 363 North American granitoid rocks (Chayes, 1985)
** Estimated composition of the upper crust (Taylor and McLennan, 1985)
*** For explanation of A/CNK see Table 1.1

Fig. 1.3 The relationship between classifications based on modal mineralogy and chemical composition of granitoid rocks. The mineralogical definition of granitoids limits their range of chemical compositions.

However, there is much more to granitoid rocks than just quartz and feldspars. A detailed mineralogical description, including all the minor and accessory minerals, would be sufficient to erect a complete classification system for granitoid rocks. However, given the large number of possible phases, this system might become somewhat unwieldy. Instead, the close relationship between mineralogy and chemistry permits the establishment of a much simpler, tripartite chemical classification that covers all cases (Shand, 1947; Table 1.1). This system uses the concept of alumina-saturation in which the ratio A/CNK (molar $[Al_2O_3/(CaO + Na_2O + K_2O)]$) can range from greater than one to less than one in igneous rocks. For a haplogranite, i.e. with quartz and two feldspars only, A/CNK = 1, because A/CNK = 1 in all varieties of feldspar. With additional minerals, this ratio will move above or below unity, depending on the type of minerals present. For example, hornblende with A/CNK = 0.7 drags the A/CNK ratio of the granitoid below unity; almandine garnet with A/CNK = infinity lifts the ratio above unity; and riebeckite with A/CNK = 0 and C = 0 creates a condition in the whole rock where A < NK. In this system, granitoid rocks are peraluminous[2] (A/CNK > 1), metaluminous (A/CNK < 1), and peralkaline (A < NK). If only modal analyses are available, the characteristic minerals listed in Table 1.1 should permit categorization into chemical types. Figure 1.4a is a graphic portrayal of the concept of alumina-saturation, and Table 1.2 gives some average compositions for real metaluminous, peraluminous, and peralkaline granitoid rocks.

1.2.3 Chemical–tectonic–genetic classifications (measured to inferred parameters)

Just as a close connection exists between the mineralogical and major element chemical classifications of granitoid rocks, so there exist many attempts to link major and even trace element chemical characteristics directly to tectonic and/or genetic significance. (For a thorough review of the relationship between granitoid type, tectonic setting, and presumed source rocks, see Barbarin, 1990). Of necessity there is some blurring between measured parameters (e.g. chemical compositions and observed field relations, especially with respect to the tectonic setting) and interpreted parameters (e.g.

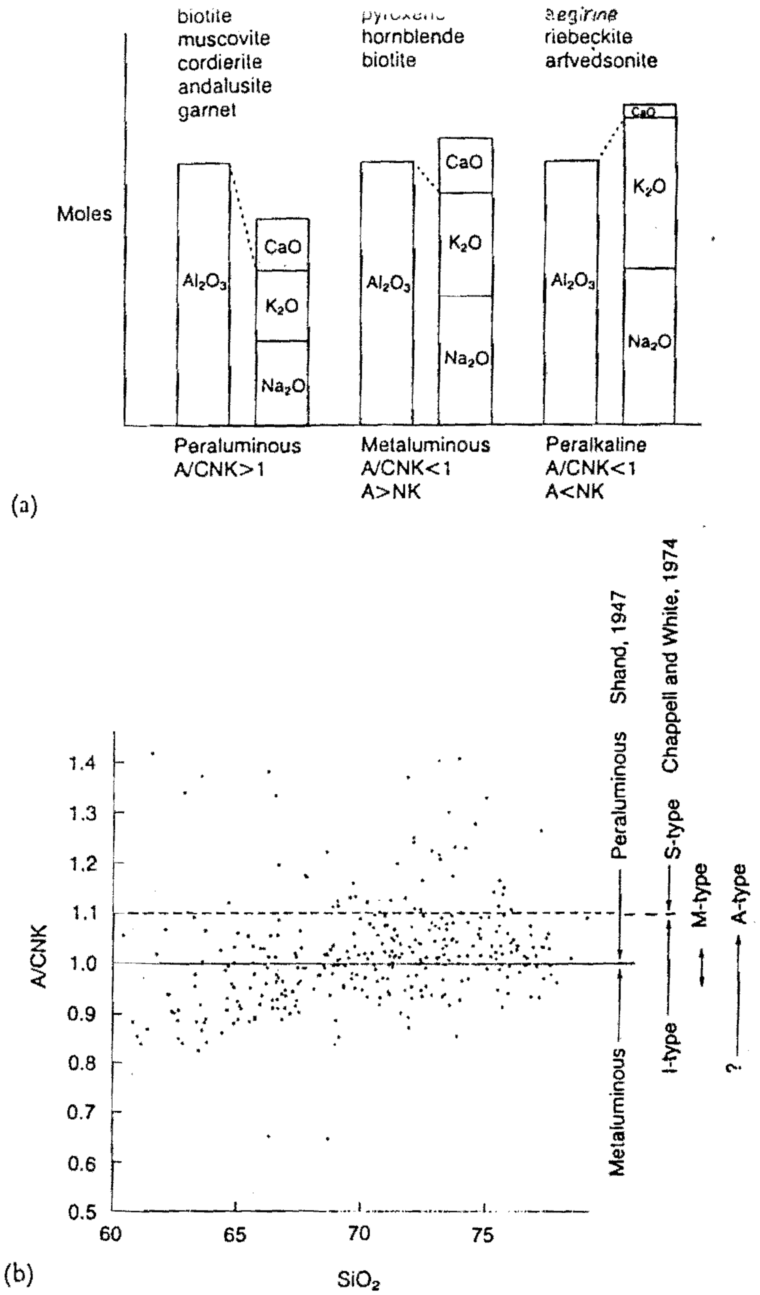

Fig. 1.4 Relationships between classifications: (a) mineralogical and a schematic representation of chemical composition (the alumina-saturation of Shand, 1947); and (b) chemical composition and presumed origin (I–S scheme of Chappell and White, 1974). The data points are the 363 North American granitoids from Chayes (1985).

---

[2] Clarke (1981) suggested that the term 'peraluminous' be used for those rocks in which the excess alumina could be attributed to crystal-melt equilibria, and 'hyperaluminous' for rocks in which generally higher values of excess alumina were acquired through the action of aqueous fluid phases.

Table 1.1 Tripartite chemical classification of granitic rocks

		*The granitoid family**	
		QAP *60% > Quartz > 20%* *Alkali-feldspar/(Alkali-feldspar + Plagioclase) = 0–1*	
	Peraluminous	*Metaluminous*	*Peralkaline*
Definition (Shand, 1947)	A > CNK**	CNK > A >NK**	A < NK**
Characteristic minerals (*Chapter 3*)	aluminosilicates, cordierite, garnet, topaz, tourmaline, spinel, corundum	orthopyroxene, clinopyroxene, cummingtonite, hornblende, epidote	fayalitic olivine, aegirine, arfvedsonite, riebeckite
Other common minerals	biotite, muscovite	biotite, minor muscovite	minor biotite
Oxide minerals	ilmenite, tapiolite	magnetite	magnetite
Accessory minerals	apatite, zircon, monazite	apatite, zircon, titanite, allanite	apatite, zircon, titanite, allanite, fluorite, cryolite, pyrochlore
Other chemical features	F/Cl > 3	–	low CaO, Al_2O_3, H_2O, Ba, Sr, Eu high SiO_2, Fe/Mg, Na + K, Zr, Nb, Ta, ΣREEs, Y F/Cl < 3
Isotopic compositions			
$^{87}Sr/^{86}Sr_i$	0.7050–0.7200	0.7030–0.7080	0.7030–0.7120
εNd_i (*Chapter 4*)	generally ≪ 0	≈ 0	highly variable
Typical mineral Deposits (*Chapter 7*)	aplite–pegmatite–greisen; polymetallic Sn–W–U–Mo–Cu and Be–B–Li–P	porphyry Cu–Mo	Sn–W–U–Mo and rare metal (Nb–Ta) greisens
General plate tectonic Environment (*Chapter 8*)	continent–continent collision tectonics involving thickened continental crust	subduction-related continental and island arc	post-tectonic or anorogenic extension resulting in intracontinental ring complexes

* For other ways to classify granitoid rocks see Pitcher (1983) and Anderson (1988)
** A = mol Al_2O_3; C = mol CaO; N = mol Na_2O; K = mol K_2O; CNK = C + N + K; NK = N + K

Table 1.2 Selected average compositions of peraluminous (Chayes, 1985), metaluminous (Chayes, 1985) and peralkaline (Chayes, 1985, with additional data) granitoid rocks

	Peraluminous	*Metaluminous*	*Peralkaline*
n	199	158	25
SiO_2	71.45	67.43	74.01
TiO_2	0.32	0.55	0.23
Al_2O_3	14.76	14.67	11.59
FeO_T	2.49	4.13	3.08
MnO	0.13	0.12	0.10
MgO	0.78	1.64	0.55
CaO	2.01	3.53	0.48
Na_2O	3.72	3.72	4.33
K_2O	3.52	3.20	5.09
P_2O_5	0.14	0.17	0.06
Total	99.32	99.16	99.52
A/CNK	1.10	0.93	0.86
NK/A	0.67	0.65	1.09

the tectonic setting, where the field relations are cryptic, and the nature of source rocks). In this type of approach it is difficult to determine where observation ends and interpretation begins.

Major elements ± trace elements

Batchelor and Bowden (1985) explored the links between the major element compositions of granitoid rocks and their tectonic settings. Their plot of a function of Si–Ti–Fe–Na–K against a function of Al–Mg–Ca shows a systematic connection between chemistry and tectonic setting. Maniar and Piccoli (1989) used a sequence of major element variation diagrams to discriminate among granitoid rocks from seven kinds of tectonic setting (island arc, continental arc, continental collision, post-orogenic, rift, continental epeirogenic uplift, and oceanic ridges and islands). Also, working from a tectonic and temporal premise, Rogers and Greenberg (1990) defined four types of biotite granite with compositions largely within the metaluminous domain (late orogenic, post-orogenic, anorthosite–rapakivi suites, and ring complex). All these approaches show that the major ± trace element compositions of granitoid rocks do bear some relationship to the tectonic environment.

Trace elements only

slednji

Mineralogy and major element geochemistry are clearly related. Trace elements are less constrained and less obviously relate to specific rock types defined by modal mineralogy. Nevertheless, trace elements, if not used for defining igneous rock types, certainly have some utility for identifying tectonic settings and making broad genetic inferences. For example, Pearce *et al.* (1984) and Whalen *et al.* (1987) use trace elements variously for the purposes of classification, determination of tectonic setting, and making inferences about the nature of source rocks. These empirical methods rest somewhat precariously on the validity of the interpretations placed on the granitoids used as reference materials, on the expectation that all unknowns will fall neatly into these predetermined categories, and on the assumption that such chemical characteristics apply over the span of geological time.

Integrated characteristics and the genetic alphabet (S-I-A-M)

One popular concept is that of the so-called alphabet granitoids, of which there are four types in common usage:

1. **I-type** granitoids have A/CNK < 1.1, $^{87}Sr/^{86}Sr_i < 0.705$, and $\delta^{18}O < 9‰$, implying source rocks of mafic to intermediate *i*gneous composition or *i*nfracrustal derivation (Chappell and White, 1974; Chappell and Stephens, 1988);
2. **S-type** granitoids have A/CNK > 1.1, $^{87}Sr/^{86}Sr_i > 0.707$, and $\delta^{18}O > 9‰$, implying source rocks of *s*edimentary or *s*upracrustal protoliths (Chappell and White, 1974; White and Chappell, 1988);
3. **M-type** granitoids have A/CNK < 1.0, $^{87}Sr/^{86}Sr_i < 0.705$, and $\delta^{18}O < 9‰$, implying *m*antle sources, either indirectly through partial melting of subducted oceanic crust, or directly by extended fractional crystallization of basalt (White, 1979; Pitcher, 1982); and
4. **A-type** granitoids have a range of A/CNK > 1.0, $^{87}Sr/^{86}Sr_i$ and $\delta^{18}O$ comparable to that in the I-, S-, and M-types; in addition, they have low CaO, high Fe/Mg, high Ta, Nb, Zr, REEs and F, and are *a*norogenic (stable cratons and rift zones) in their tectonic setting (Loiselle and Wones, 1979; Collins *et al.*, 1982; Clemens *et al.*, 1986; Creaser *et al.*, 1991).

One of the principal rules for classification is that the basis for classification must be the same at any given level of subdivision.

Each letter of the alphabet system of classification of granitoids, therefore, must have the same connotation. The original I-type and S-type classifications are indisputably genetic, signifying igneous and sedimentary sources for the granitoids, respectively. It follows, therefore, that M-type granitoids should have mantle sources and A-type granitoids should have anorogenic(?) sources.

Now the *first* problem with the alphabet classification becomes clear. Not all of the letters have the same connotation at the same (alphabetic) level of classification. I- and S-types are **one-stage genetic types** (derived directly from the putative source), M-types are **one- or two-stage genetic types** (derived directly or indirectly from the putative source), and A-types are defined principally by their anorogenic tectonic setting. So the bases for the classification are different; such an irregular classification system is the outgrowth of uncoordinated contributions to the lexicon. Despite the letter, A-type granitoids never did belong in the original genetic alphabet, and the term 'A-type' should be discontinued because of its potential to be confused with it.

The *second* problem with the remainder of the genetic alphabet (I–S–M) is that, even within one of the tightly defined groups such as S-types, a range of magma compositions may develop as a function of temperature–pressure–composition (T–P–X) in the source region. Also, subsequent igneous differentiation and subsolidus alteration will serve to extend the original compositional range shown by the partial melts. If the range of products from a single source spans one of the genetic boundaries, as some are bound to do, then simple inferences about the source can be wrong. Unfortunately, sources of igneous rocks are very difficult to discern, and S-type (peraluminous) granitoids are known to originate in more than one way, including evolution from 'I-type' granitoids (Halliday *et al.*, 1981; Zen, 1986; Liggett, 1990; Miller *et al.*, 1990), so genetic classifications are equivocal at best.

The *third* problem with the genetic alphabet (I-S-M) classification is one of oversimplification, i.e. could any crustally derived granitoid develop exclusively from either an igneous or a sedimentary source? *Given the chemical and genetic complexity of the crust, granitoids with hybrid sources must be the rule.* What, then, is the point of designating a granitoid as S-type when it probably has a source that is not exclusively sedimentary?

The inescapable conclusion is that the alphabetic classification of granitic rocks, so enlightening and so useful in its original conception, requires some overhaul. First the A-types should be discarded because they do not belong; then the question of overlap between M-type and I-type needs to be addressed (perhaps by indicating clearly that M-types are only a subset of I-types and that M-types should also be dropped); and, finally, the remainder of the alphabet (I-S) needs the caveat that the letter may only suggest the dominant source.

1.2.4 Summary

Mineralogical classifications based on modal mineralogy are dependable but time-consuming. Chemical classifications, the closer they are related to the mineralogy, are useful. Chemical – tectonic – genetic classifications, the more they extrapolate from the measurable and meaningful, are controversial. The subdivisions of the alphabetic genetic classification system smear over the clearly measurable chemical subdivisions of Table 1.1 and Fig. 1.4b (e.g. anorogenic A-types can be peraluminous, metaluminous and peralkaline, and I-types can be both metaluminous and peraluminous). Should we adopt a classification system that cannot provide clear, objective, measurable distinctions between its groups? The alphabeticists, defining as they go, become so entangled in spongy semantics, that it is preferable to leave the pseudo-genetic classifications alone. Obviously, it is much easier to determine the chemistry than the origin, so why leap to genetic conclusions? To quote Whitten *et al.* (1987a, pp. 337–338), 'A natural classification differentiates genetically distinct igneous rocks; if separation into classes were based on arbitrary observational criteria that are independent of genetic differences, the resulting classification would almost certainly be obfuscatory.' [Remember the second nearest opera house!] And, 'Such arguments do not support classification of igneous rocks by genetic environment but favor classification based on petrographic and chemical descriptive parameters explicitly having genetic, rather than arbitrary, significance.'

Thus, this book concentrates on the observations and evidence required to map and interpret the evolution and origin of any granitoid body. It adopts the straightforward tripartite chemical classification of Shand (1947) as a first step in understanding the petrogenesis of granitoid rocks. It does not specifically deal with the special problems of any one chemical type of granitoid; in fact, Chapter 8 gives several distinctly different petrogenetic case studies.

$$\mathrm{OMAG} = f(\mathrm{d}S/S) + f(\mathrm{d}W/W) + f(\mathrm{d}C/C) - f(R)$$

where OMAG is the composition of orogenic metaluminous granite;
f is a fraction;
$S = f(\mathrm{MORB}) + f(\mathrm{GABB}) + f(\mathrm{SED})$ where S is the bulk composition of the subducted slab (MORB = mid-oceanic ridge basalt, GABB = gabbro of the oceanic crust, and SED = sediments dragged down a subduction zone), the proportions (f) and compositions of which are unknown and ($\mathrm{d}S/S$) is an unknown derivative thereof;
$W = f(\mathrm{PERID}) + f(\mathrm{ECLOG})$ where W is the bulk composition of the mantle wedge overlying the subducted slab (PERID = mantle peridotite and ECLOG = mantle eclogite), the proportions and compositions of which are unknown and ($\mathrm{d}W/W$) is an unknown derivative thereof;
$C = f(\mathrm{LC}) + f(\mathrm{UC})$ where LC and UC are the compositions of the lower and upper crust, respectively, the proportions and compositions of which are *really* unknown and ($\mathrm{d}C/C$) is an unknown derivative thereof;
and $R = fRc + fRv + fRs + fRa + fRf$ where R is that portion of the magma which is removed or lost through reaction with the crust (Rc), vapour loss (Rv), surface waters (Rs), atmosphere (Ra), and through fractional crystallization processes (Rf), the proportions and compositions of which are naturally unknown.

It should be emphasized that the four terms in the equation are dependent on, or are controlled by, parameters such as temperature, pressure, distribution coefficients, melt compositions, melt structures, viscosities, densities, $f\mathrm{O}_2$, $f\mathrm{CO}_2$, $f\mathrm{H_2O}$, etc., needless to say, none of which is known. Also there are other imponderable variables such as rate of subduction, the positions of relevant solidus curves, the thickness of the crust, etc., none of which is known either. Can you solve this equation in which there is one known (OMAG) and more than 35 unknowns? (I never was very good at mathematics!) Although this example was cited for orogenic metaluminous granite, it could apply to Any Igneous Rock (AIR) and would have been no less complex. Its composition is the sum of the effects of the source and subsequent processes (herein referred to as $\Sigma(S + P)$), and until the magnitude of each and every source and process can be established, we are not making much petrogenetic progress (but see Bryan, 1986).

26

4.4.5 The ultimate control on magma compositions

As a magma forms in the source region, ascends through a tortuous path or plumbing system to the surface, and intrudes country rocks or erupts to the surface, it is continually adjusting to new sets of conditions. In short, it is attempting to reach both mechanical and chemical equilibrium. Changes in the mechanical system may cause changes in the chemical one, and vice versa. For instance, cooling of the magma may increase viscosity which in turn retards the achievement of chemical equilibrium; or, the evolution of a vapour phase may create mechanical overpressure and explosive, non-equilibrium, ascent. In such a complex and dynamic system, the probability of perfect equilibrium ever being achieved is effectively zero. Nevertheless the very fact that granitoid rocks have restricted ranges of compositions centred on invariant points in phase diagrams, or strung out along cotectic lines in phase diagrams, demonstrates that equilibrium is being approached in many cases. This is no less true under conditions of post-magmatic alteration, but in most cases this added complexity can be avoided by collecting fresh rocks. Petrological diversity in igneous rocks is thus the result of the failure of the mechanical and chemical systems to come to the equilibrium dictated by the external parameters such as temperature, pressure, and time. And, as stated in Chapter 1, we rely on this failure to attain or maintain equilibrium to help us unravel petrogenetic problems.

4.5 TRANSITIONS BETWEEN PERALUMINOUS, METALUMINOUS, AND PERALKALINE GRANITOIDS

In many areas, more than one chemical type of granitoid can occur. Indeed, a complete continuum in mineralogical and chemical compositions exists in the granitoid family (e.g. Fig. 14); therefore subdivisions (however useful) are arbitrary. The particular peraluminous – metaluminous – peralkaline subdivisions used here have very precise chemical limits, but these boundaries are permeable to varying degrees. On the reasonable assumption that all three chemical types of granitoid magmas can be born (i.e. they are *primary* magmas whose A/CNK composition is governed in part by the source rock composition; see section 4.4.1 above), then must they retain that chemical stamp forever? Certainly not! If any of the processes described in sections 4.4.2 or 4.4.3 can change the relative

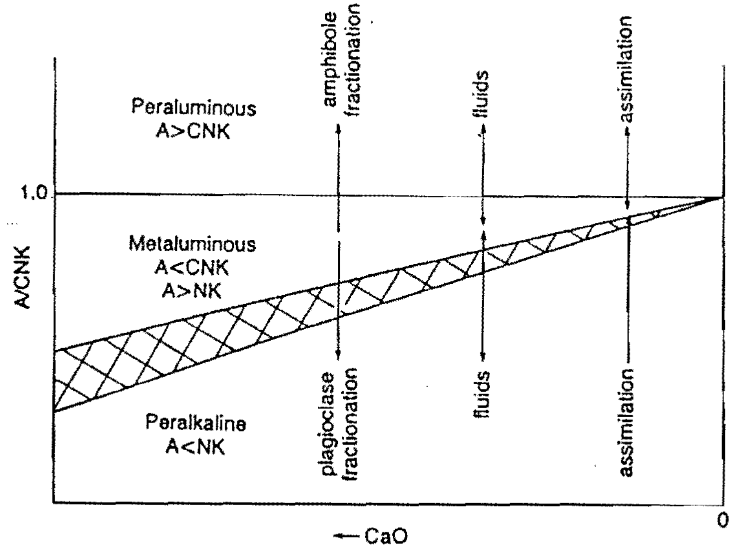

Fig. 4.4 Processes that cause transitions among peraluminous, metaluminous, and peralkaline granitoids. Some affect the course of a magma during cooling, others may operate on the solid rocks. The lower the CaO content, the greater is the possibility that peraluminous and peralkaline granitoid plutons may be found together (e.g. Nigeria). The scales are open-ended towards low values of A/CNK and high values of CaO. The cross-hatched area indicates that the boundary between peralkaline and metaluminous is not clearly defined in terms of the ordinate.

amounts of alumina and alkalis, then they can also cause transitions from one A/CNK group to another. Halliday *et al.* (1981), and many others cited therein, defined several processes that can change the chemical character of a granitoid magma or solid rock. Figure 4.4 shows some of these transitions.

4.6 CHEMISTRY AND TECTONIC ENVIRONMENT

We are now absolutely clear that the chemical composition of a granitoid rock, or any igneous rock, reflects $\Sigma(S + P)$. But if we map out the occurrences of peraluminous, metaluminous and peralkaline granitoids globally, we find that each one dominates a particular type of tectonic environment, but usually not to the complete exclusion of the other types (Table 1.1). Briefly, peraluminous granitoids are strongly associated with zones of continental collision, metaluminous granitoids with zones of ocean–continent or ocean–ocean collision, and peralkaline granitoids with zones of crustal extension. Therefore, do we immediately conclude that tectonic environment may be read directly from chemical composition? To be both correct and consistent, we must insist that their compositions are controlled by $\Sigma(S + P)$, and then go on to point out that each tectonic environment must have a dominant and reproducible combination of sources and processes that ultimately becomes reflected in the composition of the felsic igneous rocks.

Because of the infinite variety of sources, the primary magmas are smeared over the compositional range, and the subsequent magmatic and subsolidus processes smear them even more. Reproducible conditions result in broadly reproducible chemical characteristics (Farmer and DePaolo, 1983; Brown *et al.*, 1984; Pearce *et al.*, 1984; Batchelor and Bowden, 1985; Harris *et al.*, 1986; Maniar and Piccoli, 1989; Rogers and Greenberg, 1990). But the fact that different tectonic environments have dominantly one type of granitoid leads us to conclude that the amount of source + process smearing is limited, but not limited enough to permit safe snap judgements about sources or tectonic environments based on chemical composition alone.

Examples of the petrogenesis of each chemical type of granitoid are described in Chapter 8.

4.7 A GALLERY OF VARIATION DIAGRAMS WITH PRESUMED PETROGENETIC SIGNIFICANCE

4.7.1 Overview

Aware of all the problems, but undaunted, we try to extract some genetic information from geochemical data. Many types of variation diagrams exist, but all suffer from the same shortcomings:

1. major elements suffer from the problem of closure, i.e. they have a constant sum of 100% and, therefore, correlations between these variables appear better than they really are (see Chayes, 1960);
2. a restricted number of variables (e.g. divariate or trivariate diagrams) cannot adequately show all the variation in the samples as a whole and, as a result, each one provides us with only a small window to consider the causes of the variation, so we must integrate what we learn from each diagram to discover the entire evolutionary history; and

3. a perfect linear correlation ($r = 1$) on a variation diagram may (or may not) be attributable to a single cause, but most geochemical data scatter to some extent, and each point lying off the general trend does so for some very good reason; we are not yet at the stage where we worry about minor departures from perfect straight lines or curves, but the time will inevitably come.

Probably only when we learn to use multivariate techniques will we realize the full power of geochemical data. Given that this day is distant, in this section we will briefly review some of the commonly used variation diagrams and indicate what they purport to show.

Table 4.3 divides chemical variation diagrams into seven rather arbitrary categories based partly on the elements used, and partly on the purposes for which they are intended. For reasons of purpose as well as cost, few data sets represent complete quantitative analyses for 'all' major elements, trace elements, and isotopes. Examples of the variation diagrams are largely taken from 110 samples in just one pluton (the Halifax Pluton, Fig. 4.5; MacDonald and Clarke, 1991) within the South Mountain batholith (SMB) of southern Nova Scotia. For the REE and isotopic diagrams, data come from the batholith as a whole, and for the territorial map data come from both the SMB and its satellite plutons (Fig. 4.6).

Non-graphical techniques of modelling geochemical data (e.g. Allen *et al.*, 1986; Drummond *et al.*, 1988) also attempt to discover the reasons for chemical diversity in suites of granitoid rocks but, given the complexity of the problems and the uncertainties in the values of distribution coefficients between a silicate melt and its crystals (see Chapter 6), these methods are not notably more successful than inspection of a number of variation diagrams, their inadequacies notwithstanding.

4.7.2 An integrated picture of the South Mountain batholith

In the interest of brevity, the essence of each of the 22 chemical variation diagrams in Fig. 4.6 is reduced in the caption to one or two simple statements. Individually, these deductions mean little; combined, and in support of one another, they begin to paint a complete picture of the origin and evolution of the Halifax Pluton (HP) and South Mountain batholith (SMB).

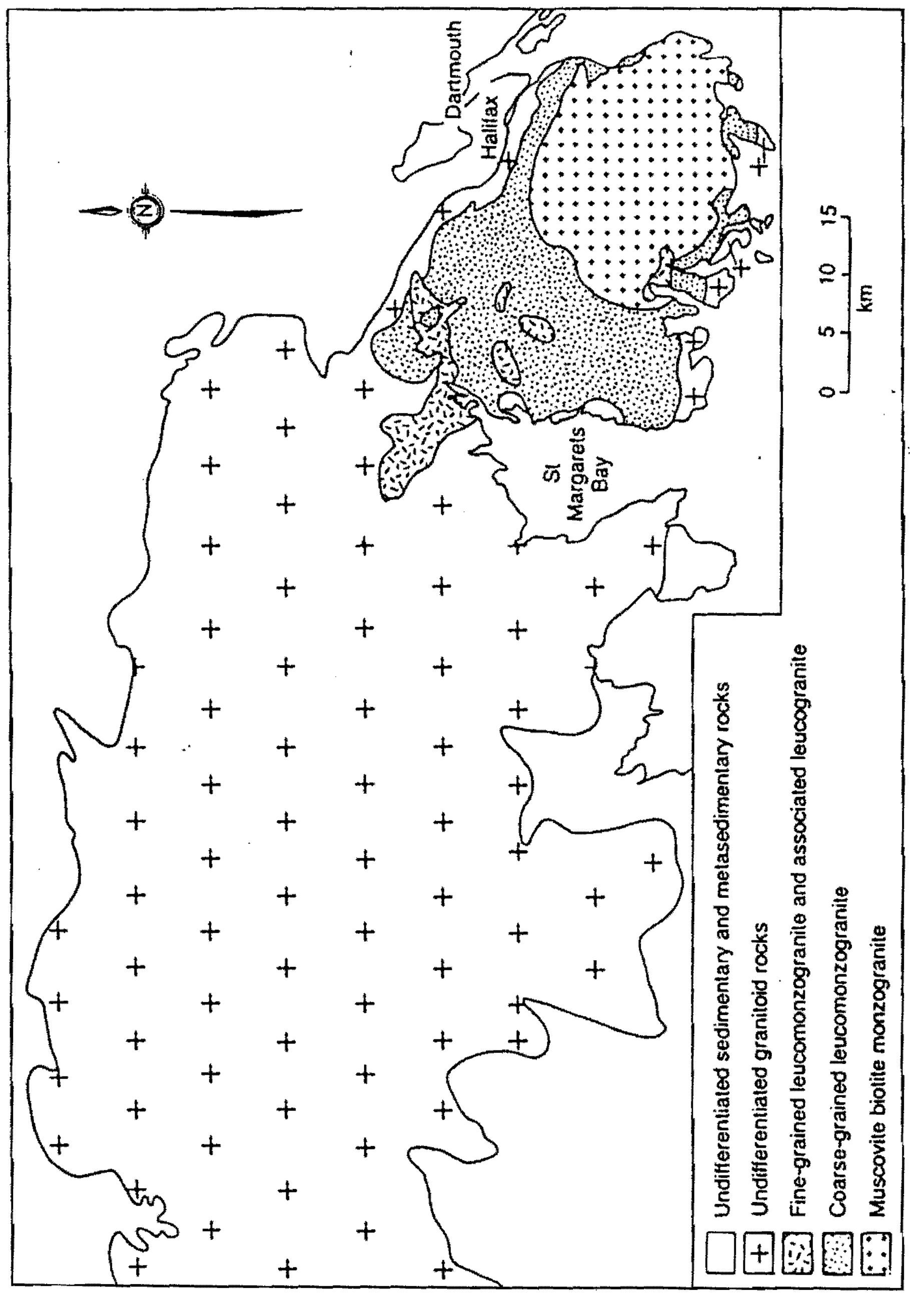

Fig. 4.5 Location of the Halifax Pluton within the South Mountain batholith.

able 4.3 Summary of the many types of geochemical variation diagrams used to unravel the origin and evolution f granitoid rocks

hemical components	*Alleged purpose of diagram*	*Examples (Fig. 4.6)*
ny component or derivative	primarily to show regional variation in the pluton at a glance, or for regional comparisons, but not generally intended for petrogenetic purposes:	
	simple histograms	a
	contour diagrams	b
	trend surface plots	c
	multivariate statistical territorial maps	d
Major – major	to show covariation of two or three elements for the purpose of defining trends in comagmatic suites, and for identifying major mineral phases responsible for those trends:	
	'Harker-type' variation diagrams	e,f,g
	rectilinear or triangular variation diagrams	h
Major – trace	to show covariation of major and trace elements to illustrate dependent or independent behaviour in any attempt to identify processes of differentiation:	
	major – compatible trace	i,j
	major – incompatible trace	k
Trace – trace	to show covariation of two or three elements, usually with similar geochemical behaviour and competing for the same lattice sites to help define the processes of chemical evolution:	
	large ion lithophile – large ion lithophile	l
	high field strength – high field strength	m,n
Normalized trace	diagrams in which the chemical composition of the granitoid is compared with some standard to make inferences about stages of evolution, processes of differentiation or even sources:	
	REE diagrams	o
	spider diagrams	p
	enrichment – depletion diagrams	q
Various components or derivatives	the purpose is more concerned with discovering the type of tectonic environment in which the granitoid was created, rather than how it was formed and evolved:	
	divariant discriminant plots	r
	multi-element discriminant functions	s
Isotope ratio – isotope ratio	normally related isotopic systems combined in a bivariate plot to learn about processes, but especially about sources of granitoid rocks:	
	stable isotopes	t
	radiogenic isotopes	u,v

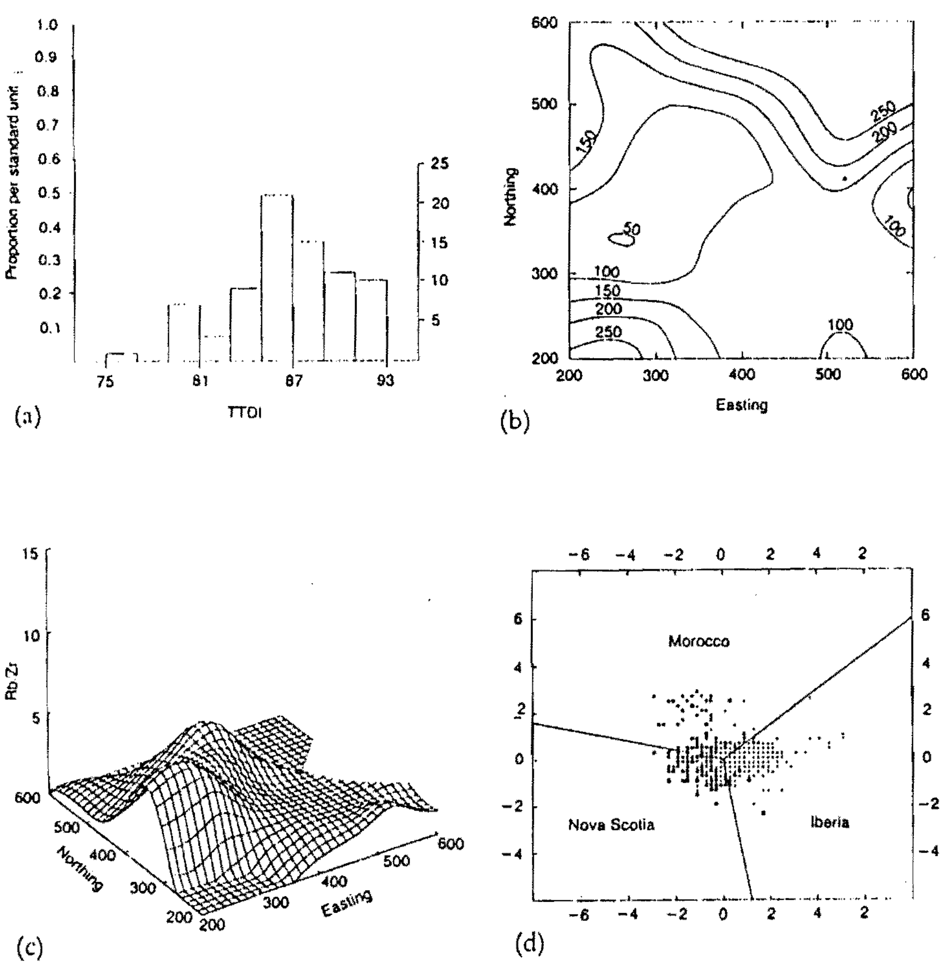

Fig. 4.6 A gallery of chemical variation diagrams.

(a) The histogram of differentiation index [Σ(Q + Ab + Or); Thornton and Tuttle, 1960] shows a broad skewed continuum of compositions, possibly with two or three modes, that may be genetically related.
(b) The contours of Zr content show systematic variation over the exposed part of the pluton suggesting a regular process of control.
(c) In normal granitic differentiation sequences, Zr decreases and Rb increases, therefore the Rb/Zr ratio (although geochemically dissimilar elements) should vary systematically. Now the highly differentiated west central portion of the pluton shows clearly.
(d) In this diagram, two discriminant functions have been calculated to produce the best separation possible between the peraluminous granitoids of Nova Scotia, Morocco and Iberia. Richard and Clarke (1989) used the degree of overlap in these populations to assess the possible correlation between these regions. (Symbols: squares – Nova Scotia; circles – Morocco; triangles – Iberia.)

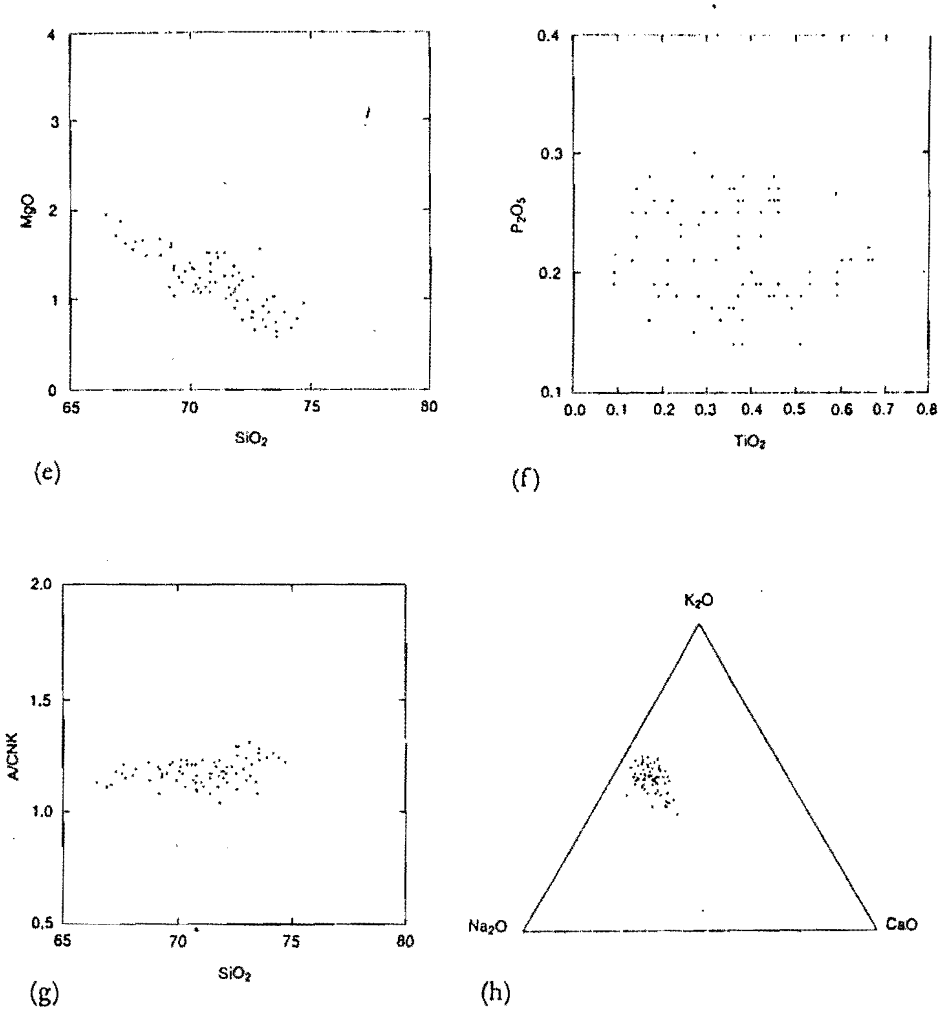

(e) Most differentiation sequences develop an inverse correlation between MgO and SiO_2, and the HP is no exception. The correlation is far from linear, however, and the 'off-trend' points suggest that several processes, other than the principal control, produce their compositions.
(f) Even though TiO_2 is highly correlated with Zr ($r^2 = 0.9x$), and therefore decreases regularly with differentiation, phosphorus is tied up principally in small quantities of apatite and monazite, minerals that also appear to decrease modally with differentiation. Perhaps surprisingly, P_2O_5 shows no correlation whatsoever with differentiation, suggesting that its concentrations are not solely related to crystal–liquid fractionation processes.
(g) The plot of A/CNK against S_iO_2 not only defines these rocks as peraluminous, but shows an increase of the excess alumina with differentiation. Some of the higher A/CNK ratios may only be attainable from interaction with hydrous fluid phases.
(h) The $CaO-Na_2O-K_2O$ diagram suggests control of chemical evolution in the pluton by removal of plagioclase.

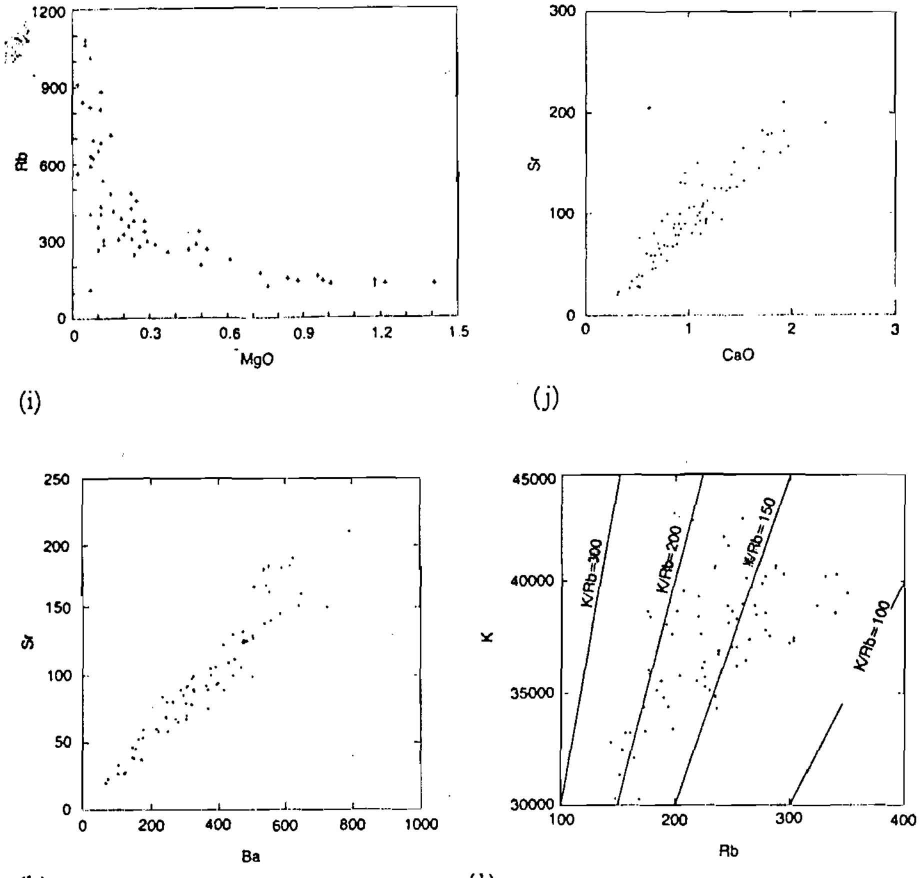

(i) (j)

(k) (l)

(i) In the MgO–Rb diagram for the whole SMB, the exponential increase of Rb with decreasing MgO may be attributed to either the MgO concentration becoming stagnated at some pseudo-eutectic point where Rb is still free to increase in late-stage differentiates, or to the action of fluid phases, or both.
(j) Strontium is strongly partitioned into plagioclase, and the CaO–Sr diagram confirms plagioclase fractionation in the HP.
(k) The decrease of Ba concomitant with Sr shows that both K-feldspar and plagioclase are being removed in the differentiation sequence.
(l) Conventional wisdom suggests that high K/Rb ratios are typical of magmatic processes and that lower values can only be reached by fluid interaction. If applicable here, the HP shows both magmatic and fluid interaction effects.

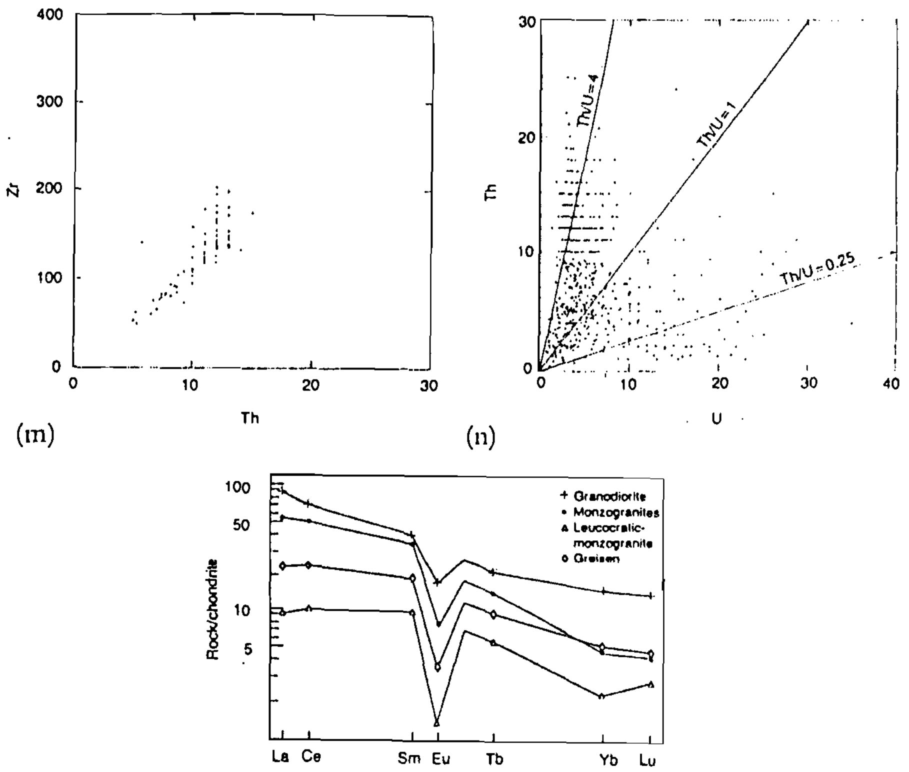

(m) (n)

(o)

(m) Zr and Th decrease together and are probably removed by the same mineral, zircon.
(n) If Th decreases with crystal–liquid fractionation, then U is either being concentrated as an incompatible element during differentiation, or its high solubility in the U^{6+} valence state may permit its concentration by late-stage fluids.
(o) Interpretation of REE patterns normally involves four steps: first, defining the slope of the pattern (chondrite–normalized La/Yb ratio) and commenting on the degree of light REE enrichment (or depletion, but not common in granitoid rocks); secondly, examining the magnitude of the Eu/Eu^* anomaly (>1 is 'positive'; <1 is 'negative'); thirdly, measuring the total REE content (ppm); and fourthly, looking for trends of variation within the plutonic suite. From early granodiorites through monzogranites and leucomonzogranites, the SMB (of which the HP is part) shows flattening La/Yb ratios suggestive of preferential removal of the LREE, increasingly negative Eu anomalies betraying removal of plagioclase, and a decrease in the total REE content suggesting removal of some phase, or phases, with bulk ΣREE greater than the bulk composition of the magma. Corey and Chatterjee (1990) demonstrate that the REEs are also mobile under metasomatic conditions.

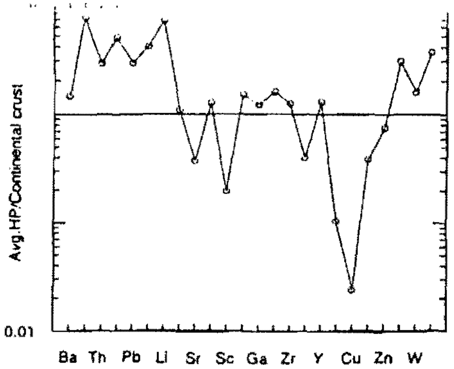

(p)

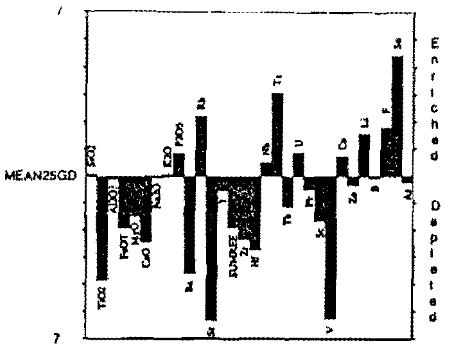

(q)

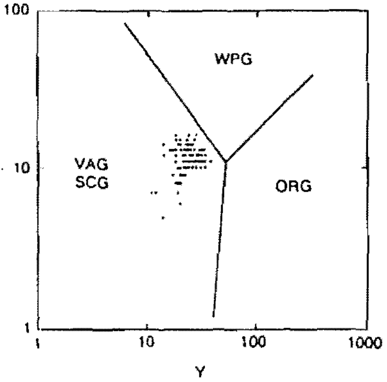

(r)

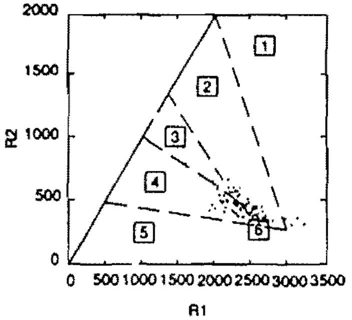

(s) 6 – anatectic two-mica syn-collisional granites

(p) Spider diagrams permit comparison with any other composition, usually a general 'standard', at a glance. This figure shows the average SMB compared with the average continental crust (Taylor and McLennan, 1985). As expected, the LILs show enrichment and the HFS elements show less enrichment or depletion relative to the average crust. The detailed pattern is the product of all the effects of source materials and processes, and granitoid rocks in a particular region may show rather similar fingerprints. For example, many granitic plutons in southern Nova Scotia have a pronounced positive Li anomaly.

(q) For comparisons within plutons, and especially to show the increasing or decreasing tendencies of a number of elements simultaneously, an enrichment–depletion diagram is used. These diagrams readily show that no two elements experience the same degree of enrichment or depletion over a fixed range of differentiation, an expression of many factors including bulk distribution coefficients and their relative mobility in fluid phases. This diagram illustrates the enrichments of several elements in the late-stage leucomonzogranites of the SMB relative to the early granodiorites.

(r) The HP shows little variation in the Nb–Y diagram (Pearce *et al.*, 1984). The relative immobility of these elements makes them useful for characterizing the tectonic environment in which these granitoids were formed. The best interpretation for the HP is that it is a volcanic arc granitoid or a syn-collisional granitoid.

(s) An example of the use of major element chemical compositions to make inferences about the tectonic environment of granitoid rocks is given by Batchelor and Bowden (1985). According to their scheme, the HP is an anatectic two-mica syn-collisional granitoid body, a deduction that is in agreement with the second possibility permitted by the Nb–Y diagram in (r).

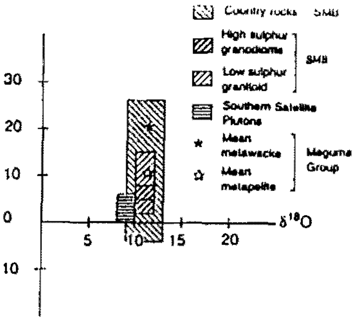

(t)

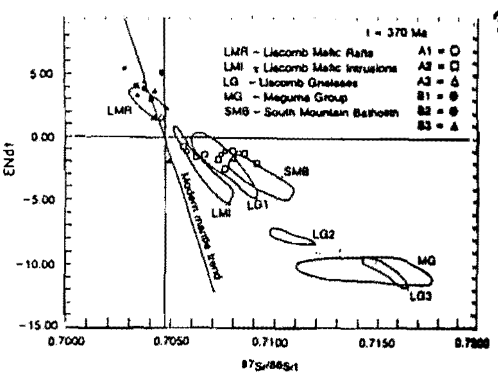

(u)

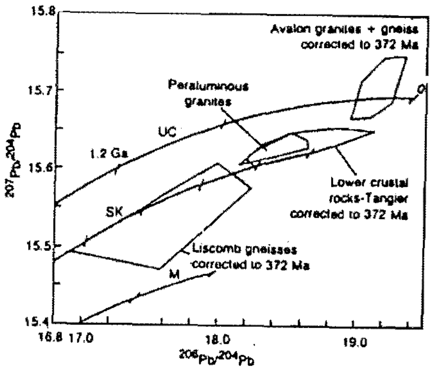

(v)

(t) Detailed stable isotopic investigations specifically of the HP have not been done; however, there exist some data for the SMB as a whole. This figure combines available sulphur (Kubilius and Ohmoto, 1982) and oxygen isotopic data (Longstaffe *et al.*, 1980). The spread of the sulphur data suggests that later differentiates of the tightly constrained early granodiorites have become contaminated with sulphur from the country rocks. The high $\delta^{18}O$ values are typical of crustal-derived magmas, and the slightly lower values in the Southern Satellite Plutons suggest a more primitive source.

(u) The Nd–Sr isotopic ratios of the SMB are quite unlike its host rocks, but very similar to the high-grade gneisses of the Liscomb Complex and deep crustal xenoliths from the Tangier lamprophyric dyke exposed much farther east in southern Nova Scotia. From an isotopic standpoint, these high-grade metamorphic rocks are suitable sources for the peraluminous granitoids; furthermore, the trend of the SMB toward the host rocks, and the trend of the xenoliths of the host rock toward the SMB, suggest that the granitic magma and host are mixing in a process of assimilation. In fact, the latent heat of crystallization is probably providing the energy for assimilation of the country rocks in this AFC process (Clarke and Halliday, 1980).

(v) Lead isotopic data demonstrate that, of three possible basement sources for the origin of the peraluminous granitoid rocks of southern Nova Scotia (Avalon, Liscomb, Tangier), only the Tangier deep crustal xenoliths have compositions that overlap with the granitoids, further refining the interpretation based on Sr–Nd above. (Unpublished Pb isotopic data courtesy of A. K. Chatterjee, Nova Scotia Department of Mines and Energy.)

In summary, although most of the atoms in the hand sample have come from the source (except for the contaminants), few are able to say so definitively (after all, what is the difference between a silicon atom from the source and one from the country rock?). Nevertheless, we potentially learn that the **source region** is dominantly metasedimentary (high A/CNK, high $^{87}Sr/^{86}Sr$, high $\delta^{18}O$) not so much from the fact that the Halifax Pluton is peraluminous, as that *all* granitoids in southern Nova Scotia are peraluminous. And, finally, identification of middle to lower crustal metasedimentary (and meta-igneous) rocks with suitable Nd–Sr isotopic ratios exposed as a xenoliths in the Tangier dyke provides a satisfactory solution to the problem of the source for the peraluminous granitoids in southern Nova Scotia.

From the evidence examined, chemical variation in the Halifax Pluton appears to be controlled primarily by fractional crystallization of plagioclase (CaO–Sr, Eu/Eu*), biotite (MgO, FeO), zircon (Zr, Th) and monazite (LREEs, Th) (Montel, 1986). Further evidence for fluid interaction, either by evolution of fluid phases from the magma itself or by hydrothermal alteration of the solid rocks of the batholith, comes from some low K/Rb ratios, high A/CNK ratios, trend of increasing U, dramatic decrease in the REEs of some leucomonzogranites, and variable $\delta^{18}O$. And, although there is ample field evidence of the assimilation of country rocks, the only reliable chemical data are the strontium and particularly neodymium isotopic ratios. These are the principal **processes** that have affected the present chemical composition of the Halifax Pluton, but identification of the processes is one thing, and determining their absolute or even relative contributions to the observed chemical variation is much more problematic.

Finally, there is little evidence to support either a batch melting model or the restite model (Clarke and Muecke, 1985; Wall *et al.*, 1987), both of which attach major importance to the source region to explain the observed chemical variation, in the SMB. Further information about these peraluminous granitic rocks is contained in contributions by Clarke and Chatterjee (1988) and Kontak and Barr (1988).

4.8 CONSTRAINTS PLACED ON THE ORIGIN AND EVOLUTION OF GRANITOID ROCKS BY MAJOR AND TRACE ELEMENT GEOCHEMISTRY

For petrogenetic studies, the task of the geochemist is to define the effects of all processes, make deductions about the source regions *after* the effects of all the processes are removed, and place chemical constraints on the origin of the suite that must be combined with similar constraints from the field, petrographic, geochronological and experimental data to determine the entire petrogenetic history of the granitoid. Table 4.4 summarizes the limitations of chemical data. Geochemistry is powerful, but, like all

Table 4.4 Summary of the use of geochemical data to interpret the origin and evolution of granitoid rocks. The more capitalization in the 'Use' column, the greater the degree of usefulness of the elements

Elements	*Considerations*	*Use*
Major element concentrations	variation in major element concentrations normally reflects melt–crystal–fluid differentiation processes and contamination, but effectiveness to reveal information even about differentiation declines as the magma becomes trapped at the low temperature invariant point (Chapter 6); only if granitoids are primary magmas (unlikely) can the bulk compositions yield some indirect information about the source region	PROCESSES source
Trace element concentrations	trace element concentrations (ppm) are a function of their concentration in the source, the degree and style of partial melting, and all of the subsequent processes of melt–cystal–fluid differentiation	PROCESSES Source
Trace element ratios	with high degrees of partial melting of the source region (likely in the case of voluminous granitoids), trace element ratios in the melt fraction may be identical to those in the source and will remain so until some differentiation process removes one element relative to the other; identification of exactly which trace element ratios in the granitoid are still reliable indicators of the source is problematic	Processes Source

TWO CONTRASTING GRANITE TYPES

B.W. CHAPPELL* and A.J.R. WHITE**

* Australian National University, Canberra, Australia.
** La Trobe University, Bundoora, Melbourne, Australia.

Expanded abstract

Granites of the major batholiths in the Tasman Orogenic Zone of eastern Australia are of two contrasting types which are of widespread occurrence and which may be distinguished by chemical, mineralogical, field and other criteria. We interpret these granites as being derived by partial melting of two different types of source material—igneous and sedimentary. Differences in the derived granites are inherited from the source rocks so that we recognize an I-type and an S-type respectively.

Some of the distinctive chemical properties of the two types are shown in the following table:—

I-types	S-types
Relatively high sodium, Na_2O normally $\geq$ 3.2% in felsic varieties, decreasing to $>$ 2.2% in more mafic types	Relatively low sodium, Na_2O normally $<$ 3.2% in rocks with approx. 5% K_2O, decreasing to $<$ 2.2% in rocks with approx. 2% K_2O
Mol $Al_2O_3/(Na_2O + K_2O + CaO) < 1.1$	Mol $Al_2O_3/(Na_2O + K_2O + CaO) > 1.1$
C.I.P.W. normative diopside *or* $<$ 1% normative corundum	$>$ 1% C.I.P.W. normative corundum
Broad spectrum of compositions from felsic to mafic	Relatively restricted in composition to high SiO_2 types
Regular inter-element variations within plutons; linear or near-linear variation diagrams	Variation diagrams more irregular

These chemical properties result from the removal of sodium into sea water (or evaporites) during sedimentary fractionation, and calcium into carbonates, with subsequent relative enrichment of the main sedimentary pile in aluminium. S-type granites come from a source that has been subjected to this prior chemical fractionation.

Petrographic features reflect the differences in chemical composition. Hornblende is common in the more mafic I-types and is generally present in felsic varieties, whereas hornblende is absent, but muscovite is common, in the more felsic S-types; biotite may be very abundant, up to 35%, in more mafic S-types. Sphene is a common accessory in the I-type granites whereas monazite may be found in S-types. Alumino-silicates, garnet and cordierite may occur in S-type xenoliths or in the granites themselves. All of these features result from the high aluminium content relative to alkalis and calcium in S-type granites and the converse in I-types. Apatite inclusions are common in biotite and hornblende of I-type granites whereas it occurs in larger discrete crystals in S-types.

Detailed studies in the Berridale Batholith (COMPSTON, SHIRAHASE, CHAPPELL & WHITE *in preparation*) have shown that strontium is more radiogenic in S-type granites (initial $Sr^{87}/Sr^{86} > 0.708$) because their source rocks had been through an earlier sedimentary cycle. I-types have initial Sr^{87}/Sr^{86} ratios in the range 0.704–0.706. Isochrons of I-types give a regular linear set of points whereas those of S-types show a scatter of points within a broad envelope, reflecting variations in the initial Sr^{87}/Sr^{86} within a single pluton as a consequence of more heterogeneous source material.

Field relationships of the two types may be distinctive. More mafic I-types contain mafic hornblende-bearing xenoliths of igneous appearance whereas hornblende-bearing xenoliths are rare in the S-types but metasedimentary xenoliths may be common. When both types occur together in composite batholiths the S-types are usually early in the intrusive sequence and they often have a strong secondary foliation truncated by later I-type intrusions which are either massive or have a dominant primary foliation.

Economic minerals are also different in their association with the two types. Tin mineralization appears to be confined to highly silicic S-type granites whereas tungsten and porphyry-type copper and molybdenum deposits are associated with I-types.

Chemical Geology, 16 (1975) 207—219

THE RELATION BETWEEN Rb, Ba AND Sr IN GRANITIC ROCKS

A.M. EL BOUSEILY and A.A. EL SOKKARY

Geology Department, Alexandria University, Alexandria (Egypt)
Geology Department, Atomic Energy Establishment, Cairo (Egypt)

(Received February 17, 1975; revised and accepted July 16, 1975)

ABSTRACT

El Bouseily, A.M. and El Sokkary, A.A., 1975. The relation between Rb, Ba and Sr in granitic rocks. Chem. Geol., 16: 207—219.

The ternary relation between the elements Rb, Ba and Sr in granitoid rocks is discussed. This relation proved to be useful in tracing differentiation trends in acidic suites. Moreover, it has a potentiality for being used as a criterion in genetic problems of granites, i.e. in distinguishing magmatic from metasomatic or granitized granites. The averages of these three elements in the various types of granites are calculated. The Turekian and Wedepohl (1961) two-fold subdivision of granites into high- and low-Ca rocks is elaborated so as to comprise four distinctive types: quartz diorites and granodiorites, normal granites, strongly differentiated granites beside the group of anomalous granites.

INTRODUCTION

Rubidium, Ba and Sr are widely distributed in acidic igneous rocks. The three elements are known to replace K particularly in feldspars. They are usually present at concentration levels from a few to several hundred parts per million, and are readily detectable by several techniques.

The geochemistry of Rb (1.47 Å) was reviewed by Heier and Adams (1963) who stated that the strong coherence between K and Rb in igneous rocks of the main stages makes it difficult to use the K/Rb ratio in tracing moderate differentiation processes.

Barium (1.34 Å), being almost identical in size with K (1.33 Å), behaves according to the classical capture principle. It is concentrated relative to K in the early minerals, and hence in the earlier rocks. However, Ba is not depleted in the magma until very late stages of the differentiation sequence (Nockolds and Allen, 1953). Turekian and Wedepohl (1961) gave values of 420 and 840 ppm Ba for high- and low-Ca granites respectively, which implies an increase of Ba with differentiation. However, Kolbe and Taylor (1966) observed a sharp decline of Ba at the extreme-acid end. Taylor and Heier (1960) found that the Ba/Rb ratio is more sensitive than the K/Rb ratio in tracing differentiation in potassium feldspars.

While the geochemistry of Rb and Ba is comparatively simple, since they are selective in their substitution for K among the common cations, that of Sr (1.18 Å) is more complicated by the fact that it isomorphously replaces not only K but also Ca (1.02 Å). When a trace element can substitute for two major elements and is intermediate in size between them, a simple relation is not to be expected. In basic rocks, Sr increases with decreasing Ca (Wager and Mitchell, 1951; Butler and Skiba, 1962), whereas in acidic rocks it decreases as the Ca content decreases (Sen et al., 1959; Hall, 1967). This may be attributed to the fact that Sr has a higher ionic radius than Ca, causing it to be admitted in the structure of Ca-bearing minerals less readily than Ca itself. It is only in granitic rocks that the Ca/Sr ratio starts to rise due to the presence of large amounts of alkali feldspars which remove from the magma some of the Sr which would otherwise go to plagioclases.

The foregoing discussion shows that elemental ratios with two elements have their difficulties when used to trace differentiation processes. It is thought that considering the three elements Rb, Ba and Sr together in a ternary relation might be more useful in tracing differentiation trends in igneous suites.

PRESENTATION OF DATA

Some 139 published analyses of Rb, Ba and Sr from different well-documented igneous assemblages varying in acidity were investigated and used in this study. The data are mainly from the following rock types: diorites, quartz diorites, granodiorites, normal granites, strongly differentiated granites, beside the so-called "anomalous granites". Under the term "normal granites" are included those types similar to the well-known low-Ca granites of Turekian and Wedepohl (1961). Strongly differentiated granites are those with distinct impoverishment in Ba and enrichment in Rb. These represent a very late stage of differentiation. The term "anomalous granites" is meant to include the following granite types: metasomatised, granitized, rapakivi, magmatic granites subjected to metasomatism and granites that suffered from chemical changes or were not formed by a simple mechanism. The rock types together with the number of analyses, localities and cited references are listed in the Appendix.

THE PROPOSED TERNARY RELATION Rb—Ba—Sr

The collected data, recalculated to 100, are plotted on a Rb—Ba—Sr ternary diagram (Fig. 1). Boundaries are drawn to delimit fields for each of the different rock types from diorites to strongly differentiated granites. It is clear that the points representing each type tend to cluster in a particular field within the triangle.

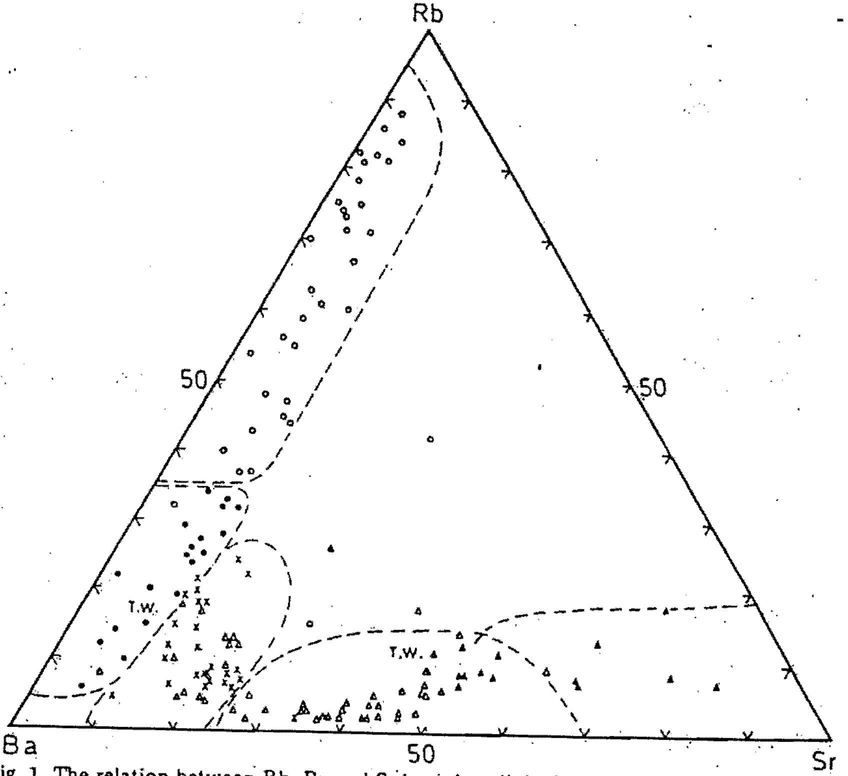

Fig. 1. The relation between Rb, Ba and Sr in various "granite groups". ▲ = diorites; △ = quartz diorites—granodiorites; x = anomalous granites; • = normal granites; ○ = strongly differentiated granites; ▵ T.W. = high-Ca granites; • T.W. = low-Ca granites (Turekian and Wedepohl, 1961).

Diorites

A limited number of analyses (11 analyses) are given for this group. They are mainly clustered around the Sr apex of the triangle. In comparison with the other "granitic" groups, diorites are relatively enriched in Ca with which element Sr shows a certain association. On the other hand, Sr^{2+} has a smaller ionic radius as well as a higher electrostatic charge than K^+. Consequently, Sr should tend to be relatively concentrated in the early formed K-bearing minerals (Nockolds and Allen, 1953). The effect of charge becomes more dominant in the latest stages leading to a decrease in Sr with differentiation.

Quartz diorites and granodiorites

With increasing acidity diorites gradually pass to quartz diorites and granodiorites. This is reflected in an increase of Ba relative to Sr, whereas Rb does not show any significant increase in concentration. Nockolds and Allen (1953) and Turekian and Wedepohl (1961) mentioned that the Ba content increases steadily as the more acidic rocks are approached. Despite the close association of Sr and Ca, Heier and Taylor (1959a) demonstrated that the Sr—Ba correlation is more pronounced than that of Sr—Ca.

The high values of both Ba and Sr together with a low Rb level make these quartz diorites and granodiorites more affiliated with the high-Ca granites of Turekian and Wedepohl (1961).

Normal granites

This group is characterised by normal distribution of the three index trace elements. By normal distribution is meant values close to those of the reference low-Ca granites of Turekian and Wedepohl (1961). The nineteen analyses representing this group are mainly clustered near the Ba apex. High-Ba concentrations are typically associated with high-temperature (least differentiated) K-feldspars in normal granites (Taylor et al., 1960).

Strontium shows more or less uniform distribution in the normal granites group, while the increase in Ba is accompanied by a decrease in Rb.

Strongly differentiated granites

It is the Ba/Rb ratio which characterises the change from normal granites to strongly differentiated types. Rubidium enrichment has long been known to occur in highly differentiated granites (Ahrens et al., 1952; Taylor et al., 1956). Such Rb enrichment is usually explained by the classical geochemical principle of radius difference between K and Rb.

Anomalous granites

The members of this group show a somewhat unusual distribution of the three index trace elements. In the ternary diagram the 24 analyses representing this anomalous group occupy a field overlapping that of quartz diorites and granodiorites. The anomalous granites field is marked from that of quartz diorites—granodiorites by their relatively high Rb level which is still below that of normal granites.

The group of anomalous granites is selected to cover types that suffered from metasomatism. Their low Rb content relative to that of normal granites may be attributed to Rb fractionation during metasomatism. While considerable attention has been focussed upon Rb fractionation during magmatic processes, recent studies have shown that similar fractionation could be triggered by metamorphic processes. Biotite in metamorphic rocks is observed to concentrate Rb by a factor of 3—4 relative to potassium feldspar (White, 1966). This is due to the preference of the larger Rb^+ ion for the larger 12-coordinated alkali sites of the micas relative to the 8—10-coordination sites available in the feldspars. In addition, gradual breakdown of the layer-structure silicates under metamorphic conditions might be expected to produce an impoverishment of Rb relative to K in intensely metamorphosed rocks (Heier, 1965; Lambert and Heier, 1968; Whiteny, 1969).

APPLICATION OF THE TERNARY RELATION

Fig. 2 illustrates the ternary relation Rb—Ba—Sr in the form of a model diagram applied to another 132 analyses notably from: (a) Palmer granite,

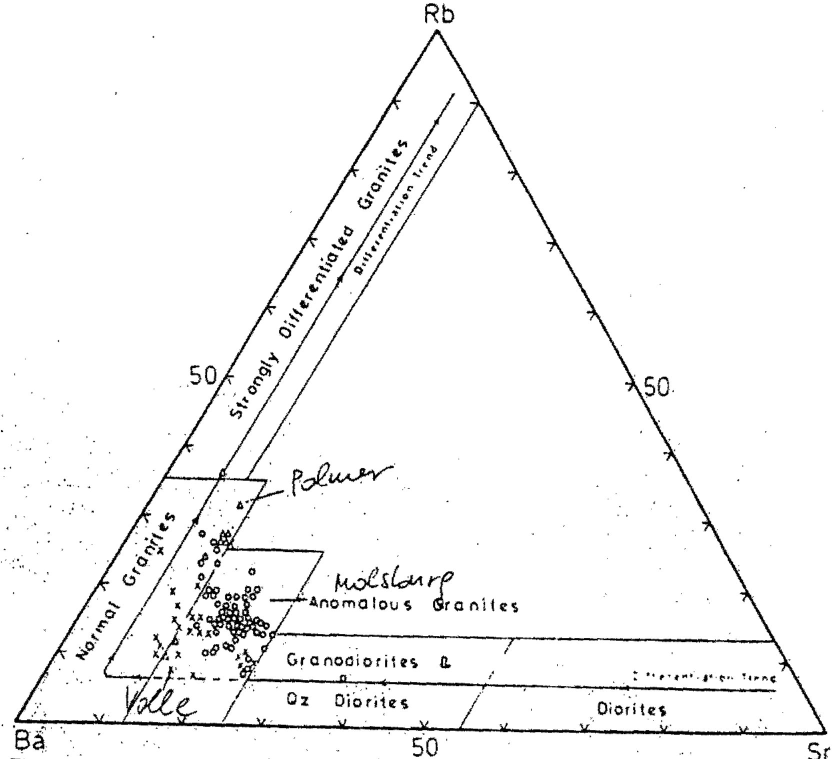

Fig. 2. The application of the different fields of the ternary relation Rb—Ba—Sr on some other investigated granites.
▵ = Palmer granite, South Australia (White et al., 1967); ○ = Malsburg granite, southern Black Forest (Weinheimer and Ackermann, 1967); × = Valle granite, southern Norway (Oweiss and Khalil, 1972).

South Australia, seven analyses from the main granite body and two averages from the associated migmatites and gneisses (White et al., 1967); (b) Malsburg granite, southern Black Forest, 99 analyses (Weinheimer and Ackermann, 1967); and (c) Valle granite, southern Norway, 24 analyses (Oweiss and Khalil, 1972). The origin of each of these granites will be discussed below in the light of the Rb—Ba—Sr ternary diagram.

(a) Palmer granite

The Palmer granite outcrops in a metamorphic environment associated with migmatites and high-grade schists and gneisses. Rattigan and Wegner (1951) have relied on the general structural concordance with the envelope rocks, gradational contacts and crystalloblastic textures in assigning a metasomatic origin for the Palmer granite. White (1956) disputed the gradational contacts and found small-scale cross-cutting relationships indicating that the granite was intrusive. White et al. (1967) have confirmed the intrusive origin in the light of petrochemical, structural and chronological data.

The representation of the Palmer granite on the Rb—Ba—Sr ternary diagram is shown as small triangles in Fig. 2. The seven analyses from the main granite body plot in the upper part of the normal-granite field, whereas the two averages of the associated migmatites and gneisses plot in the lower part at the contact with the anomalous-granite field. Therefore, the high Rb level of the Palmer granite relative to that of the envelope rocks, as well as its tendency to be clustered in the normal-granite field agree with the intrusive origin argued by White (1956) and White et al. (1967).

(b) Malsburg granite

Weinheimer and Ackermann (1967) mentioned that the Malsburg granite is an illustrative example of the continuous process of crystallisation—differentiation. They gave the following average modal composition: quartz 22.4, plagioclase 37.8, potassium feldspar 25.8, biotite 13.0, and hornblende 1.3 vol. %. The average major elements chemical composition is: SiO_2 67.80, Al_2O_3 15.05, Fe_2O_3 2.69, CaO 1.47, MgO 1.62, K_2O 4.81, and Na_2O 3.89 wt. %. These modal and chemical data are more affiliated with granodiorites than with normal granites.

The representation of the Malsburg granite on the ternary diagram (open circles in Fig. 2) does not reflect a clear differentiation trend. The analyses are mainly clustered in the anomalous-granites field. Those points plotting in the normal-granites field are from a type referred to by the previous authors as late-stage acid rocks. However, these so-called "late-stage acid rocks" are still away from the strongly differentiated granites region in Fig. 2. Their K/Rb ratios are in the range 156—207. Taylor et al. (1956) gave a K/Rb ratio of less than 100 for late-stage granites.

Weinheimer and Ackermann (1967) mentioned that the contact of the Malsburg granite with the syntectic rocks in the eastern side is gradational with "Schliern" and inclusions. This favours the anomalous character, as clearly indicated from the ternary diagram.

(c) Valle granite

The Valle granite is a part of the Precambrian basement complex that covers the greater part of southern Norway. It is surrounded by a vast area of migmatite rocks. Oweiss (1969) listed several features, such as pronounced foliation, position in the trough of granitic systems and normal behaviour of major and trace elements which led him to suggest that magmatic conditions prevailed during the formation of the granite. However, the representation of the Valle granite on the Rb—Ba—Sr ternary diagram (crosses in Fig. 2) reveals its possible anomalous character. The following features mentioned by Oweiss (1969) are also quoted to show the probability of metasomatic origin: Country-rock inclusions are widely distributed throughout the granite body, being more concentrated along its contacts. Granitic patches with diffused and irregular boundaries are observed in these inclusions. Feldspar porphyroblasts and augen crystals in the inclusions are similar to those found in the granite itself. Therefore, if the magmatic origin assigned by Oweiss is accepted, then the Valle granite still bears the imprint of being anomalous, as is clear from its plot in the ternary diagram.

RELATIVE GEOCHEMICAL BEHAVIOUR OF Rb, Ba AND Sr

The distribution of Rb, Ba and Sr in alkali feldspars has been discussed by Heier and Taylor (1959a, b). They found that, in a differentiation series, Ba decreases more readily than Sr, so that the Ba/Sr ratio decreases with increasing fractionation. This is not in accord with the principle that the smaller Sr ion is preferentially incorporated in the feldspar structure. It is the more ionic character of the Ba—O bond that leads to the preferential entry of Ba compared with Sr. This concept can be held true with respect to the concentration of the two elements in the feldspar structure. However, with respect to the whole-rock concentration of Ba and Sr, the relative decrease in the proportion of the two elements with differentiation is different. From the ternary diagram, it is clear that in the differentiation sequence: diorites → quartz diorites—granodiorites → normal granites it is the Sr which decreases while Ba increases. In such a series it is mainly the potassium feldspar/plagioclase ratio which governs the differentiation sequence. Strontium decreases readily with differentiation since it replaces Ca in plagioclase as well as K in K-feldspars, while Ba replaces only K in K-feldspars. The Rb content remains essentially unchanged from diorites to quartz diorites—granodiorites. It starts to increase in the normal granites as a result of increase of the amount of K-feldspars.

On the other hand, with respect to the differentiation sequence: normal granites → strongly differentiated granites, it is the Ba/Rb ratio which shows the greatest variation, the Sr concentration remains virtually constant.

It is clear from the ternary diagram that low-Ba granites are enriched either in Sr or Rb but not in both. Thus the Ba content seems to govern the Rb/Sr ratio. In the differentiation sequence: diorites → quartz diorites—granodiorites → normal granites, the Rb/Sr ratio increases on account of the decrease of Sr relative to Ba, while the Rb content tends to increase. In the sequence: normal granites → strongly differentiated granites, the Rb/Sr ratio also increases.

AVERAGES OF Rb, Ba AND Sr IN THE VARIOUS GRANITE GROUPS

The averages of Rb, Ba and Sr in the various granite groups presented here (271 analyses) are given in Table I. Actually the number of analyses is much more than 271 since some of the data are averages for more than one analysis (see Appendix).

TABLE I

Averages of Rb, Ba and Sr for the various granite groups as compared with the corresponding values for high- and low-Ca granites of Turekian and Wedepohl (1961)

Rock type	Rb (ppm)	Ba (ppm)	Sr (ppm)	Rb, Ba and Sr recalculated to 100% Rb (%)	Ba (%)	Sr (%)
quartz diorites and granodiorites	140	1,170	810	7	55	38
normal granites	190	550	70	23	69	8
strongly differentiated granites	260	140	20	62	33	5
anomalous granites	210	1,030	280	14	68	18
high-Ca granites	110	420	440	11	43	46
low-Ca granites	170	840	100	15	76	9

Hitherto, the most useful approach to estimating the average composition of granitic rocks, especially for trace elements, appears to be the major two-fold subdivision (high- and low-Ca granites) suggested by Turekian and Wedepohl (1961). The average Rb, Ba and Sr values for these high- and low-Ca granites are included in Table I for comparison.

It seems that the low-Ca granites of Turekian and Wedepohl (1961) correspond approximately to the normal-granites group. A comparison of the high-Ca granites with the quartz diorite—granodiorite group shows some differences. The average Ba and Sr concentrations of the high-Ca granites are much lower.

With respect to the average Ba concentration, Turekian and Wedepohl (1961) assigned values of 420 and 840 ppm to high- and low-Ca granites, resp. This implies a two-fold increase with differentiation which does not seem to be the case with the sequence: quartz diorites—granodiorites → normal granites, where the average Ba concentration is found to decrease with differentiation (being 1,170 and 550 ppm, resp.). However, a closer examination of the Ba value relative to that of both Sr and Rb shows that Ba relatively increases with differentiation in both series (see Table I). This reflects the importance of using the relative proportion between the three index trace elements rather than their absolute values in tracing differentiation trends.

The sharp decline of Ba in very acidic rocks makes the estimation of an average Ba content for low-Ca granites especially difficult. This is why the present authors further subdivided low-Ca granites into normal and strongly differentiated types. On the basis of the present data, the average Ba content decreases from 550 ppm in normal granites to 100 ppm in strongly differentiated types. This is accompanied by an increase of Rb from an average value of 190—260 ppm resp.

Anomalous granites show unusual distributions of the three index trace elements. El Sokkary (1970), during a study on the geochemistry of Egyptian granites, introduced the term "anomalous granites" to describe certain low-Ca types with peculiar distribution of the three index trace elements. Table I shows that the average Rb value of anomalous granites is slightly higher than that of normal granites (being 210 and 190 ppm, resp.). However, a consideration of the average Rb value relative to those of Ba and Sr shows that anomalous granites are lower in their relative Rb content.

CONCLUDING REMARKS

(1) The problem of granite genesis is highly controversial, and there is no line of evidence which would definitely indicate one conclusive interpretation. However, if the metasomatic origin of the group named "anomalous granites" is accepted, then the ternary diagram Rb—Ba—Sr possesses the advantage of being both classificatory and genetic. It facilitates the classification of granitic rocks into various groups according to the extent of probable differentiation. As a genetic factor, the diagram may help in indicating whether the granites are magmatic or not.

(2) Barium and Sr appear to be specifically sensitive indicators for tracing possible differentiation trends.

(3) Within the ternary diagram, granitic rocks depleted in Ba are enriched either in Rb or in Sr, but not in both. It is the Ba content which seems to govern the Rb/Sr ratio.

(4) It is difficult to rely on either the absolute values of Rb, Ba and Sr or on the binary relation between any two of them in tracing differentiation trends in granitic rocks exhibiting a wide range of acidity. It is better to refer to differentiation trends in terms of two different factors within the mentioned ternary relation. In the differentiation sequence: diorites → quartz

diorites—granodiorites → normal granites, the Ba/Sr ratio is the governing factor, and is found to increase with differentiation. In the sequence: normal granites → strongly differentiated granites, it is the Ba/Rb ratio which shows the rapid decrease.

(5) Single acid magmatic plutons, although differentiated, may plot in one field within the ternary diagram. This is because each one of the granitic groups occupies a wide range within the ternary diagram.

ACKNOWLEDGEMENTS

The authors wish to express their thanks to Prof. A.M. Gheith, Chairman, Geology Department, Boston University, for critically reviewing the manuscript and constructive suggestions, but the views expressed are the authors' responsibility.

REFERENCES

Ahrens, L.H., Pinson, W.H. and Kearns, M.M., 1952. Association of rubidium and potassium and their abundance in common igneous rocks and meteorites. Geochim. Cosmochim. Acta, 2: 229—242.

Butler, J.R. and Skiba, W., 1962. Strontium in plagioclase feldspars from four layered basic masses in Somalia. Mineral. Mag., 33: 213—225.

Condie, K. and Howard, H.L., 1971. Trace elements geochemistry of the Louis Lake batholith of early Precambrian age, Wyoming. Geochim. Cosmochim. Acta, 35: 1099—1119.

El Bouseily, A.M., 1973. On the rapakivi granite in contact with the biotite granite, Drammen, Norway. Bull. Fac. Sci., Alexandria Univ., 13 (in press).

El Bouseily, A.M. and Mahmoud, B.E., 1972. Geological studies of the Drammen granite, Oslo region, Norway — Part II, Geochemistry. Bull. Fac. Sci., Alexandria Univ., 12 (in press).

El Sokkary, A.A., 1970. Geochemistry of some granites in Egypt. Ph.D. Thesis, Alexandria University, Alexandria, 230 pp.

Hall, A., 1967. The distribution of some major and trace elements in feldspars from the Rosses and Ardara granite complexes, Donegal, Ireland. Geochim. Cosmochim. Acta, 31: 835—847.

Heier, K.S., 1965. Metamorphism and chemical differentiation of the crust. Geol. Fören. Stockholm Förh., 87: 249—256.

Heier, K.S. and Adams J.A.S., 1963. The geochemistry of alkali metals. In: L.H. Ahrens, S.K. Runcorn and H.C. Vrey (Editors), Physics and Chemistry of the Earth, 5. Pergamon, London, pp. 253—381.

Heier, K.S. and Taylor, S.R., 1959a. Distribution of Li, Na, K, Cs, Pb and Tl in southern Norwegian Precambrian alkali feldspars. Geochim. Cosmochim. Acta, 15: 284—304.

Heier, K.S. and Taylor, S.R., 1959b. Distribution of Ca, Sr and Ba in southern Norwegian alkali feldspars. Geochim. Cosmochim. Acta, 17: 286—304.

Kolbe, P. and Taylor, S.R., 1966. Major and trace element relationships in granodiorites and granites from Australia and South Africa. Contrib. Mineral. Petrol., 12: 202—222.

Lambert, I.B. and Heier, K.S., 1968. Geochemical investigation of deep seated rocks in the Australian Shield. Lithos, 1: 30—53.

Mukherjee, B., 1969. Genetic significance of trace elements in certain rocks of Singhbum, India. Mineral. Mag., 36: 661—670.

Nockolds, S.R. and Allen, R., 1953. The geochemistry of some igneous rock series. Geochim. Cosmochim. Acta, 4: 105—142.

Nockolds, S.R. and Mitchell, R.L., 1948. The geochemistry of some Caledonian plutonic rocks. A study in the relationship between the major and trace elements of igneous rocks and their minerals. Trans. R. Soc. Edinburgh, 61: 533—575.

Oweiss, G.A., 1969. Petrological and geochemical studies on some pre-Cambrian rocks in southern Norway. Ph.D. Thesis, Alexandria Univeristy, Alexandria, 252 pp.

Oweiss, G.A. and Khalil, S.O., 1972. Distribution and significance of Ba, Rb and Sr in Valle granite, Norway. Bull. Fac. Sci., Alexandria Univ., 12 (in press).

Rattigan, J.H. and Wegner, C.F., 1951. Granites of the Palmer area and associated granitized sediments. Trans. R. Soc. South Aust., 74: 149—164.

Sen, N., Nockolds, S.R. and Allen, R., 1959. Trace elements in minerals from rocks of the S. California batholith. Geochim. Cosmochim. Acta, 16: 58—78.

Taylor, S.R. and Heier, K.S., 1960. Petrological significance of trace element variations in alkali feldspars. Proc. 21nd Int. Geol. Congr., Norden, 14: 47—61.

Taylor, S.R., Emeleus, C.H. and Exley, C.S., 1956. Some anomalous K/Rb ratio in igneous rocks and their petrological significance. Geochim. Cosmochim. Acta, 10: 224—229.

Taylor, S.R., Heier, K.S. and Sverdrup, P.L., 1960. Contribution to the mineralogy of Norway, No. 5. Trace element variations in three generations of feldspars from the Landsverk I pegmatite, Evje, southern Norway. Nor. Geol. Tidsskr., 40: 133—156.

Turekian, K.K. and Wedepohl, W.H., 1961. Distribution of the elements in some major units of the earth's crust. Bull. Geol. Soc. Am., 72: 175—192.

Wager, L.R. and Mitchell, R.L., 1951. The distribution of trace elements during fractionation of basic magma — a further study of the Skaergaard intrusion, east Greenland. Geochim. Cosmochim. Acta, 1: 129—208.

Weinheimer, P.H. and Ackermann H., 1967. Geological investigation of differentiated granite plutons of southern Black Forest, II. The zoning of the Malsburg granite as indicated by the elements titanium, zirconium, phosphorus, barium, rubidium, potassium and sodium. Geochim. Cosmochim. Acta, 31: 2197—2214.

White, A.J.R., 1956. The granites and associated metamorphic rocks of Palmer, South Australia. Ph.D. Thesis, University of London, London, 221 pp.

White, A.J.R., 1966. Genesis of migmatites from Palmer region of southern Australia. Chem. Geol., 1: 156—200.

White, A.J.R., Compston, W. and Kleeman, A.W., 1967. The Palmer granite — A study of a granite within a regional metamorphic environment. J. Petrol., 8: 29—50.

Whiteny, P.R., 1969. Variation of K/Rb ratio in migmatitic paragneisses of northwestern Adirondacks. Geochim. Cosmochim. Acta, 33: 1203—1211.

25. Iz analiz svežega in preperelega diabaza izračunaj izgube in obogatitve prvin ob predpostavki, da je

- Al nemobilen (Krauskopf, 1982)
- Al mobilen, razmerje Al : Fe : Ti stalno (Cheswort, 1981)
- vse prvine so mobilne, izgube in obogatitve so podane kot utežno razmerje med oksidom v sveži in prepereli kamnini, pomnoženo s 100 (Garrels & Mackenzie, 1971)

a.) Rezultate grafično predstavi in jih primerjaj.

b.) Rezultate pod prvo točko primerjaj z rezultati preperevanja gnajsa iz tabele 13-2 in jih komentiraj

c.) glede na kemijsko analizo predpostavi mineralno sestavo preperelega diabaza in gnajsa

	svež	preperel
SiO_2	47.28	44.44
Al_2O_3	20.22	23.19
TiO_2	1.45	1.22
Fe_2O_3	3.66	12.70
FeO	8.89	-
MgO	3.17	2.82
CaO	7.09	6.03
Na_2O	3.94	3.93
K_2O	2.16	1.75
H_2O	2.73	2.73

TABLE 13-2

Analyses of quartz–feldspar–biotite gneiss and weathered material derived from it[1]

Column I gives the analysis of a sample of fresh rock, and columns II, III, and IV give analyses of weathered material. In general, the degree of weathering increases from II to IV, but there is no assurance that the original material was precisely the same or that IV represents a longer time of weathering than II or III.

Chemical composition (weight percent)	(I)	(II)	(III)	(IV)
SiO_2	71.54	68.09	70.30	55.07
Al_2O_3	14.62	17.31	18.34	26.14
Fe_2O_3	0.69	3.86	1.55	3.72
FeO	1.64	0.36	0.22	2.53
MgO	0.77	0.46	0.21	0.33
CaO	2.08	0.06	0.10	0.16
Na_2O	3.84	0.12	0.09	0.05
K_2O	3.92	3.48	2.47	0.14
H_2O	0.32	5.61	5.88	10.39
Others	0.65	0.56	0.54	0.58
Total	100.07	99.91	99.70	100.11
Approximate mineral composition (volume percent)				
Quartz	30	40	43	25
K-feldspar	19	18	13	1
Plagioclase	40	1	1	?
Biotite (+ chlorite)	7	Trace	Trace	0.2
Hornblende	1	None	None	Trace
Magnetite, ilmenite, secondary oxides	1.5	5	2	6
Kaolinite	None	36	40	66

[1] Reprinted by permission from Goldich (1938).

increase. Nothing in the analyses themselves enables us to choose between these alternatives.

If we had independent evidence as to how the mass or volume of rock has changed during weathering, our problem would be solved. Such evidence is usually not obtainable, so in most cases we can proceed only by making an arbitrary assumption that will allow computation of elemental gains and losses during weathering. One assumption commonly used is that alumina does not change appreciably during weathering—a guess that seems reasonable on the grounds that Al_2O_3 in analyses of weathered material generally shows the greatest *apparent* increase and that of all common rock constituents Al is least abundant in surface waters. Inasmuch as Al is not completely absent from stream and groundwaters, however, the assumption cannot be strictly accurate. In some weathering profiles there is good evidence that substantial Al has been removed from the rock, and for these it may be more appropriate to assume that a trace element like Ti or Zr is immobile during the weathering process for the purpose of calculating chemical gains or losses.

The calculation goes by the following steps, as illustrated in Table 13-3:

1. Recalculate analyses to 100 percent by distributing the analytical error (columns I and III).
2. Assume Al_2O_3 constant. During weathering, 100 g of fresh rock has decreased in weight so that Al_2O_3 has apparently increased from 14.61 to 18.40%. Hence the total weight has decreased in the ratio 14.61/18.40, or from 100 to 79.40 g. The amount of each constituent in the 79.40 g can be found by multiplying each number in column III by this same ratio. This gives the numbers in column A.
3. The decrease (or increase) in each constituent is found by subtracting the numbers in column A from those in column I, giving the numbers in column B.
4. The percentage decrease or increase of each constituent is computed by dividing the numbers in column B by those in column I, giving the numbers in column C.

This same method of calculation is often used with analyses showing other kinds of rock alteration, for example, hydrothermal alteration near veins and igneous intrusions. The assumption of constant aluminum is on shakier ground here,

TABLE 13-3

Calculation of gains and losses during weathering

Columns I and III, giving composition in weight percent, are repeated from Table 13-2, except that the analytical error in each has been distributed so that the totals are 100.00. Column A shows the calculated weight in grams of each oxide remaining from the weathering of 100 g of fresh rock, on the assumption of constant Al_2O_3. Column B shows the gains and losses of the different oxides in grams, and column C shows the same gains and losses in percentages of the original amounts.

	(I)	(III)	(A)	(B)	(C)
SiO_2	71.48	70.51	55.99	−15.49	−22
Al_2O_3	14.61	18.40	14.61	0	0
Fe_2O_3	0.69	1.55	1.23	+0.54	+78
FeO	1.64	0.22	0.17	−1.47	−90
MgO	0.77	0.21	0.17	−0.60	−78
CaO	2.08	0.10	0.08	−2.00	−96
Na_2O	3.84	0.09	0.07	−3.77	−98
K_2O	3.92	2.48	1.97	−1.95	−50
H_2O	0.32	5.90	4.68	+4.36	+1,360
Others	0.65	0.54	0.43	−0.22	−34
Total	100.00	100.00	79.40	−20.60	

Geochimica et Cosmochimica Acta Vol. 45, pp. 1235 to 1243, 1981
Printed in Great Britain.

0016-7037/81/071235-09$02.00/0

The weathering of basalt and relative mobilities of the major elements at Belbex, France

WARD CHESWORTH[1], JEAN DEJOU[2] and PIERRE LARROQUE[3]
[1] University of Guelph, Guelph, Canada. [2] I.N.R.A., Clermont—Ferrand, France.
[3] Maison des Volcans, Aurillac, France

(*Received* 17 *January* 1980; *accepted in revised form* 13 *March* 1981)

Abstract—A basalt and its weathered profile have been analysed for major elements. Graphical examination shows Al, Fe and Ti to have been essentially immobile. Determining mobility sequences for this deposit is complicated by the long pedogenetic history of the area. Three different sequences are presented, two for different stages of weathering integrated over time, and one that reflects the weathering regime of the present day.

INTRODUCTION

NO UNIQUE mobility sequence of the elements during weathering exists, though as TARDY (1969) points out in a thorough search of the literature, there is a great similarity between many of the sequences proposed. The major factors normally stressed as determining the sequence are: (a) the nature of the parent material; (b) the nature of newly formed phases; and (c) the inherent solubility of the elements (e.g. KARPOFF, 1973, pp. 58–59). Three equally important factors, rarely stressed, are the size of the system, the stage of weathering, and the ambient conditions in the system and its surroundings.

A sequence such as POLYNOV'S (1973):

$$\mathrm{Ca} > \mathrm{Na} > \mathrm{Mg} > \mathrm{K} > \mathrm{Si} > \mathrm{Fe} > \mathrm{Al}$$

and the similar Goldschmidt-Mason scheme (MASON, 1966) are strictly applicable only on global or perhaps continental scales. On smaller scales, for example on that of the soil profile considered here, different sequences can be expected. The behaviour of Al illustrates this. Though relatively immobile in Polynov's scheme, in podzolic soils, Al moves readily from A to B horizons.

As regards the stage of weathering being important in determining the relative mobilities of elements, it should be obvious that the elements contained in the most easily weathered minerals will be released first, those in less easily weathered minerals, later. In the case of elements with a low inherent solubility, this will not affect their mobilities, other things being equal; but with more mobile elements, changes in the sequence may be quite marked (POLYNOV, 1945). Many published studies of the relative mobilities of elements hide this effect of stage, by determining a sequence from a comparison of the most weathered material with parent rock (e.g. JOHNSON *et al.*, 1968). In effect such studies result in an integration over time, of all changes that have taken place between the beginning and end points.

The effect of ambient conditions becomes most critical for the smaller scale systems. Here is where the greatest variety is found. For example, at the scale of the soil profile the geochemical environment remains ill-defined. Yet PEDRO (1968) claims four chemically distinguishable soil-forming environments on the earth, while GAUCHER (1977) recognises at least ten. Soils that have developed on landscapes stable for many thousands of years, particularly those in areas undisrupted by recent glaciations, tectonism or volcanism, are likely to have weathered under more than one pedogenic regime. Different mobility sequences are appropriate to different regimes, and again schemes worked out by comparing least weathered with most weathered materials in such areas, will result in an integration of the effects of more than one regime.

These points are illustrated below in terms of the weathering of basalt and its overlying soil at Belbex.

GEOLOGICAL BACKGROUND

Belbex, in the Cantal, at the southern end of the Massif Central (Fig. 1) is dominated by the remains of the largest European Cenozoic volcano, a stratovolcano active from 21 to 3.8 Myr ago (BELLON *et al.*, 1972). Near the city of Aurillac, on the southwest flank of the volcano, flows of alkali olivine basalt of Pontian age, are found.

Two such flows, on the eastern side of the city at Puy Courny, have been dated at 7.3 ± 0.4 Myr and 6.5 ± 0.1 Myr respectively (GILBERT, 1972). The lower flow also outcrops at Belbex, 2 km west of Aurillac. Emplacement here was in a paleovalley cut into Stampian marls. Later erosion produced an inversion of relief so that the basalt now forms a small butte.

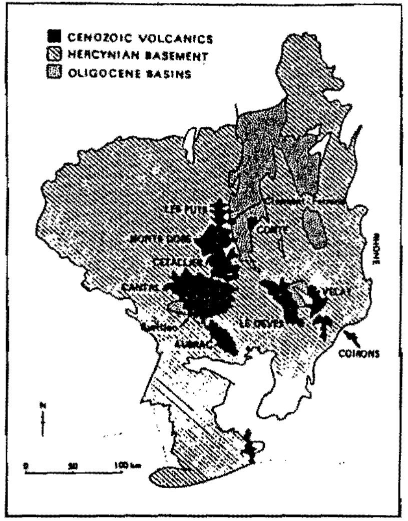

Fig. 1. Generalised geology of the Massif Central, France. The Belbex basalt outcrops 2 km west of Aurillac.

THE BASALT AND ITS WEATHERED PROFILE

The Belbex basalt is alkaline in nature and contains phenocrysts of olivine in a groundmass of clinopyroxene (salite), labradorite, titaniferous magnetite and glass. Within the glass, small needles of apatite occur. Except for the absence of modal feldspathoid, the rock displays the characteristics of a basanite.

The profile of alteration from bedrock to soil can be divided into six horizons on the basis of macroscopic features visible in the field, (Fig. 2). The pedochemical environment of the present day is one of brunification (GAUCHER, 1977; DUCHAFOUR, 1977, Chap. 9). An earlier pedochemical regime is indicated by horizon 5 (Fig. 2). Rubefaction, characteristic of a hotter climate than the current humid, temperate one is displayed there. That a hotter climate prevailed in this part of Europe, in Tertiary times is attested to by several studies (e.g. COINCON *et al.*, 1975).

EXPERIMENTAL RESULTS

A description of the samples is given in the Appendix. Bulk chemical analyses were performed by XRF, individual phases were analysed by microprobe and clay mineralogy was determined by diffraction techniques.

Chemistry

Bulk analyses are given in Table 1. In terms of the triangular projection used by CHESWORTH (1973b); the trend of alteration, as expected, is clearly towards residua relatively enriched in SiO_2, Al_2O_3, and Fe_2O_3 and relatively impoverished in CaO, MgO, K_2O and Na_2O (Fig. 3). The behaviour of the accumulating components is more clearly seen in Fig. 4. On weathering, the material moves towards the base of the tetrahedron. Once the spheroids are completely disintegrated, beginning at level 4, there is a marked enrichment of SiO_2 in the residuum relative to Al_2O_3 and Fe_2O_3.

Mineralogy

Compositions of unaltered phases in the bedrock are shown, in Table 2. The sequence of breakdown of these phases, determined from observations on thin sections is: (1) glass; (2) olivine; (3) clinopyroxene; (4) plagioclase. In horizons 4, 5 and 6, allochthonous phases of quartz and

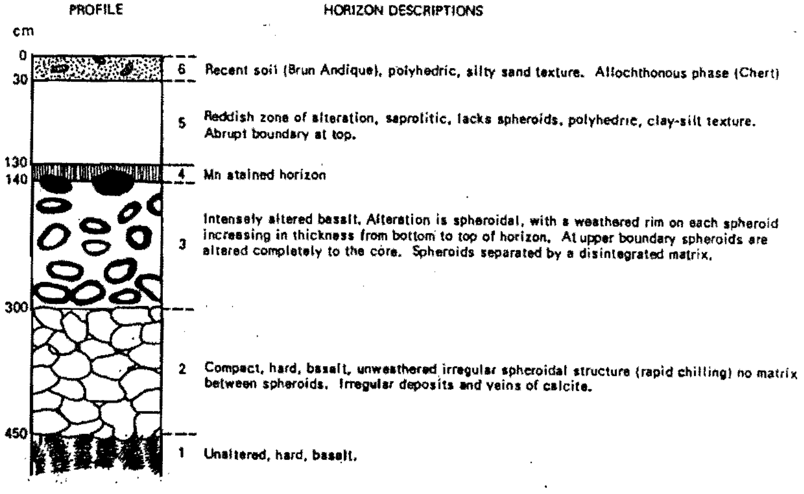

Fig. 2. The weathered profile at Belbex.

Table 1. Bulk chemical analyses of Belbex basalt and its weathered products

	Coherent samples												Non-coherent samples		
	Fresh basalt (level 1)			Spheroid (level 2)	Spheroid cores (level 3)				Spheroid envelopes (level 3)				(level 4)*	(level 5)†	(level 6)‡
	1	2	3	4	5	6	7	8	9	10	11	12	13	14	15
SiO_2	45.07	45.26	45.32	44.79	45.09	42.31	41.71	41.23	43.31	40.63	39.17	35.69	50.25	54.91	53.40
Al_2O_3	12.92	12.91	13.06	14.09	14.94	14.78	14.95	15.20	17.32	19.05	21.51	22.61	21.45	21.06	19.06
Fe_2O_3	12.66	11.85	11.41	13.38	13.47	13.68	13.92	14.42	15.84	20.08	21.85	20.62	19.94	16.22	17.20
MgO	9.70	9.61	8.90	8.93	7.55	8.87	8.21	7.71	5.76	4.26	3.94	3.18	0.91	0.64	2.55
CaO	12.12	12.14	12.72	13.16	12.96	12.48	12.32	12.68	12.35	8.59	7.09	7.36	0.87	0.72	1.92
Na_2O	2.03	2.26	2.57	1.18	1.41	1.50	1.29	1.17	0.76	0.24	0.19	0.18	0.03	0.00	0.33
K_2O	1.73	1.89	2.09	0.86	0.91	0.56	0.73	0.44	0.31	0.26	0.16	0.16	0.46	0.73	1.06
TiO_2	2.96	2.84	2.75	3.18	3.42	3.40	3.49	3.68	4.02	5.15	5.52	5.90	4.89	5.11	3.91
MnO	0.21	0.24	0.19	0.22	0.17	0.11	0.10	0.14	0.32	0.19	0.15	0.11	0.58	0.24	0.37
P_2O_5	0.65	1.00	0.98	0.11	0.16	2.31	3.28	3.34	0.31	1.58	0.23	4.19	0.26	0.16	0.37
L.O.I.	2.94	3.84	3.62	2.72	5.70	6.83	7.31	8.12	18.52	12.55	13.90	n.d.	12.47	11.23	14.01

* Mn-stained layer.
† Zone of rubefaction.
‡ Present day soil, (solum).

chert appear. The clay minerals produced during weathering are smectite, halloysite, hematite/goethite and an amorphous phase (Dejou and Chesworth, 1979).

INTERPRETATION

In a thermodynamic sense, weathering systems are invariably open. Two general models may be considered, the distinction being whether or not there are any components that can be classed as immobile:

Model 1:

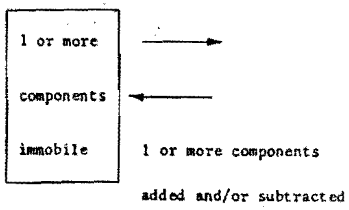

Model 2:

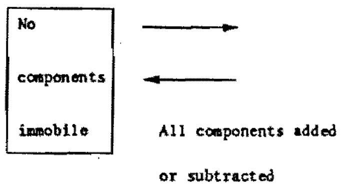

The principal agent of mobilisation is water, which, reacting with minerals in the weathering zone to produce an aqueous solution, moves downwards in the gravitational field and modifies the composition of a given system by leaching. Since all components in the soil are soluble to some degree, *model 2* is the only one that is rigorously tenable. However, weathered profiles generally have only short existences in terms of the geological time scale so that during the lifetime of a deposit, components with extremely low aqueous solubilities will not be significantly mobilised. In such cases *model 1* is appropriate.

Several methods are used to determine the relative mobilities of elements in systems of this kind. For example Harris and Adams (1966) contrast soil with parent rock; an internal standard of comparison may be used (Al in Goldich, 1938, quartz in Lelong and Souchier, 1979); or parent material may be compared with soil water (e.g. Tardy, 1969). Each has its usefulness though as the following account shows, a complex pedogenetic history presents problems, especially for the first.

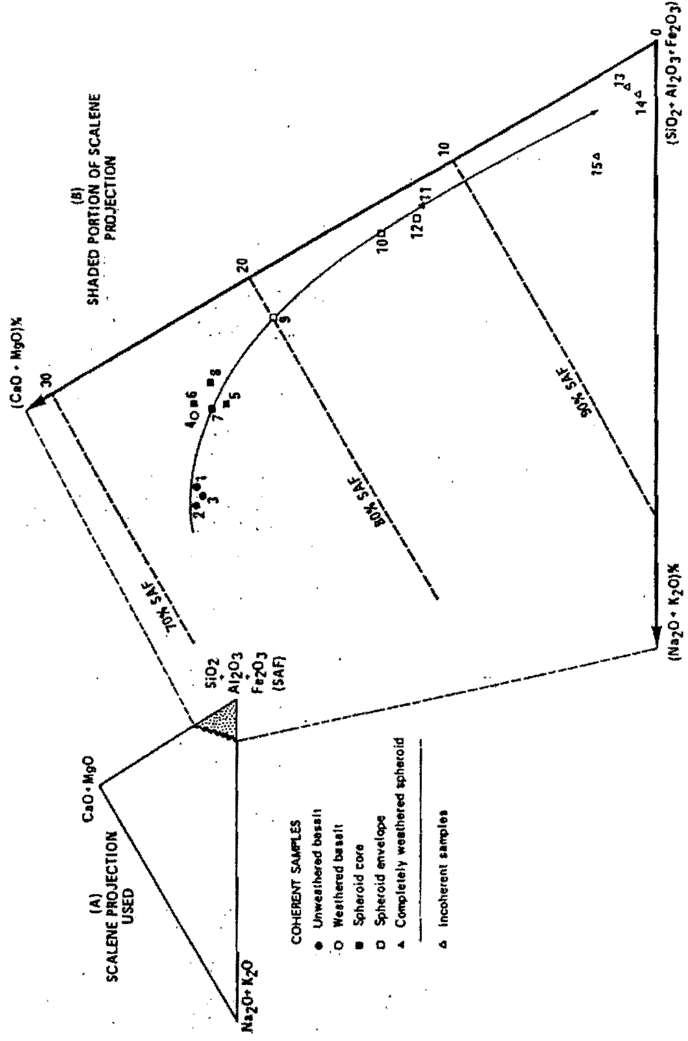

Fig. 3. The overall geochemical trend from unaltered basalt to soil at Belbex.

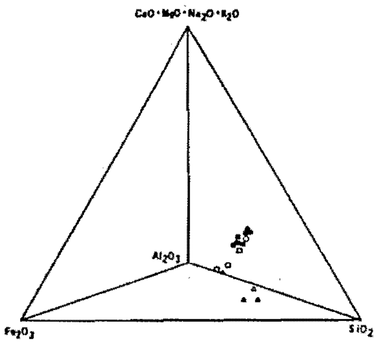

Fig. 4. Tetrahedral plot to show the trend of Fig. 3 in more detail.

A CHECK FOR IMMOBILE COMPONENTS

The easiest way to check for immobility amongst components is to determine intercomponental ratios. In the present case these show that the ratio Al:Fe:Ti is sensibly constant (Fig. 5). One, two or all therefore may be used as internal standards against which to measure the comings and goings of other components.

Table 2. Composition of unaltered phases in the bedrock

1. Olivine (av. of 4)	Si	5.94
	Fe	2.43
	Mg	9.62
	O	24
2. Clinopyroxene (av. of 5)	Si	6.88
	Al	1.30
	Ti	0.21
	Fe	0.92
	Mg	2.71
	Ca	3.14
	O	24
3. Plagioclase (av. of 5)	Si	7.09
	Al	4.96
	Fe	0.08
	Ca	1.78
	Na	0.85
	K	0.07
	O	24
4. Opaques (av. of 2)	Al	1.29
	Ti	3.50
	Fe	13.15
	Mg	1.53
	O	24
5. Glass (av. of 3)	SiO_2	57.06
	Al_2O_3	23.22
	ZrO_2	0.01
	TiO_2	1.01
	FeO	4.42
	MnO	0.12
	CaO	1.39
	Na_2O	4.80
	K_2O	7.78
	P_2O_5	0.01
	Cl	0.17
		100

Analyses 1–4 are expressed in atomic proportions with respect to 24 oxygens. Analysis 5 is in weight percent.

It is possible, of course, for components to maintain a constant ratio with each other if they leave or enter a system at rates proportional to their concentrations in the parent material. Physical processes might accomplish this rather easily, (e.g. by erosion), but the chances of it happening chemically, with elements as distinct as Al, Fe and Ti, must be accorded a very low probability.

It is interesting to note that GOLDICH (1938) studying the Morton gneiss, used Al as an internal standard. However, his analyses (Fig. 5) come closer to showing a relatively constant Fe_2O_3/TiO_2 ratio implying virtual immobility for these two components, and implying equally a loss of Al during weathering. Thus Al in this case was a poor standard of comparison.

WEATHERING TRENDS

Since Al_2O_3, Fe_2O_3 and TiO_2 can be assumed immobile, their sum can be taken as a measure of degree of alteration and the behaviour of other components can be contrasted with them.

In looking for trends it is convenient to divide the samples into two groups, coherent and non-coherent. By coherent, we mean those materials such as bedrock, spheroid cores, and envelopes of spheroids, that have notable coherency and retain some part at least, of the original rock structure. Thus on visual evidence alone, a genetic relation between samples can be assumed. The non-coherent samples are those that are loose and particulate and which on structural evidence alone cannot be unequivocally shown to have developed solely from the underlying basalt.

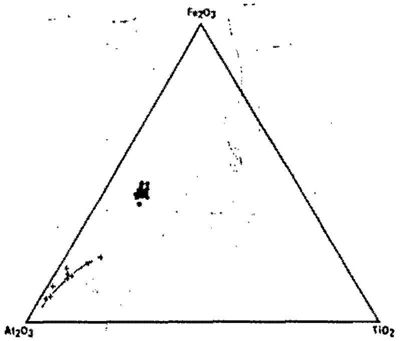

Fig. 5. All samples (dots) plotted in triangular coordinates to show the constancy of mutual ratios between Al_2O_3, Fe_2O_2 and TiO_2. The crosses represent analyses of the Morton gneiss and its weathered products. The arrow indicates the weathering trend which can be interpreted to show a loss of Al relative to Fe and Ti. GOLDICH'S (1938) choice of Al as an internal standard is hard to justify.

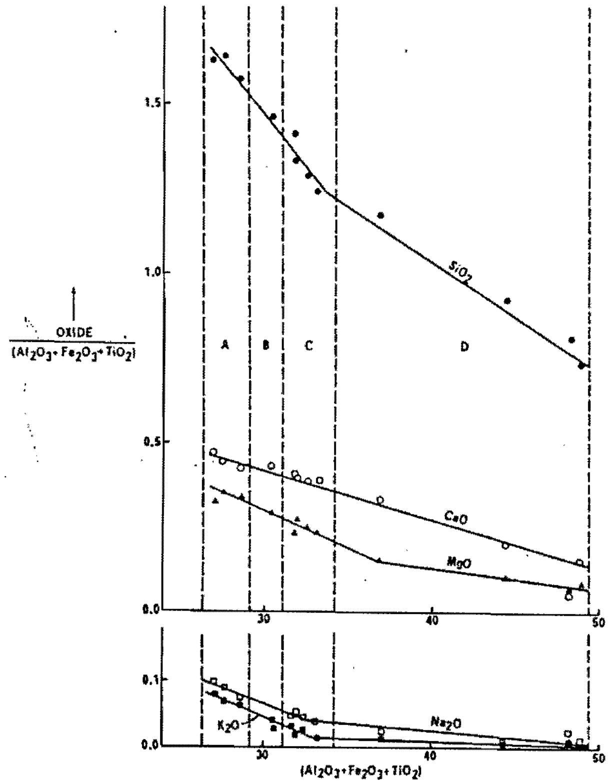

Fig. 6. Rates of loss of major oxides with respect to $Al_2O_3 + Fe_2O_3 + TiO_2$ used here as an index of weathering. (A) unweathered basalt; (B) weathered basalt; (C) spheriod core; (D) spheroid envelope and completely weathered spheroid.

Coherent samples

Major oxide components, normalised with respect to $Al_2O_3 + Fe_2O_3 + TiO_2$ are plotted against $Al_2O_3 + Fe_2O_3 + TiO_2$ (Fig. 6). The linear relationship, of course, is built in (CHAYES, 1960). However, the rate of decrease of the normalised values on the graphs is proportional to the rate of loss of a component, given the sum $Al_2O_3 + Fe_2O_3 + TiO_2$ as a measure of the degree of alteration. Noteworthy breaks in slope occur for SiO_2, MgO, Na_2O and K_2O, implying a slowdown in the rates of loss of these components when the envelope stage of alteration is reached.

Non-coherent samples

Bulk samples of the manganese stained layer, the reddish zone of alteration and soil, again show a virtual constancy in Al_2O_3–Fe_2O_3–TiO_2 ratios, so that

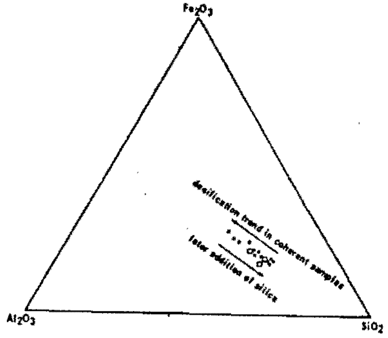

Fig. 7. Desilication of coherent samples (dots), and resilication of incoherent samples (squares).

Belbex basalt can still be claimed as a parent material, (Fig. 3). However, a marked increase in SiO_2 to the system is obvious (Fig. 7) indicating an addition of SiO_2 to the system in the upper levels of the profile. Later, this will be related to the geomorphological history of the area.

DISCUSSION

The behaviour of the weathering system at Belbex is in accordance with model 1. Specifically it involved two steps:

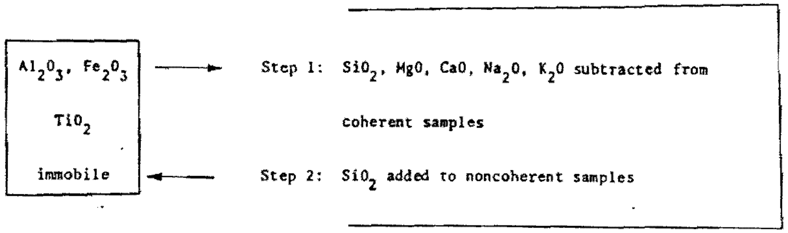

Data from the coherent materials allows us to deduce an order of mobility for major components. Before the weathered material has altered to the stage of a separable envelope on the spheroids, the slopes of the curves in Fig. 6 indicated the following order of decreasing mobility:

Si > K, Na, Mg > Ca > Fe, Al, Ti.

At the envelope stage the rates of loss of Si, Mg, Na and K decrease, and the mobility sequence changes slightly:

Si > Ca > K, Na, Mg > Fe, Al, Ti.

The mobility sequences can be explained in terms of the factors emphasized by KARPOFF (1973). First the nature of the parent material: fresh basalt at Belbex contains two easily weathered phases (glass and olivine) and two that are weathered less easily (pyroxene and plagioclase). While glass and olivine are still present, they release their components relatively rapidly giving rise to the initial high mobilities of Si, Mg, Na and K indicated by the steeper parts of the curves in Fig. 6. When these phases are exhausted the rate of release of Si, Mg, Na and K is governed by the slower breakdown of the other phases. Ca, the bulk of which is to be found in pyroxene and plagioclase is released and mobilised at a steady rate throughout. Secondly the effect of the secondary phases becomes clear at the envelope stage. Smectite and halloysite form to fix and 'slow down' some of the Si, Mg, Na, K and Ca. Thirdly, the effect of an inherently low solubility for a component is most obvious in the cases of Al, Fe and Ti which precipitate virtually on release from primary phases, partly in amorphous, but also in crystalline forms, such as hematite, goethite and the clay minerals.

An important feature of mobility sequences of the kind given above, is that they represent an integration of weathering changes over time. They may not therefore be representative of the present day pedogenic regime. This must be true of most studies of geochemical mobilities in soil, certainly of soils found on landscapes such as that at Belbex which predate the late Cenozoic glaciations.

The study by HARRIS and ADAMS (1966) is a case in point. Their Georgia profiles were collected in an area covered by acrisols, relatively ancient soils, that were probably preceded by podzols. To what extent the mobility sequence they propose relates to the present environment is impossible to say from the evidence published. Furthermore, their technique of comparing soil with bedrock is only valid if it can be shown that physical processes have not intervened to modify the composition of the weathering system. At Belbex this was patently not the case, and although dramatic geomorphological changes may not have occurred on the Georgia landscapes studied, aeolian additions or subtractions to a soil are common.

At Belbex the basalt has weathered under at least two pedogenic regimes, the present one of brunification and an earlier one of rubefaction. The latter produced the reddish zone (level 5) which then became the parent material of the present day soil. A present day (or 'instantaneous' as opposed to integrated) mobility sequence can be estimated by comparing the composition of the reddish zone with the composition of waters draining soils formed on basic rocks in the Massif Central (TARDY, 1969, Table 38). Omitting Ti (not determined by Tardy) the sequence is Na > Ca > Mg > K > Si > Fe > Al which is almost identical to POLYNOV'S (1937) global sequence. The notable change between this and the two earlier sequences is in the position of Si, and is a reflection of the addition of forms of SiO_2 of low solubility to the weathered basalt. This contamination of the profile by SiO_2 was revealed geochemically in Fig. 7. It is explainable on the basis of the complex geomorphological history of the region. The basalt was originally emplaced in a valley cut into Stampian marls. In this situation, the upper surface of the flow would be in a position to receive detritus derived from the valley

sides. That this happened is indicated by the presence of brownish fragments of chert in the upper, noncoherent part of the Belbex profile, identical to chert found in the Stampian marls. The carbonate component of the added marls would tend to be removed by CO_2-charged leaching waters and would only reprecipitate when the pH had increased to about 7.8 (KRUMBEIN and GARRELS, 1952). This appears to have happened in the lower part of the profile where calcite is found on rock surfaces and in cracks in spheroids.

CONCLUSIONS

The final version of model 1 that can be advanced for the Belbex deposit is shown diagrammatically.

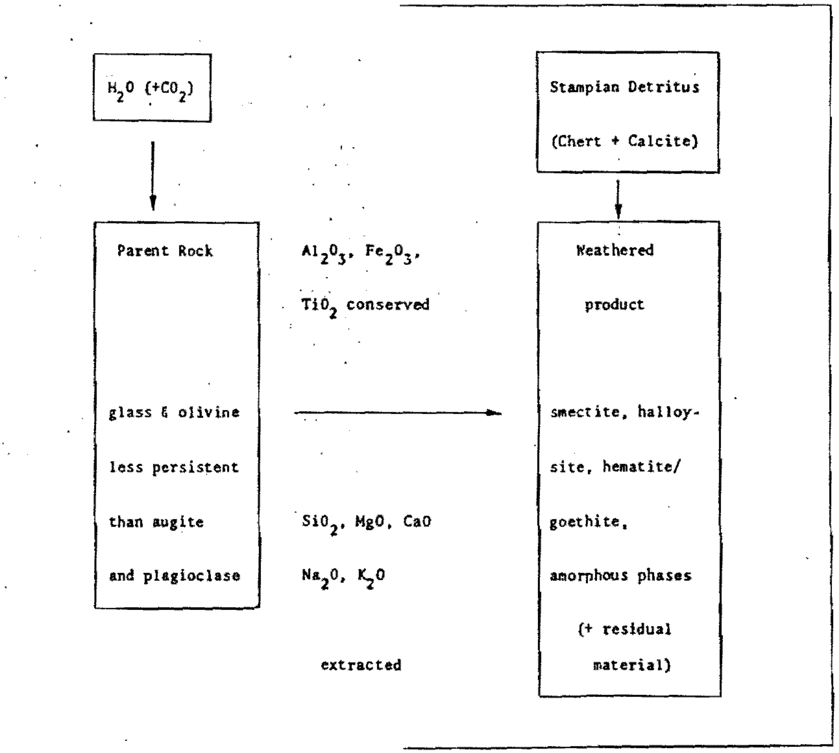

The basalt weathered over a period of time which encompassed at least two different pedogenic regimes, an early one of rubefaction and a later of brunification.

At the present day the order of mobility of major components is:

Na > Ca > Mg > K > Si > Fe > Al.

This, which can be looked upon as an instantaneous order, compares with two sequences integrated over time:

Si > K, Na, Mg > Ca > Fe, Al, Ti.

(earlier stage of basaltic weathering)

Si > Ca > K, Na, Mg > Fe, Al, Ti.

(later stage of basaltic weathering)

Many such sequences must exist, especially on the scale of a soil profile. At this scale, not only such commonly recognised factors as: (a) nature of parent material; (b) nature of secondary phases; and (c) inherent solubility of components, are important in determining the order, but the nature of the pedogenic environment becomes important, several distinct environments having been identified (GAUCHER, 1977).

Acknowledgements—We are grateful to BOB MCNUTT of McMaster University who supervised the XRF analyses, and to JOHN RUCKLEDGE, who allowed one of us to use the microprobe at the University of Toronto.

26.) Primerjaj vsebnost težkih mineralov v dveh vzorcih peska, od katerih je en iz vrha drugi pa iz dna terase. Nastanek terase je trajal vsaj nekaj 100.000 let, izvor materiala pa se v tem času ni spreminjal. Kateri od naštetih mineralov bodo v večji količini prisotni v vzorcu iz spodnjega dela: cirkon, rogovača, granati, olivin, biotit, labradorit, avgit, turmalin, magnetit, apatit.

27.) Napiši ravnotežne enačbe za navedene reakcije. Enačbe naj bodo geološko logične, v smislu, da so produkti stabilni in lahko skupaj nastopajo v naravnem okolju (pH).

a.) raztapljanje kalcita v ogljikovi kislini,
b.) grossularit ($Ca_3Al_2Si_3O_{12}$) reagira v ogljikovi kislini,
c.) raztapljane sfalerita v ogljikovi kislini,
d.)hidrolizira nefelina ($NaAlSiO_4$).

28.) Navedi glavne produkte preperevanja

a.) gabbra
b.) apnenca
c.) granita
d.) eklogita
e.) glinavca

29.) Primerjaj in komentiraj kemični formuli illita in montmorillonita.

30.) Montmorillonit ima glede na kaolinit večjo plastičnost, sposobnost absorbcije vode in ionsko izmenjevalno kapaciteto. Zakaj?

31.) Razvrsti navedena okolja glede na

a.) padajoč pH

b.) padajoč Eh:

A. morska voda blizu površja v tropih

B. voda v tleh iz A horizonta podzola

C. voda v tleh iz A horizonta černozema

D. potočna voda, ki teče preko skrilavcev, ki vsebujejo precej pirita

E. voda iz močvirja v severni Kanadi

32.) Kateri od navedenih procesov zajemajo oksidacijo, kateri redukcijo in kateri ne enega ne drugega?

a.) izločanje sadre pri izhlapevanju morske vode

b.) izguba organske snovi iz sedimenta zaradi razpada

c.) nastanek pirita v morskem okolju nekaj centimetrov pod mejo sediment-voda

d.) obarjanje fluorapatita iz morske vode

e.) izkosmičenje sola Fe oksida, ki ga reka prinese v morje

f.) obarjanje MnO_2 iz podtalnice, ki teče skozi peščenjake

g.) obarjane kremenice iz vode iz vročega izvira

h.) rast kristalov sadre v glinah bogatih z organsko snovjo

i.) nastanek glinenih mineralov z reakcijo med raztopljeno koloidno kremenico in glinico v morski vodi.

Nina Zupančić

OSNOVE FIZIKALNE KEMIJE

0. zakon termodinamike

Če sta dva sistema v termičnem ravnotežju s tretjim (med njimi ni toplotnega toka) sta v ravnotežju tudi med seboj. Vsi trije imajo enako temperaturo.

$0°C = 273K$

- pogoji ravnotežja (T, p, koncentracije)
- kinetika procesov - metastabilna stanja

1. Zakon termodinamike ali zakon o ohranitvi energije

Celotna energija sistema je konstantna. Skupna sprememba *notranje energije* je enaka vloženemu *delu* in spremembi *toplote*.

$\Delta U = Q - W = Q - p\Delta V \qquad W = p\Delta V$

$\Delta H = Q + V\Delta p$

$p = \text{konst.} \Rightarrow \Delta H = \Delta Q$

U	*notranja energija*
Q	*toplota*
W	*delo*
p	*tlak (pritisk)*
V	*volumen (prostornina)*
H	*entalpija*
$H^0{}_f$	*formacijska entalpija*

Spremembe *entalpije* (toplotne vsebnosti) posameznih procesov imajo svoja imena: izparilna toplota, reakcijska toplota, formacijska toplota... *Toplota formacije* neke komponente je sprememba toplote, ki nastane pri reakciji potrebnih elementov pod standardnimi pogoji (*ss = 25°C, 1 bar*).

$\Delta H^0{}_f = 0$ za elemente

2. Zakon termodinamike

Smer reakcije določata *toplotni tok* (pri večini reakcij se toplota oddaja) in stopnja urejenosti - *entropija*. Oba faktorja povezuje *Gibbsova funkcija*.
Reakcija poteka, če je upadanje Gibbsove funkcije zaradi spremembe urejenosti večja kot njeno naraščanje zaradi absorbcije toplote. Toplote ne moremo 100% efektno pretvoriti v delo. Pri obrnljivih (idealnih) procesih je absorbirana toplota enaka opravljenemu delu in produktu temperature in spremembe entropije.

$\Delta S = Q/T$

S	*entropija*
T	*temperatura*

Vrste reakcij:

- toplota se oddaja, urejenost se niža (viša se entopija) — *možno*
  primer: gorenje premoga
- toplota se oddaja, urejenost se viša — $Q>S$ — *možno*
  primer: voda prehaja v led
- toplota se sprejema, urejenost se niža — *možno*
  primer: voda prehaja v paro

toplota se sprejema, urejenost se viša — *ni možno*

3. zakon termodinamike

Vsaka popolnoma urejena in kristalizirana snov ima pri absolutni ničli (-273°C) enako entropijo. Entropijo snovi pri drugi temperaturi lahko izračunamo s pomočjo *specifične toplote*.

$\mathbf{c_p = dQ/dT}$

$\mathbf{\Delta S_T = \Delta S_{298K} + {}_{298}\int^T c_p/T\, dT}$

$\mathbf{\Delta H_T = \Delta H_{298K} + {}_{298}\int^T c_p\, dT}$

c_p	*specifična toplota*

298K = 25°C (ss)

Gibbsova funkcija

Standardna prosta energija formacije je sprememba *proste energije* zaradi nastanka komponente iz njenih gradbenih elementov pod standardnimi pogoji.

$\Delta H = T\Delta S + V\Delta p$

$\Delta G = V\Delta p - S\Delta T$

$\Delta G = \Delta H - T\Delta S$

$\Delta G_f = G_{produktov} - G_{reaktantov}$

$\Delta G_f = 0$ za elemente

Gf	*standardna prosta energija formacije ali standardna Gibbsova prosta energija*
G	*Gibbsova prosta energija*

Ravnotežje in ravnotežna konstanta

Smer poteka reakcije ugotovimo z Gibbsovo prosto energijo:

$\Delta G < 0$reakcija poteka v desno
$\Delta G = 0$reakcija je v ravnotežju
$\Delta G > 0$reakcija poteka v levo

Za idelano raztopino je pri dani temperaturi reakcije

$aA + bB \Leftrightarrow cC + dD$

ravnotežna konstanta (K):

$K = [C]^c[D]^d/[A]^a[B]^b$

[ ]	*koncentracija*
a,b...	*število ionov v reakciji*

Pri realnih raztopinah koncentracijo nadomestimo z *aktivnostjo (a)*. Aktivnosti trdnih snovi in navadno tudi vode so po dogovoru 1.

$\Delta G = -RT\ln K$

R = 8.31 J/mol deg

Topnost

Koncentracije so podane v enotah teža/teža (mg/kg = ppm = mg/l), teža/volumen (mg/l = ppm), molarnost (mM/l = (mg/l)/molska teža), mEq/l (upošteva količino naboja - npr.: $SO_4^{2-} \Rightarrow$ 2mM/l = mEq/l). *Topnost* določamo s pomočjo ravnotežne konstante, imenovane *topnostni produkt*. Topnost je enaka aktivnosti kationa ali aniona.

$AgCl \Leftrightarrow [Ag^+][Cl^-]$

K_{sp} = **produkti/reaktanti** $= [Ag^+][Cl^-]$

$s = [Ag^+] = [Cl^-] = \sqrt{K_{sp}}$

s	*topnost*
K_{sp}	*topnostni produkt*

pH

pH izraža aktivnost vodikovega iona.

$H_2O \Leftrightarrow H^+ + OH^-$

$pH = -\log[H^+]$

$[H^+] = 10^{-pH}$

Ravnotežna konstanta reakcije pri standardnih pogojih je

$K = [H^+][OH^-] = 10^{-14}$

pH je nevtralen (7), kadar je koncentracija (ali aktivnost) kationov eneka koncentraciji anionov. Raztopine s pH > 7 so bazične in s pH < 7 kisle.

Eh

$H_2 \Leftrightarrow 2H^+ + 2e^-$ $E^0 = 0.00V$

E^0 standardni potencial

Če neka snov reducira H^+ je po dogovoru E^0 negativen, če pa H_2 reducira neko snov in pri tem prehaja v H^+ je po dogovoru E^0 pozitiven. Reakcije z negativnim potencialom potekajo v levo, s pozitivnim pa v desno.

Pri standardnih pogojih za redoks reakcije velja

$\Delta G = -RTlnK = NE^0F$

N število elektonov (e^-)
F = 9650 J/mol (23.06 kcal/mol)

Redoks potencial je mera za tendenco raztopine, da dovoli nastop neke reakcije.

$Eh = E^0 + (RT/NF)lnK$

Pri standardnih pogojih velja:

$Eh = E^0 + (0.059/N)logK$

1.) Ali grafit lahko preide v diamant pri 1atm in a.) 25°C b.) 500°C?

2.) Katera faza je obstojna, kristalni kremen ali kremenovo steklo pri 1 atm in a.) 25°C b.) 1500°C?

3.) Kakšna je smer reakcije periklaz + kremen = enstatit pri 1atm in a.) 25oC b.) 500oC? Ali lahko pričakujemo, da se pri visokih temperaturah smer reakcije obrne?

4.) V procesu nastajanja osončja je utegnila biti pomembna reakcija med grafitom, vodikom in metanom: $C + 2H_2 = CH_4$. Kaj je obstojno pri a.) standardnih pogojih, b.) 500°C, c.) kakšna je temperatura ravnotežja?

5.) Kolika je standardna prosta Gibbsova energija nastanka galenita? Oceni G pri 1000°C.

6.) Kolikšen je G reakcije $Pb^{2+} + S^{2-} = PbS$ pri ss. Ocena pri 500°C. Koliko znaša ravnotežna konstanta?

7.) Izračunaj ravnotežno konstato pri standardnem stanju za reakcijo $N_2 + 2H_2 = 2NH_3$. Ali bo v vulkanskem plinu iz fumarole pri 250°C dušik navzoč predvsem kot amonijak, ali kot prosti dušik? G NH_3 je -16,7kJ/mol, S za NH_3 192,55, N_2 191,50 in H_2 130,6 J/mol,st.

8.) Apnenec, ki vsebuje kremen, preide pod vplivom kontaktne metamorfoze v wollastonit po reakciji: $CaCO_3 + SiO_2 = CaSiO_3 + CO_2$
a.) v katero smer teče reakcija pri standardnih pogojih?
b.) pri 650 K
c.) temperatura ravnotežja?

9.) Izračunaj G prehoda aragonita v kalcit pri ss. Kateri je obstojen? Kateri polimorf bo obstojen pri višjih temperaturah in zakaj? Oceni pri kateri T sta v ravnotežju? $V_{m,ca} = 36,93$ cm^3, $V_{m,ar} = 34,15$ cm^3; kateri bo obstojen pri visokih tlakih in zakaj? Pod 80 K ima aragonit nižjo G od kalcita. Skiciraj diagram obstojnostnih področij aragonita in kalcita v odvisnosti od P in T.

10a.) Izračunaj spremembo notranje energije (U) reakcije andaluzit = sillimanit pri ss. $V_{m,an} = 51,53$ in $V_{m,sil} = 49,90$ cm^3.
b.) kakšna je G pri teh pogojih?
c.) z enačbo $dG = VdP - SdT$ izrazi dP/dT za ravnotežje med obema.

11.) Domnevajo, da je bila za navzočnost kovinskega železa v procesu nastajanja osončja pomembna reakcija: $3Fe + 4H_2O = Fe_3O_4 + 4H_2$. Kam teče reakcija pri ss, kam pri 1000 K? Temperatura ravnotežja?

12.) Zračunaj G reakcije $CaSO_4.2H_2O = CaSO_4 + 2H_2O$ pri 25 in 50°C. Kateri mineral je stabilen pri 25 in kateri pri 50°C? Specifične toplote $c_{p,an} = 14,1 + 0,033T$cal/st.mol, $c_{p,sa} = 21,84 + 0,076T$ in $c_{p,aq} = 18,02$.

13.a) Zračunaj G in ravnotežno konstanto K za reakcijo: $2CaCO_3(ca) + Mg^{2+} = CaMg(CO_3)_2 + Ca^{2+}$
b.) zakaj te konstante ne moremo porabiti, da napovemo, v katero smer teče reakcija v morski vodi?
c.) kam bo tekla reakcija v morski vodi, če so tam koncentracije Ca^{2+} 0,0025 mol/kg in Mg^{2+} 0,017 mol/kg?

14.a) Zračunaj S pri segrevanju 1 mola vode od 0 do 100°C. Specifična toplota vode Cp = 18,02 cal/st.mol. b.) zračunaj S pri izparjenju 1 mola vode. Toplota izparjanja vode je 540cal/g.

15.) Kakšna je topnost $CaCO_3$ v morski vodi, če sta aktivnosti Ca^{2+} 0,0000054 in CO_3^{2-} 0,0025 mol/kg?

16.) Kakšna je topnost apnenca v vodi?

17.) Kakšna koncentracija Cu^{2+} je potrebna, da se iz morske vode obarja malahit? Aktivnost OH^- in karbonatnega iona je približno 10^{-6}.

18.a) Kakšna je topnost anhidrita v čisti vodi pri 25°C ?
b.) napiši izraz za K reakcije sadra = anhidrit. Privzemi, da je v reakciji udeležena izparevajoča morska voda z aktivnostjo manjšo od 1.
c.) Kateri mineral je obstojen pri ss?
d.) S poskusom so določili, da je K za reakcijo pod (b) pri 25°C 0,61 in pri 50°C 0,85. Na diagramu aktivnost-temperatura nariši obstojnostna območja sadre in anhidrita.

19.) Izračunaj ravnotežno konstanto za reakcijo: $2CaCO_3(kalcit) + Mg^{2+} = CaMg(CO_3)_2 + Ca^{2+}$ pri standardnih pogojih. b.) Zamisli si, da teče voda, ki vsebuje 10x več Ca^{2+} kakor Mg^{2+}, čez apnenec. Ali se bo tvoril dolomit namesto kalcita?

20.) Ali je na zemeljskem površju obstojen hematit ali siderit?
Reakcija: $2FeCO_3 + O_2 + 2H_2O = Fe_2O_3 + 2H_2CO_3$
G siderita je -674, H_2CO_3 pa -623,4 kJ/mol.

21.) Kakšna je koncentracija vodikovega iona v vodni raztopini s pH = 8,3 ?

22.) Koliko je pH raztopine s koncentracijo vodikovega iona 0,00002 mol/l.

23.) Kolika je vsebina vodikovih ionov v raztopini s pH 0?

24.) Kakšen je pH raztopine, v kateri je koncentracija OH^- 10-3,7mol/l?

25.) Koliko je Eh reakcije $Cu = Cu^{2+} + 2e^-$, če je aktivnost bakrovega iona 10^{-3}.

26.) Talnica ima vrednost pH = 7 in Eh = 0,6 V. Če se ta voda pretaka skozi svinčevo rudišče, koliko Pb^{2+} v raztopini je potrebno, da se začne obarjati PbO_2 ?
Reakcija: $Pb^{2+} + 2H_2O = PbO_2 + 4H^+ + 2e^-$ $E^\circ = 1{,}46$ V
b.) se bo količina oborjenega plattnerita zvečala ali zmanjšala, če postane raztopina alkalnejša?

27.a) V potoku so izmerili vrednost Eh 0,92V in pH 5,5. Katera oblika , Mn^{2+} ali Mn^{3+}, bo obilnejša v vodi? b.) Izračunaj razmerje Mn^{2+}/Mn^{3+} v vodi. c.) Nariši Eh - pH diagram.

28.a) Izračunaj vrednost E° za reakcijo: $2Fe^{2+} + 3H_2O = Fe_2O_3 + 6H^+ + 2e^-$
b.) načrtaj na diagramu Eh-pH premico, ki predstavlja to enačbo. Privzemi za Fe2+ vrednost 10^{-6}M.
c.) če teče prek ležišča hematita potok s pH 6 in Eh 0,47V, kakšna koncentracija železovih ionov v vodi bo v ravnotežju s hematitom?

29.) Voda vsebuje raztopljen CO_2 v naslednjih oblikah: H_2CO_3, HCO_3 in CO_3. Izračunaj razmerje med temi oblikami pri pH 6, 8,3 in 10. Reakcije in ravnotežne konstante so:
$H_2CO_3 = H^+ + HCO_3$ $K_1=10^{-6,4}$
$HCO_3 = H^+ + CO_3$ $K_2=10^{-10,3}$
b.) Oceni koncentracije H_2CO_3, HCO_3 in CO_3 v raztopini pri pH 7 in skupnem raztopljenem CO_2 0,001 mol.

30.) Podzemna voda, ki privre na dan, začne obarjati kalcijev karbonat. Zakaj?

31.) Kakšna koncentracija Fe^{2+} je lahko v stiku z $Fe(OH)_3$ pri pH 6,5 in +Eh 0,3V, ter pH 8,4 in Eh -0,3V?

Element	Symbol	Atomic number	Atomic weight
Silver	Ag	47	107.87
Sodium	Na	11	22.99
Strontium	Sr	38	87.62
Sulfur	S	16	32.06
Tantalum	Ta	73	180.95
Tellurium	Te	52	127.60
Terbium	Tb	65	158.93
Thallium	Tl	81	204.37
Thorium	Th	90	232.04
Thulium	Tm	69	168.93
Tin	Sn	50	118.69
Titanium	Ti	22	47.90
Tungsten	W	74	183.85
Uranium	U	92	238.03
Vanadium	V	23	50.94
Xenon	Xe	54	131.30
Ytterbium	Yb	70	173.04
Yttrium	Y	39	88.91
Zinc	Zn	30	65.38
Zirconium	Zr	40	91.22

APPENDIX VI

IONIC RADII AND ELECTRONEGATIVITIES

Element	Ion[1]	Radius for 6-coordination, octahedral (Å)[2]	Commonly occurring coordination numbers[3]	Electro-negativity[4]	Approximate ionic character of bond with oxygen[5]
Aluminum	Al^{3+}	0.535	4, 6	1.5	60
Antimony	Sb^{3+}	0.80 (5)	6		66
	Sb^{5+}	0.60	4, 6	1.9	48
Arsenic	As^{3+}	0.58	4, 6		60
	As^{5+}	0.46	4, 6	2.0	38
Barium	Ba^{2+}	1.35	8–12	0.9	84
Beryllium	Be^{2+}	0.27 (4)	4	1.5	63
Bismuth	Bi^{3+}	1.03	6, 8	1.9	66
Boron	B^{3+}	0.11 (4)	3, 4	2.0	43
Bromine	Br^{-}	1.96		2.8	
Cadmium	Cd^{2+}	0.95	6, 8	1.7	66
Calcium	Ca^{2+}	1.00	6, 8	1.0	79
Carbon	C^{4+}	0.15 (4)	3, 4, 6	2.5	23
Cerium	Ce^{3+}	1.01	6, 8	1.1	74
Cesium	Cs^{+}	1.67	12	0.7	89
Chlorine	Cl^{-}	1.81		3.0	
Chromium	Cr^{3+}	0.615	6	1.6	53
	Cr^{6+}	0.26			23
Cobalt	Co^{2+}	0.745	6	1.8	65
Copper	Cu^{+}	0.77	6, 8	1.9	71
	Cu^{2+}	0.73	6	2.0	57
Fluorine	F^{-}	1.33		4.0	

(Continued)

Element	Ion[1]	Radius for 6-coordination, octahedral (Å)[2]	Commonly occurring coordination numbers[3]	Electro-negativity[4]	Approximate ionic character of bond with oxygen[5]
Gallium	Ga^{3+}	0.62	4, 6	1.6	57
Germanium	Ge^{4+}	0.73	4	1.8	49
Gold	Au^{+}	1.37	8–12	2.4	62
Hafnium	Hf^{4+}	0.71	6	1.3	70
Indium	In^{3+}	0.80	6	1.7	62
Iodine	I^{-}	2.20		2.5	
	I^{5+}	0.95	6		54
Iron	Fe^{2+}	0.78	6	1.8	69
	Fe^{3+}	0.643	6	1.9	54
Lanthanum	La^{3+}	1.032	8	1.1	77
Lead	Pb^{2+}	1.19	6–10	1.8	72
Lithium	Li^{+}	0.76	6	1.0	82
Magnesium	Mg^{2+}	0.72	6	1.2	71
Manganese	Mn^{2+}	0.83	6	1.5	72
	Mn^{3+}	0.645	6		51
	Mn^{4+}	0.53	4, 6		38
Mercury	Hg^{2+}	1.02	6, 8	1.9	62
Molybdenum	Mo^{4+}	0.65	6		58
	Mo^{6+}	0.59	4, 6	1.8	47
Nickel	Ni^{2+}	0.69	6	1.8	60
Niobium	Nb^{5+}	0.64	6	1.6	56
Nitrogen	N^{5+}	0.13	3	3.0	9
Oxygen	O^{2-}	1.40		3.5	
Palladium	Pd^{2+}	0.86	6	2.2	61
Phosphorus	P^{5+}	0.17 (4)	4	2.1	35
Potassium	K^{+}	1.38	8–12	0.8	87
Radium	Ra^{2+}	1.48	8–12	0.9	83
Rare-earth metals	Ce^{3+}–Sm^{3+}	1.01–0.958	6, 8	1.1–1.2	73–75
	Eu^{3+}–Lu^{3+}	0.947–0.861	6	1.2	76
	Eu^{2+}	1.17	8		
Rhenium	Re^{4+}	0.63	6		63
	Re^{7+}	0.53	4, 6		51
Rubidium	Rb^{+}	1.52	8–12	0.8	87
Scandium	Sc^{3+}	0.745	6	1.3	65
Selenium	Se^{2-}	1.98		2.4	
	Se^{6+}	0.28	4		26
Silicon	Si^{4+}	0.26 (4)	4	1.8	48
Silver	Ag^{+}	0.94	8, 10	1.9	71
Sodium	Na^{+}	1.02	6, 8	0.9	83
Strontium	Sr^{2+}	1.18	8	1.0	82
Sulfur	S^{2-}	1.84		2.5	
	S^{6+}	0.12 (4)	4		20
Tantalum	Ta^{5+}	0.64	6	1.5	63
Tellurium	Te^{2-}	2.21		2.1	
	Te^{6+}	0.56	4, 6		36

(Continued)

Element	Ion[1]	Radius for 6-coordination, octahedral (Å)[2]	Commonly occurring coordination numbers[3]	Electro-negativity[4]	Approximate ionic character of bond with oxygen[5]
Thallium	Tl^{+}	1.50	8–12		79
	Tl^{3+}	0.67	6, 8	1.8	58
Thorium	Th^{4+}	0.94	6, 8	1.3	72
Tin	Sn^{2+}	1.27 (8)	6, 8	1.8	73
	Sn^{4+}	0.69	6	1.9	57
Titanium	Ti^{3+}	0.67	6		60
	Ti^{4+}	0.605	6	1.5	51
Tungsten	W^{6+}	0.60	4, 6	1.7	57
Uranium	U^{4+}	1.00 (8)	6, 8		68
	U^{6+}	0.73	6	1.7	62
Vanadium	V^{3+}	0.64	6	1.6	57
	V^{4+}	0.58	6		45
	V^{5+}	0.54	4, 6		36
Yttrium	Y^{3+}	0.90	6	1.2	74
Zinc	Zn^{2+}	0.74	4, 6	1.7	63
Zirconium	Zr^{4+}	0.72	6	1.4	65

---

[1] Only ions commonly found in naturally occurring minerals are listed.

[2] *Sources:* Shannon, R. D.: "Revised effective ionic radii and systematic studies of interatomic distances in halides and chalcogenides," *Acta Cryst.*, A32, p. 751–767, 1976, and Shannon, R. D., and C. T. Prewitt: "Effective ionic radii in oxides and fluorides," *Acta Cryst.*, B25, pp. 925–946, 1968. All are radii for 6-coordination except a few for which a different coordination is indicated by a number in parentheses. In general, radii for 4-coordination can be estimated from the 6-coordination radii by subtracting 0.13 Å, and radii for 8-coordination by adding 0.13 Å; for most ions these rules give radii within 0.02 Å of the correct values.

[3] *Source:* Smith, F. G.: *Physical Geochemistry*, Addison-Wesley, Reading, Massachusetts 1963.

[4] *Source:* Pauling, L.: *The Nature of the Chemical Bond*, 3d ed., Copyright © by Cornell University. Used by permission of the publisher, Cornell University Press, N.Y., 1960. The numbers are in arbitrary units, ranging from 0.7 for Cs to 4.0 for F.

[5] *Source:* Smith, *op. cit.*, calculated by Smith from electronegativity values estimated by A. S. Povarennykh, *Dokl. Akad. Nauk SSSR*, vol. 109, pp. 993–996, 1956.

APPENDIX VIII

STANDARD FREE ENERGIES, ENTHALPIES, AND ENTROPIES

Standard state thermodynamic data for geologic substances come from a bewildering array of sources. A variety of experimental and theoretical techniques have been used to obtain the data, and the results are continually modified by new experiments and theoretical algorithms. In the table below, values for standard molal Gibbs free energies, enthalpies, and third-law entropies are those recommended by the National Bureau of Standards for inorganic substances commonly encountered in geochemistry. A full discussion of available data bases can be found in Chapter 12 and Appendix D of Nordstrom, D. K., and J. L. Munoz: *Geochemical Thermodynamics*, The Benjamin/Cummings Publishing Co., 1985.

The second column of the table gives the physical state of each substance, insofar as it is known. Abbreviations: s, solid, form not specified in source; l, liquid; g, gas; aq, dissolved in water at unit activity. The columns headed ΔG° and ΔH° give standard free energies and enthalpies of formation from the elements at 25°C and 1 bar, in kilojoules per mol. The column headed S° gives entropies in standard entropy units, joules per mol per degree kelvin. To find the standard free energy change for a reaction, subtract the sum of ΔG° values for the reactants from the sum of ΔG° for the products [Eqs. (7-49) and (7-67)]. To find the equilibrium constant for a reaction at 25°C and 1 bar, use the relation [Eq. (8-49)]

$$\log K = -\Delta G^\circ / 5709.$$

By using this equation in reverse, approximate free energies of formation for many compounds and ions not given in the table may be calculated from the equilibrium constants in Appendix VII. Numbers in the table are of widely varying accuracy, and are subject to continual revision as new data are reported in the literature.

At temperatures greater than 25°C, approximate values for standard Gibbs free energies of reaction (ΔG°_T) can be found from the equation

$$\Delta G^\circ_T = \Delta H^\circ - 0.001 T \Delta S^\circ,$$

on the assumption that ΔH° and ΔS° are constant (or that $\Delta C^\circ_p \approx 0$). If the heat capacity of the reaction is small, as it is for most solid–solid reactions, this equation will give a close estimate of ΔG°_T for temperatures to a few hundred degrees. To find free energies at higher temperatures, or in general to obtain accurate values for thermodynamic properties of a reaction at elevated temperatures and pressures, requires additional information on the variation of heat capacity and volume of all substances in the reaction [cf. Eqs. (7-41), (7-62), (8-18), and Prob. 8-8].

kJmol kJmol Jmol/deg

Formula	**Form**	ΔG°	ΔH°	S°
	Aluminum			
Al	**s**	0	0	28.3
Al_2O_3	**corundum**	−1582.3	−1675.7	50.9
AlOOH	**boehmite**	−915.9	−990.9	48.5
$Al(OH)_3$	**gibbsite**	−1155.1	−1293.3	68.5
$Al_2Si_2O_5(OH)_4$	**kaolinite**	−3799.7	−4119.6	205.0
Al^{3+}	**aq**	−485	−531	−321.7
$Al(OH)_4^-$	**aq**	−1305.3	−1502.5	102.9
	Arsenic			
As	**metallic**	0	0	35.1
As	**gas**	+261.0	+302.5	174.2
As_4O_6	**arsenolite**	−1152.4	−1313.9	214.2
As_2O_5	**s**	−782.3	−924.9	105.4
AsH_3	**g**	+68.9	+66.4	222.8
As_2S_3	**orpiment**	−168.6	−169.0	163.6
H_3AsO_3	**aq**	−639.8	−742.2	195.0
H_3AsO_4	**aq**	−766.0	−902.5	184.
$H_2AsO_4^-$	**aq**	−587.1	−714.8	110.5
AsO_4^{3-}	**aq**	−648.4	−888.1	−162.8
	Barium			
Ba	**s**	0	0	62.8
BaO	**s**	−525.1	−553.5	70.4
BaF_2	**s**	−1156.8	−1207.1	96.4
BaS	**s**	−456.	−460.	78.2
$BaSO_4$	**barite**	−1362.2	−1473.2	132.2
$BaCO_3$	**witherite**	−1137.6	−1216.3	112.1
$BaSiO_3$	**s**	−1540.2	−1623.6	109.6
Ba^{2+}	**aq**	−560.8	−537.6	9.6
	Boron			
B	**s**	0	0	62.8
B_2O_3	**s**	−1193.7	−1272.8	54.0
H_3BO_3	**s**	−968.9	−1094.3	88.9
$H_4BO_4^-$	**aq**	−1153.2	−1344.0	102.5

(Continued)

Formula	Form	ΔG°	ΔH°	S°
Cadmium				
Cd	s	0	0	51.8
CdO	s	−228.4	−258.2	54.8
$Cd(OH)_2$	precipitated	−473.6	−560.7	96.
CdS	greenockite	−156.5	−161.9	64.9
$CdCO_3$	otavite	−669.4	−750.6	92.5
$CdSiO_3$	s	−1105.4	−1189.1	97.5
Cd^{2+}	aq	−77.6	−75.9	−73.2
Calcium				
Ca	s	0	0	41.4
CaO	s	−604.0	−635.1	39.8
$Ca(OH)_2$	portlandite	−898.5	−986.1	83.4
CaF_2	fluorite	−1167.3	−1219.6	68.9
CaS	s	−477.4	−482.4	56.5
$CaCO_3$	calcite	−1128.8	−1206.9	92.9
$CaCO_3$	aragonite	−1127.8	−1207.1	88.7
$CaMg(CO_3)_2$	dolomite	−2163.4	−2326.3	155.2
$CaSO_4$	anhydrite	−1321.8	−1434.1	106.7
$CaSO_4.2H_2O$	gypsum	−1797.3	−2022.6	194.1
$Ca_3(PO_4)_2$	whitlockite	−3884.7	−4120.8	236.0
$CaSiO_3$	wollastonite	−1549.7	−1634.9	81.9
$CaAl_2Si_2O_8$	anorthite	−4002.3	−4227.9	199.3
$CaMgSi_2O_6$	diopside	−3032.0	−3206.2	142.9
Ca^{2+}	aq	−553.6	−542.8	−53.1
Carbon				
C	graphite	0	0	5.7
C	diamond	2.9	1.9	2.4
CH_4	g	−50.7	−74.8	186.3
C_2H_6	g	−32.8	−84.7	229.6
C_3H_8	g	−23.5	−104.0	270.0
C_4H_{10}	g	−17.2	−126.1	310.4
C_2H_4	g	+68.2	+52.3	219.6
C_6H_6	l	+129.8	+83.0	269.2
CO	g	−137.2	−110.5	197.7
CO_2	g	−394.4	−393.5	213.7
H_2CO_3	aq	−623.1	−699.7	187.4
HCO_3^-	aq	−586.8	−692.0	91.2
CO_3^{2-}	aq	−527.8	−677.1	−56.9
CN^-	aq	+172.4	+150.6	94.1
Chlorine				
Cl_2	g	0	0	223.1
HCl	g	−95.3	−92.3	186.9
Cl^-	aq	−131.3	−167.2	56.5
Chromium				
Cr	s	0	0	23.8
$FeCr_2O_4$	chromite	−1343.8	−1444.7	146.0
CrO_4^{2-}	aq	−727.8	−881.2	50.2
$Cr_2O_7^{2-}$	aq	−1301.1	−1490.3	261.9
Copper				
Cu	s	0	0	33.2
Cu_2O	cuprite	−146.0	−168.6	93.1

(Continued)

Formula	Form	ΔG°	ΔH°	S°
CuO	tenorite	−129.7	−157.3	42.6
$Cu(OH)_2$	s	−357.		
CuCl	s	−119.9	−137.2	86.2
Cu_2S	chalcocite	−86.2	−79.5	120.9
CuS	covellite	−53.6	−53.1	66.5
$Cu_2(OH)_2CO_3$	malachite	−893.6	−1051.4	186.2
Cu^+	aq	+50.0	+71.7	40.6
Cu^{2+}	aq	+65.5	+64.8	−99.6
$CuCl_2^-$	aq	−240.1		
Fluorine				
F_2	g	0	0	202.8
HF	g	−273.2	−271.1	173.8
HF	aq	−296.8	−320.1	88.7
F^-	aq	−278.8	−332.6	−13.8
Gold				
Au	s	0	0	47.4
$AuCl_2^-$	aq	−151.1		
$AuCl_4^-$	aq	−235.1	−322.2	266.9
$Au(CN)_2^-$	aq	+285.8	+242.3	172.
Hydrogen				
H_2	g	0	0	130.7
H^+	aq	0	0	0
Iron				
Fe	s	0	0	27.3
$Fe_{0.947}O$	wüstite	−245.1	−266.3	57.5
Fe_3O_4	magnetite	−1015.4	−1118.4	146.4
Fe_2O_3	hematite	−742.2	−824.2	87.4
$Fe(OH)_2$	precipitate	−486.5	−569.0	88.
$Fe(OH)_3$	precipitate	−696.5	−823.0	106.7
FeS	troilite	−100.4	−100.0	60.3
Fe_7S_8	pyrrhotite	−748.5	−736.4	485.8
FeS_2	pyrite	−166.9	−178.2	52.9
$FeCO_3$	siderite	−666.7	−740.6	92.9
Fe_2SiO_4	fayalite	−1379.0	−1479.9	145.2
Fe^{2+}	aq	−78.9	−89.1	−137.7
Fe^{3+}	aq	−4.7	−48.5	−315.9
Lead				
Pb	s	0	0	64.8
Pb	g	+161.9	+195.0	175.4
PbO	s (red)	−188.9	−219.0	66.5
PbO_2	s	−217.3	−277.4	68.6
$Pb(OH)_2$	s	−452.2		
$PbCl_2$	cotunnite	−314.1	−359.4	136.0
PbS	galena	−98.7	−100.4	91.2
$PbSO_4$	anglesite	−813.1	−919.9	148.6
$PbCO_3$	cerussite	−625.5	−699.1	131.0
$PbSiO_3$	s	−1062.1	−1145.7	109.6
Pb^{2+}	aq	−24.4	−1.7	10.5
$Pb(OH)_3^-$	aq	−575.6		

(Continued)

Formula	Form	ΔG°	ΔH°	S°
Magnesium				
Mg	s	0	0	32.7
MgO	periclase	−569.4	−601.7	26.9
$Mg(OH)_2$	brucite	−833.5	−924.5	63.2
MgF_2	sellaite	−1070.2	−1123.4	57.2
MgS	s	−341.8	−346.0	50.3
$MgCO_3$	magnesite	−1012.1	−1095.8	65.7
$MgCO_3.3H_2O$	nesquehonite	−1726.1		
$MgSiO_3$	clinoenstatite	−1462.1	−1549.0	67.7
Mg_2SiO_4	forsterite	−2055.1	−2174.0	95.1
Mg^{2+}	aq	−454.8	−466.9	−138.1
Manganese				
Mn	s	0	0	32.0
MnO	manganosite	−362.9	−385.2	59.7
Mn_3O_4	hausmannite	−1283.2	−1387.8	155.6
Mn_2O_3	s	−881.1	−959.0	110.5
MnO_2	pyrolusite	−465.1	−520.0	53.1
$Mn(OH)_2$	precipitate	−615.0	−695.4	99.2
MnS	alabandite	−218.4	−214.2	78.2
$MnCO_3$	rhodochrosite	−816.7	−894.1	85.8
$MnSiO_3$	rhodonite	−1240.5	−1320.9	89.1
Mn_2SiO_4	tephroite	−1632.1	−1730.5	163.2
Mn^{2+}	aq	−228.1	−220.8	−73.6
MnO_4^-	aq	−447.2	−541.4	191.2
Mercury				
Hg	l	0	0	76.0
Hg	g	+31.8	+61.3	175.0
HgO	s, red	−58.5	−90.8	70.3
Hg_2Cl_2	calomel	−210.7	−265.2	192.5
HgS	cinnabar	−50.6	−58.2	82.4
Hg_2^{2+}	aq	+153.5	+172.4	84.5
Hg^{2+}	aq	+164.4	+171.1	−32.2
$HgCl_4^{2-}$	aq	−446.8	−554.0	293.
Hg_2^{2-}	aq	+41.9		
Molybdenum				
Mo	s	0	0	28.7
MoO_3	s	−668.0	−745.1	77.7
MoS_2	molybdenite	−225.9	−235.1	62.6
$CaMoO_4$	powellite	−1434.6	−1541.4	122.6
MoO_4^{2-}	aq	−836.3	−997.9	27.2
Nickel				
Ni	s	0	0	29.9
NiO	s	−211.7	−239.7	38.0
$Ni(OH)_2$	s	−447.2	−529.7	88.
NiS	s	−79.5	−82.0	53.0
$NiCO_3$	s	−612.5		
Ni^{2+}	aq	−45.6	−54.0	−128.9
Nitrogen				
N_2	g	0	0	191.6
N_2O	g	+104.2	+82.1	219.9

(Continued)

Formula	Form	ΔG°	ΔH°	S°
NO	g	+86.6	+90.3	210.8
NH_3	g	−16.5	−46.1	192.5
NH_4OH	aq	−263.7	−366.1	181.2
NO_3^-	aq	−108.7	−205.0	146.4
NH_4^+	aq	−79.3	−132.5	113.4
Oxygen				
O_2	g	0	0	205.1
H_2O	l	−237.1	−285.8	69.9
H_2O	g	−228.6	−241.8	188.8
OH^-	aq	−157.2	−230.0	−10.8
Potassium				
K	s	0	0	64.2
KCl	sylvite	−409.1	−436.7	82.6
$KAlSiO_4$	kaliophilite	−2005.3	−2121.3	133.1
$KAlSi_2O_6$	leucite	−2871.4	−3034.2	200.0
$KAlSi_3O_8$	microcline	−3742.9	−3968.1	214.2
$KAl_3Si_3O_{10}(OH)_2$	muscovite	−5608.4	−5984.4	306.3
K^+	aq	−283.3	−252.4	102.5
Silicon				
Si	s	0	0	18.8
SiO_2	α-quartz	−856.6	−910.9	41.8
SiO_2	α-cristobalite	−855.4	−909.5	42.7
SiO_2	α-tridymite	−855.3	−909.1	43.5
SiO_2	glass	−850.7	−903.5	46.9
$SiCl_4$	g	−617.0	−657.0	330.7
SiF_4	g	−1572.7	−1614.9	282.5
SiH_4	g	+56.9	+34.3	204.6
H_4SiO_4	aq	−1316.6	−1468.6	180.
Silver				
Ag	s	0	0	42.6
Ag_2O	s	−11.2	−31.1	121.3
AgCl	cerargyrite	−109.8	−127.1	96.2
Ag_2S	acanthite	−40.7	−32.6	144.0
Ag^+	aq	+77.1	+105.6	72.7
$AgCl_2^-$	aq	−215.4	−245.2	231.4
Sodium				
Na	s	0	0	51.2
NaCl	halite	−384.1	−411.2	72.1
$NaAlSiO_4$	nepheline	−1978.1	−2092.8	124.3
$NaAlSi_2O_6$	jadeite	−2852.1	−3030.9	133.5
$NaAlSi_3O_8$	low albite	−3711.5	−3935.1	207.4
$NaAlSi_2O_6.H_2O$	analcite	−3082.6	−3300.8	234.3
Na^+	aq	−261.9	−240.1	59.0
Strontium				
Sr	s	0	0	52.3
SrO	s	−561.9	−592.0	54.4
$SrSO_4$	celestite	−1340.9	−1453.1	117.
$SrCO_3$	strontianite	−1140.1	−1220.1	97.1
$SrSiO_3$	c	−1549.7	−1633.9	96.7
Sr^{2+}	aq	−559.5	−545.8	−32.6

(Continued)

Formula	Form	ΔG°	ΔH°	S°
	Sulfur			
S	s, orthorhombic	0	0	31.8
S_2	g	+79.3	+128.4	228.2
H_2S	g	−33.6	−20.6	205.8
H_2S	aq	−27.8	−39.7	121.
SO_2	g	−300.2	−296.8	248.2
SO_3	g	−371.1	−395.7	256.8
S^{2-}	aq	+85.8	+33.1	−14.6
HS^-	aq	+12.1	−17.6	62.8
SO_4^{2-}	aq	−744.5	−909.3	20.1
HSO_4^-	aq	−755.9	−887.3	131.8
	Tin			
Sn	s	0	0	51.6
SnO	s	−256.9	−285.8	56.5
SnO_2	cassiterite	−519.6	−580.7	52.3
$Sn(OH)_2$	precipitated	−491.6	−561.1	155.
$SnCl_4$	g	−432.2	−471.5	365.8
SnS	s	−98.3	−100.	77.0
Sn^{2+}	aq	−27.2	−8.8	−17.
Sn^{4+}	aq	+2.5	+30.5	−117.
SnOHCl	aq	−392.0	−453.5	−126.
	Titanium			
Ti	s	0	0	30.6
TiO_2	anatase	−884.5	−939.7	49.9
TiO_2	rutile	−889.5	−944.7	50.3
$TiCl_4$	g	−726.7	−763.2	354.9
	Uranium			
U	g	0	0	50.2
UO_2	uraninite	−1031.7	−1084.9	77.0
UO_3	s	−1145.9	−1223.8	96.1
$UO_2(OH)_2$	s	−1394.8	−1533.9	126.
UF_6	g	−2063.7	−2147.4	377.9
U^{4+}	aq	−531.0	−591.2	−410.
UO_2^{2+}	aq	−953.5	−1019.6	−97.5
	Zinc			
Zn	s	0	0	41.6
Zn	g	+95.1	+130.7	161.0
ZnO	zincite	−318.3	−348.3	43.6
$Zn(OH)_2$	s	−553.5	−641.9	81.2
ZnS	sphalerite	−201.3	−206.0	57.7
$ZnCO_3$	smithsonite	−731.5	−812.8	82.4
Zn_2SiO_4	willemite	−1523.2	−1636.7	131.4
Zn^{2+}	aq	−147.1	−153.9	−112.1
$Zn(OH)_4^{2-}$	aq	−858.5		

Source: Wagman, D. D., W. H. Evans, V. B. Parker, R. H. Schumm, I. Halow, S. M. Bailey, K. L. Churney, and R. L. Nuttall: "NBS tables of chemical thermodynamic properties," *Journal of Physical and Chemical Reference Data,* vol. 11, supplement No. 2, 1982.

Another excellent source of similar data is Robie, R. A., B. S. Hemingway, and J. R. Fisher: "Thermodynamic properties of minerals and related substances at 298.15 K and 1 bar pressure and at higher temperatures," *U.S. Geol. Survey Bull.* 1452, 1979.

APPENDIX IX

STANDARD ELECTRODE POTENTIALS

The value of E° for each half-reaction is its potential in volts referred to the H_2–H^+ half-reaction, which is assigned the arbitrary value zero. The values are given for 25°C and 1 bar, with all substances at unit activity. Pure substances whose state is not specified in the equations are assumed to be in their standard states at 25°C and 1 bar.

The equation for each couple is written so that the reducing agent is at the left. Potential differences for complete reactions may be obtained by subtracting potentials for the appropriate half-reactions, provided that formulas of oxidizing and reducing agents are identical in the half-reactions and the complete reaction. E° values for half-reactions not shown in the table may be calculated from the free energies in Appendix VIII, by using the equation $E^\circ = \Delta G^\circ/96.5\mathbf{n}$, where **n** is the coefficient of e^- in the half-reaction.

Potentials in acid solutions	
$K \rightleftharpoons K^+ + e^-$	−2.93
$Ca \rightleftharpoons Ca^{2+} + 2e^-$	−2.87
$Na \rightleftharpoons Na^+ + e^-$	−2.71
$Mg \rightleftharpoons Mg^{2+} + 2e^-$	−2.37
$Th \rightleftharpoons Th^{4+} + 4e^-$	−1.90
$Al \rightleftharpoons Al^{3+} + 3e^-$	−1.67

(Continued)

Potentials in acid solutions	
$U \rightleftharpoons U^{4+} + 4e^-$	−1.38
$Mn \rightleftharpoons Mn^{2+} + 2e^-$	−1.18
$Si + 2H_2O \rightleftharpoons SiO_2 + 4H^+ + 4e^-$	−0.99
$Zn \rightleftharpoons Zn^{2+} + 2e^-$	−0.76
$Cr \rightleftharpoons Cr^{3+} + 3e^-$	−0.74
$Fe \rightleftharpoons Fe^{2+} + 2e^-$	−0.41
$H_2Se \rightleftharpoons Se + 2H^+ + 2e^-$	−0.40
$Co \rightleftharpoons Co^{2+} + 2e^-$	−0.28
$Ni \rightleftharpoons Ni^{2+} + 2e^-$	−0.24
$Sn \rightleftharpoons Sn^{2+} + 2e^-$	−0.14
$Pb \rightleftharpoons Pb^{2+} + 2e^-$	−0.13
$H_2 \rightleftharpoons 2H^+ + 2e^-$	−0.00
$H_2S(aq) \rightleftharpoons S + 2H^+ + 2e^-$	+0.14
$Sn^{2+} \rightleftharpoons Sn^{4+} + 2e^-$	+0.15
$Cu^+ \rightleftharpoons Cu^{2+} + e^-$	+0.15
$S^2 + 4H_2O \rightleftharpoons SO_4^{2-} + 8H^+ + 8e^-$	+0.16
$H_2SO_3(aq) + H_2O \rightleftharpoons SO_4^{2-} + H^+ + 2e^-$	+0.17
$Ag + Cl^- \rightleftharpoons AgCl + e^-$	+0.22
$As + 2H_2O \rightleftharpoons HAsO_2(aq) + 3H^+ + 3e^-$	+0.25
$U^{4+} + 2H_2O \rightleftharpoons UO_2^{2+} + 4H^+ + 2e^-$	+0.27
$Cu \rightleftharpoons Cu^{2+} + 2e^-$	+0.33
$S + 3H_2O \rightleftharpoons H_2SO_3(aq) + 4H^+ + 4e^-$	+0.45
$Cu \rightleftharpoons Cu^+ + e^-$	+0.52
$2I^- \rightleftharpoons I_2(s) + 2e^-$	+0.54
$3I^- \rightleftharpoons I_3^- + 2e^-$	+0.54
$HAsO_2(aq) + 2H_2O \rightleftharpoons H_3AsO_4 + 2H^+ + 2e^-$	+0.57
$Pd + 4Cl^- \rightleftharpoons PdCl_4^{2-} + 2e^-$	+0.59
$Pt + 4Cl^- \rightleftharpoons PtCl_4^{2-} + 2e^-$	+0.76
$Se + 3H_2O \rightleftharpoons H_2SeO_3(aq) + 4H^+ + 4e^-$	+0.74
$Fe^{2+} \rightleftharpoons Fe^{3+} + e^-$	+0.77
$2Hg \rightleftharpoons Hg_2^{2+} + 2e^-$	+0.80
$Ag \rightleftharpoons Ag^+ + e^-$	+0.80
$Hg \rightleftharpoons Hg^{2+} + 2e^-$	+0.85
$Pd \rightleftharpoons Pd^{2+} + 2e^-$	+0.95
$NO(g) + 2H_2O \rightleftharpoons NO_3^- + 4H^+ + 3e^-$	+0.96
$Fe^{2+} + 3H_2O \rightleftharpoons Fe(OH)_3 + 3H^+ + e^-$	+0.97
$Au + 4Cl^- \rightleftharpoons AuCl_4^- + 3e^-$	+1.00
$2Br^- \rightleftharpoons Br_2(l) + 2e^-$	+1.07
$2Br^- \rightleftharpoons Br_2(aq) + 2e^-$	+1.09
$HgS \rightleftharpoons S + Hg^{2+} + 2e^-$	+1.11
$H_2SeO_3(aq) + H_2O \rightleftharpoons SeO_4^{2-} + 4H^+ + 2e^-$	+1.15
$\frac{1}{2}I_2(s) + 3H_2O \rightleftharpoons IO_3^- + 6H^+ + 5e^-$	+1.20
$2H_2O \rightleftharpoons O_2 + 4H^+ + 4e^-$	+1.23

(Continued)

Potentials in acid solutions	
$Mn^{2+} + 2H_2O \rightleftharpoons MnO_2(s) + 4H^+ + 2e^-$	+1.23
$2Cr^3 + 7H_2O \rightleftharpoons Cr_2O_7^{2-} + 14H^+ + 6e^-$	+1.35
$2Cl^- \rightleftharpoons Cl_2 + 2e^-$	+1.36
$Pb^{2+} + 2H_2O \rightleftharpoons PbO_2(s) + 4H^+ + 2e^-$	+1.46
$Au \rightleftharpoons Au^{3+} + 3e^-$	+1.50
$Mn^{2+} + 4H_2O \rightleftharpoons MnO_4^- + 8H^+ + 5e^-$	+1.51
$Mn^{2+} \rightleftharpoons Mn^{3+} + e^-$	+1.54
$Au \rightleftharpoons Au^+ + e^-$	+1.69
$Co^{2+} \rightleftharpoons Co^{3+} + e^-$	+1.83
$2F^- \rightleftharpoons F_2(g) + 2e^-$	+2.89

Potentials in basic solution	
$Mg + 2OH^- \rightleftharpoons Mg(OH)_2 + 2e^-$	−2.69
$Al + 4OH^- \rightleftharpoons Al(OH)_4^- + 3e^-$	−2.33
$U + 4OH^- \rightleftharpoons UO_2 + 2H_2O + 4e^-$	−2.27
$Mn + 2OH^- \rightleftharpoons Mn(OH)_2 + 2e^-$	−1.56
$Zn + 2OH^- \rightleftharpoons Zn(OH)_2 + 2e^-$	−1.24
$SO_3^{2-} + 2OH^- \rightleftharpoons SO_4^{2-} + H_2O + 2e^-$	−0.93
$Sn(OH)_3^- + 3OH^- \rightleftharpoons Sn(OH)_6^{2-} + 2e^-$	−0.93
$Se^{2-} \rightleftharpoons Se + 2e^-$	−0.92
$Sn + 3OH^- \rightleftharpoons Sn(OH)_3^- + 2e^-$	−0.91
$Fe + 2OH^- \rightleftharpoons Fe(OH)_2 + 2e^-$	−0.89
$H_2 + 2OH^- \rightleftharpoons 2H_2O + 2e^-$	−0.83
$Fe(OH)_2 + OH^- \rightleftharpoons Fe(OH)_3 + e^-$	−0.55
$Pb + 3OH^- \rightleftharpoons Pb(OH)_3^- + 2e^-$	−0.54
$S^{2-} \rightleftharpoons S + 2e^-$	−0.44
$2Cu + 2OH^- \rightleftharpoons Cu_2O + H_2O + 2e^-$	−0.36
$Cr(OH)_3 + 5OH^- \rightleftharpoons CrO_4^{2-} + 4H_2O + 3e^-$	−0.13
$Cu_2O + 2OH^- + H_2O \rightleftharpoons 2Cu(OH)_2 + 2e^-$	−0.09
$Mn(OH)_2 + 2OH^- \rightleftharpoons MnO_2 + 2H_2O + 2e^-$	−0.05
$SeO_3^{2-} + 2OH^- \rightleftharpoons SeO_4^{2-} + H_2O + 2e^-$	+0.05
$Hg + 2OH^- \rightleftharpoons HgO(red) + H_2O + 2e^-$	+0.10
$Mn(OH)_2 + OH^- \rightleftharpoons Mn(OH)_3 + e^-$	+0.10
$Co(OH)_2 + OH^- \rightleftharpoons Co(OH)_3 + e^-$	+0.17
$PbO(red) + 2OH^- \rightleftharpoons PbO_2 + H_2O + 2e^-$	+0.25
$I^- + 6OH^- \rightleftharpoons IO_3^- + 3H_2O + 6e^-$	+0.26
$4OH^- \rightleftharpoons O_2 + 2H_2O + 4e^-$	+0.40

Sources of data: Sillén, L. G.: "Stability constants of metal-ion complexes. Sec. 1: Inorganic ligands," *Chem. Soc. London Spec. Publ.* 17, 1964; and Supplement 1, *Spec. Publ.* 25, 1971. Weast, R. C. *et al.*: *Handbook of Chemistry and Physics*, 66th ed., CRC Press, Boca Raton, Florida, pp. D-151 to D-158, 1985–86.